Building tools to identify interacting partners of Rev1 polymerase in its novel role in DNA Damage Tolerance by Template Switching

A senior honors thesis for the Department of Biology

Under the advisement of Dr. Mitch McVey

Gina Tomarchio

Abstract:

DNA replication is a dynamic and tightly regulated cellular process involving a complex cast of players but when the replication machinery encounters lesions or physical blockages in the DNA template, there is a threat to the integrity of the replication forks. If these lesions are not bypassed, replication forks will stall and eventually collapse and thus cells have evolved a set of mechanisms for bypassing lesions during replication, known as DNA Damage Tolerance (DDT). In eukaryotes, DDT is separated into two pathways, translesion synthesis (TLS) and template switching (TS). TLS involves use of specialized polymerases to synthesize past the lesion while TS uses a homology-directed mechanism and a sister chromatid template to replicate past the lesion. The coordination between the two separate DDT pathways remains to be fully understood. Also, despite the critical nature of the lesion bypass pathways, their exact mechanisms and players remain somewhat mysterious, especially in the TS pathway. Recent, unpublished work from our lab has provided evidence for a hierarchy of DDT pathway choice in *Drosophila* with TS serving as a back-up to bypass via TLS. This study aims to elucidate if this hierarchy is phenomenon specific to rapidly proliferating tissues by comparing our previous results to the effects of chemically induced fork-stalling in *Drosophila* cell culture. Also, this study was successful in building tools for further clarifying the mechanisms and players involved in the TS pathway in *Drosophila*. Specifically, we are interested in using these tools to identify new interacting partners of TLS polymerase, Rev1, which other recent unpublished studies from out lab have implicated to have a role in lesion bypass via TS, separate from its known function in TLS.

Table of Contents

Introduction

I. Genome Replication and Instability

In order for unicellular organisms to propagate and for multicellular organisms to grow and develop, cells need to divide. To maintain cellular function after division, the original cell must first replicate and then pass along a single copy of its coded instructions in the form of DNA. Since each cell receives only a single copy of its coding information, accurate duplication and division of DNA is essential to ensuring the functionality and survival of a cell. Despite this fact, the process of DNA replication is quite dynamic and involves the formation of inherently unstable and easily damaged intermediates. It is not surprising, then, that this process is accompanied by an intricate set of protein factors both for stabilization of intermediate structures and for signaling when damage has occurred. Signaling at sites of DNA damage during replication involves pathways that stall the natural course of the cell's division and pathways that bypass the site of damage so that cell division can continue. Interestingly, both of these signals have the potential to actually cause a more severe defect in the cell's functioning. Errors in cell cycle checkpoints often lead to unchecked cellular proliferation and cancers. Failure of the damage bypass pathways can create dangerous sequence mutations, replication fork stalling, collapse and generation of dangerous DNA double strand breaks. Interestingly, the DNA damage that can come from faulty attempts at damage bypass can effect genes that mediate normal cellular function so can also create cancerous cell phenotypes. In this way, it seems that faulty lesion bypass mechanisms could be at the root of many cancerous phenotypes and, therefore, it may be even more crucial to understand how our cells ensure that errors during replication do not happen in the first place. This poses the question, what are the pathways our cells have in place to address damage encountered during DNA replication? Despite their relative importance, these pathways remain relatively uncharacterized and are therefore the focus of this study

A. DNA Replication

DNA replication originates at a variety of specified locations throughout the complex genomes of eukaryotes. The starting points of DNA replication, referred to as replication origins, are denoted by specific sequences throughout the genome (Branzei and Psachye 2016). Prior to initiation of replication, factors assemble at the origin sequence in a process termed origin "licensing." During this organization of replication factors, the essential double hexameric helicase, MCM2-7, is loaded onto the replication origin (Moldovan, Pfander & Jentsch 2007). When the cell is ready to replicate its DNA, the origin will be "activated": MCM2-7 is phosphorylated and the other essential players of the replisome are recruited. At this point, MCM2-7 can carry out its catalytic strand separation activity, and DNA replication has begun. Once MCM2-7 begins to produce single-stranded DNA (ssDNA) at the replication origin, it is immediately coated with the heterotrimeric protein RPA, replication protein A (Figure 2). RPA protects the exposed base pairs of ssDNA from damage by external factors and from formation of secondary structures (Moldovan, Pfander & Jentsch 2007).

After helicase unwinding, DNA is separated into its two complementary, single strands. Each of these strands serves as a template for synthesis of a new strand. In this way, DNA replication is semi-conservative, each new molecule of DNA is composed of a newly synthesized strand hybridized to one strand of parental DNA (Lehman & Nogurmi 2012). At each replication origin, two "replication forks" move away from the initial site of unwinding in opposite directions. These forks represent the junctions where the helicase is actively separating the duplex DNA (Lehman & Nogurmi 2012). Though the replication machinery at each individual fork is coordinated and moves unidirectionally, the actual synthesis of new DNA is more complex. Because of the reactivity of DNA's deoxyribose sugar, the replicative polymerases can only move in the direction of the replication fork on one strand, termed the leading strand, and

must synthesize in the opposite direction on the complementary strand, termed the lagging strand (Lehman & Nogurmi 2012). (Figure 1). Regardless of strand orientation, DNA synthesis cannot take place without an RNA primer. RNA primers are added to the DNA template by Primase, a DNA-dependent RNA polymerase. After addition of an RNA primer, a specialized polymerase, Pol α synthesizes a short tract of DNA and is quickly replaced by the specialized, replicative polymerases Pol ε and δ. There is evidence that replicative polymerase activity is strand-specific with Pol ε on the leading strand and Pol δ on the lagging strand (Figure 1).

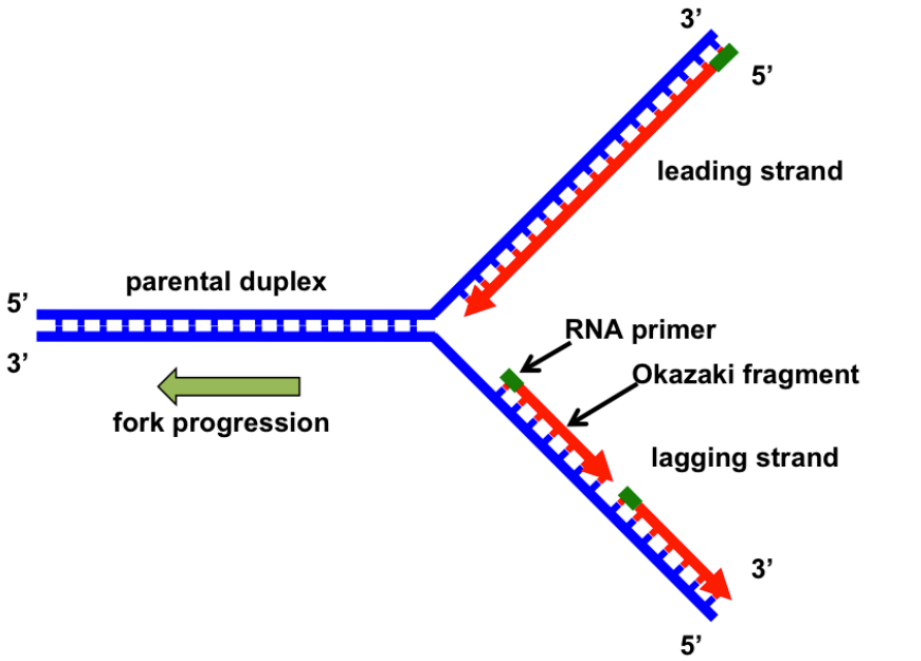

Figure 1: Strand polarity during DNA replication, leading and lagging strand synthesis. Here, parental DNA is represented in blue and nascent DNA is in red. Since DNA can only be synthesized in the 5' to 3' direction, only one of the two nascent strands can move in the direction of the fork. The nascent strands templated from the 3' to 5' strand, here the bottom strand, must be synthesized in short tracts, away from the overall direction of fork movement, to maintain appropriate polarity (Lehman & Nogurmi 2012).

The replicative polymerases have very small active sites which precludes them from allowing the mismatching of DNA base pairs. They also have 3' to 5' exonuclease activity, allowing them to proofread as they synthesize new DNA (Lehman & Nogurmi 2012). The

replicative polymerases are quite processive yet, in order to remain tethered to DNA for the megabases of distance between replication origins, they must interact with the replicative sliding clamp, proliferating cell nuclear antigen (PCNA) (Lehman & Nogurmi 2012). PCNA is loaded onto the template DNA by replication factor C (RFC), which recognizes and recruits PCNA to the RNA primer-template junctions where it will interact with the replicative polymerases and secure them to the ssDNA template (Figure 2). PCNA is a critically important signaling molecule during replication, it has various residues at which it can be chemically modified or marked by proteins as a means of signaling various alternate pathways during replication. Specifically, marking PCNA with the small protein, ubiquitin, seems to mediate the DNA Damage Response (DDR) for bypassing lesions during replication (Moldovan, Pfander and Jentsch 2007). Though there are other well studied PCNA modifications, ubiquitination is the most essential to this study because of its connection to DDT. PCNA ubiquitination and other modifications are discussed further in later sections.

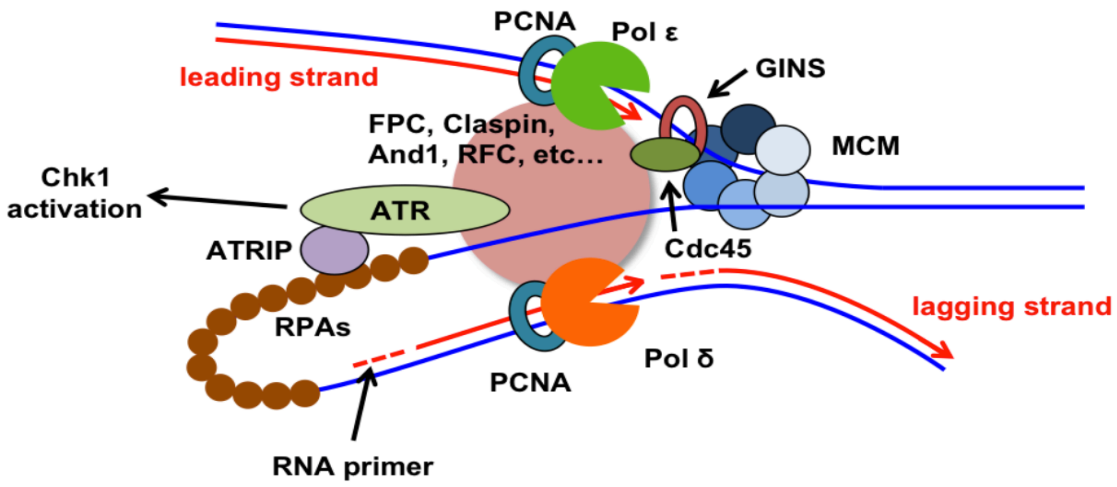

Figure 2: Model of the Eukaryotic Replication Machinery at the Replication Fork. Shown here is the trombone model for lagging strand synthesis (bottom strand) in which the ssDNA upstream of the replication machinery is looped out to allow for lagging and leading strand polymerases to move together. Also illustrated here is the coating of naked ssDNA by RPA,

PCNA increasing polymerase processivity, and MCM catalyzing strand unwinding (Lehman & Nogurmi 2012).

B. Replication Stress and Instability

Despite the complex systems of support and stability provided to the DNA polymerases and helicase by other members of the replication machinery, there are still some areas of the genome that prove difficult for this complex to replicate. Replication forks often encounter regions of DNA that cause its progression to slow or even stop. Cells encounter challenges to processive replication in a variety of contexts, some are naturally occurring sequence contexts like AT rich sequences, repeat sequences or condensed chromatin, while others are naturally occurring physical obstacles like transcriptional machinery, RNA-DNA hybrids or secondary DNA structures like hairpins, H-DNA or G quadruplexes (Mazozui, Velimezi & Loizou 2014). Stalled or slowed replication can be caused by external damaging agents like ultraviolet and ionizing radiation. Most importantly, though, there is great potential for replication damage via endogenous cellular agents. The normal functioning of cellular metabolism produces reactive oxygen species that pose a great threat to the integrity of DNA structure and DNA alkylating agents are naturally abundant in cells as well (Jena 2012). Though physical blockages can occur naturally and are not uncommon, the chemical modification of bases via endogenous agents is likely a more common occurrence in cells and warrants the presence of a well-coordinated lesion bypass system during replication.

When these endogenous physical blockages or chemical alterations occur on the template strand, the replication machinery does not have a mechanism for avoiding it and so the fork may stall or collapse (Branzei & Foiani, 2010). Though studies in *E. coli* have shown that during replication, both leading and lagging strand synthesis can re-prime downstream of a fork stalling lesion, this has yet to be shown in any higher eukaryotes (Heller & Marians 2006). When a

replication fork stalls, the replicative helicase and polymerase uncouple: the helicase continues to unwind the duplex while the polymerase remains stationary, creating extended tracts of exposed ssDNA that is prone to mutagenic base damage. DSBs can also form during replication when the replicative polymerases encounter single stranded nicks or abasic sites or when forks collapse after extended periods of stalling (Ghosa and Chen 2013). DSBs during replication are prone to the formation of very deleterious chromosome translocations, or incorrect repair via homologous recombination, creating either sizable insertions or deletions of important coding sequence (Branzei & Psakhye 2016). Considering the serious implications of DNA replication stress and fork stalling, it is not surprising that all prokaryotes and eukaryotes can activate a series of alternate pathways during replication to bypass fork-stalling blockages, or to halt the progression of the cell cycle until a fork is restarted or a converging fork can compensate. The presence of a lesion bypass mechanism across prokaryotes and eukaryotes emphasizes how important these mechanisms are to cellular survival and highlights the critical nature of understanding how they work.

C. Coping with Replication Stress and Instability

Cells have two mechanisms for dealing with replication stress: DNA Damage Response (DDR) which regulates the cell cycle and repairs collapsed forks or resulting DSBs, and DNA Damage Tolerance (DDT) which acts in the context of replication to prevent extended stalling or collapse of replication forks. It is important to note that, while the main function of DDT is during replication, DDR acts in many contexts, all triggered by DNA damage, such as coordination of the cell cycle and apoptosis (Cimprich & Cortez 2008). DDR is an incredibly complex set of signaling pathways that, in the context of replication stress, can pause the cell cycle to allow time for repair of DNA damage (Chang & Cimprich 2009). DDR is mediated by

two factors, ATR and ATM. ATR recognizes extensive tracts of RPA-coated ssDNA, a signature of replicative polymerase and helicase uncoupling. ATR interacts with and phosphorylates CHK1, a cell cycle regulating protein, which begins a signaling cascade that pauses the cell cycle so the damaged fork can be repaired through homology-directed mechanisms (Cimprich & Cortez 2008). The roles and mechanisms of ATM are somewhat less defined. It is known to act at the sites of DSBs to activate cell cycling protein CHK2 (Cimprich & Cortez 2008) and is hypothesized to stabilize replication forks as they pass through these break-sites (Branzei & Faioni, 2010). DNA Damage Tolerance (DDT) is the set of alternate pathways that occur during replication to bypass potentially fork-stalling lesion so DDT seems to be the cell's first line of defense against replication stress. DDT is the focus of this study and therefore will be discussed in further detail in the next section.

II. DNA Damage Tolerance DDT

There is an important significance to the term DNA damage tolerance, as this set of pathways should not be considered a repair pathway but instead a mechanism for "tolerating" or avoiding physical blockages to prevent the even more deleterious consequences of fork stalling or collapse. DDT allows the fork to bypass obstacles and leaves them behind to be repaired later in the cell cycle, as mentioned previously (Branzei & Szakal 2016). There are two DDT mechanisms; while both achieve the same goal of lesion bypass, the mechanisms and consequences of each pathway are quite different.

Since DDT is occurring in the context of replication, it is not surprising that the main regulatory and signaling mechanism involves a member of the replisome, the heterotirmeric sliding clamp, PCNA. Differential ubiquitination of PCNA signals which branch of DDT the cell will use to bypass a lesion. Though the exact mechanisms and players involved in this signaling

are still under study, it has been proposed that the ubiquitin conjugating enzymes and machinery likely recognize long tracts of ssDNA characteristic of replicative polymerase and helicase uncoupling at stalled forks (Chang & Cimprich 2009). Upon fork stalling in *S. cerevisiae*, PCNA is first mono- ubiquitinated at the conserved lysine residue 164 and shunted into the often-mutagenic Translesion Synthesis (TLS) bypass pathway. The ubiquitin chain can also be extended via linkage of Lys63 on the individual ubiquitin molecules creating a non-canonical poly-ubiquitin chain. This sends the stalled fork into a homology-directed, and classically error-free mechanism of repair often referred to as Template Switching (TS) (Moldovan, Pfander and Jentsch 2007) (Figure 5). PCNA can also be modified by markers other than ubiquitin, in fact, PCNA is believed to be marked by the small, ubiquitin-like modifier (SUMO) protein during normal replication in *S. cerevisiae*. Other recent studies in yeast have indicated that this SUMOylation serves to inhibit homologous recombination (HR) from occurring via recruitment of Srs2, a helicase that prevents the nucleation of Rad51 on ssDNA. In this way, SUMOylation of PCNA prevents the ssDNA present normally during replication from being able to successfully invade a homologous template and complete HR (Chang & Cimprich 2009). Coordination between PCNA ubiquitination and SUMOylation is only some of the post-translational signaling that happens on this molecule and recent studies are making it clear that PCNA modifications coordinating DDT are much more complicated than is currently understood (Branzei &Szakal 2016).

A. Translesion Synthesis (TLS)

When a replication fork encounters a fork-stalling lesion, the mono-ubiquitination of PCNA likely causes the switching of the replicative polymerase for a specified, trans-lesion synthesis (TLS) polymerase. The TLS polymerases can accommodate large lesions and bulky

adducts in their larger active sites and are therefore able to add nucleotides across from these unusual structures (Moldovan, Pfander and Jentsch 2007). TLS polymerases are also more error-prone when adding base pairs across from undamaged templates and lack exonuclease proofreading activity (Sale 2013). TLS can be an error-free process, though, depending on which polymerase is used (Chang & Cimprich 2009). The main TLS polymerases in mammalian and most eukaryotic cells are the B-family pol ζ and Y-family pol η, pol κ and Rev1 and each has lesion type specificity. In yeast, Pol η preferentially synthesizes past thymine dimers, mammalian pol κ past benzopyrene-induced guanine adducts, eukaryotic pol ζ extends after distorted or mismatched base pairs and eukaryotic Rev1 incorporates deoxycytidines across from abasic sites (Ghosal & Chen 2013). Of these TLS polymerases, pol η is the most accurate as studies have shown that it can bypass its preferred lesion, thymine dimers, without error. The exact mechanism by which the replicative polymerase is switched out for a TLS polymerase is still not clear. It seems that, in some cases there may be three polymerase-switching events in eukaryotes, though there is also evidence that pol η can do the entire process alone (Waters et al 2009). During the polymerase switching events, the replicative polymerase will first switch out for a TLS polymerase, which will add a nucleotide across from the site of the lesion. Next, this TLS polymerase will be switched out for another TLS polymerase that can synthesize after the unstable, mismatch-like structure, this is most likely pol ζ. Finally, this polymerase will again be replaced by the original, replicative polymerase. Though the other factors involved in these polymerase-switching events remain uncertain, it is often hypothesized that Rev1, itself a TLS polymerase, is involved in the recruitment of pol ζ to the site of the stalled replication fork (Figure 3). (Friedberg, Lehmann & Fuchs 2005)

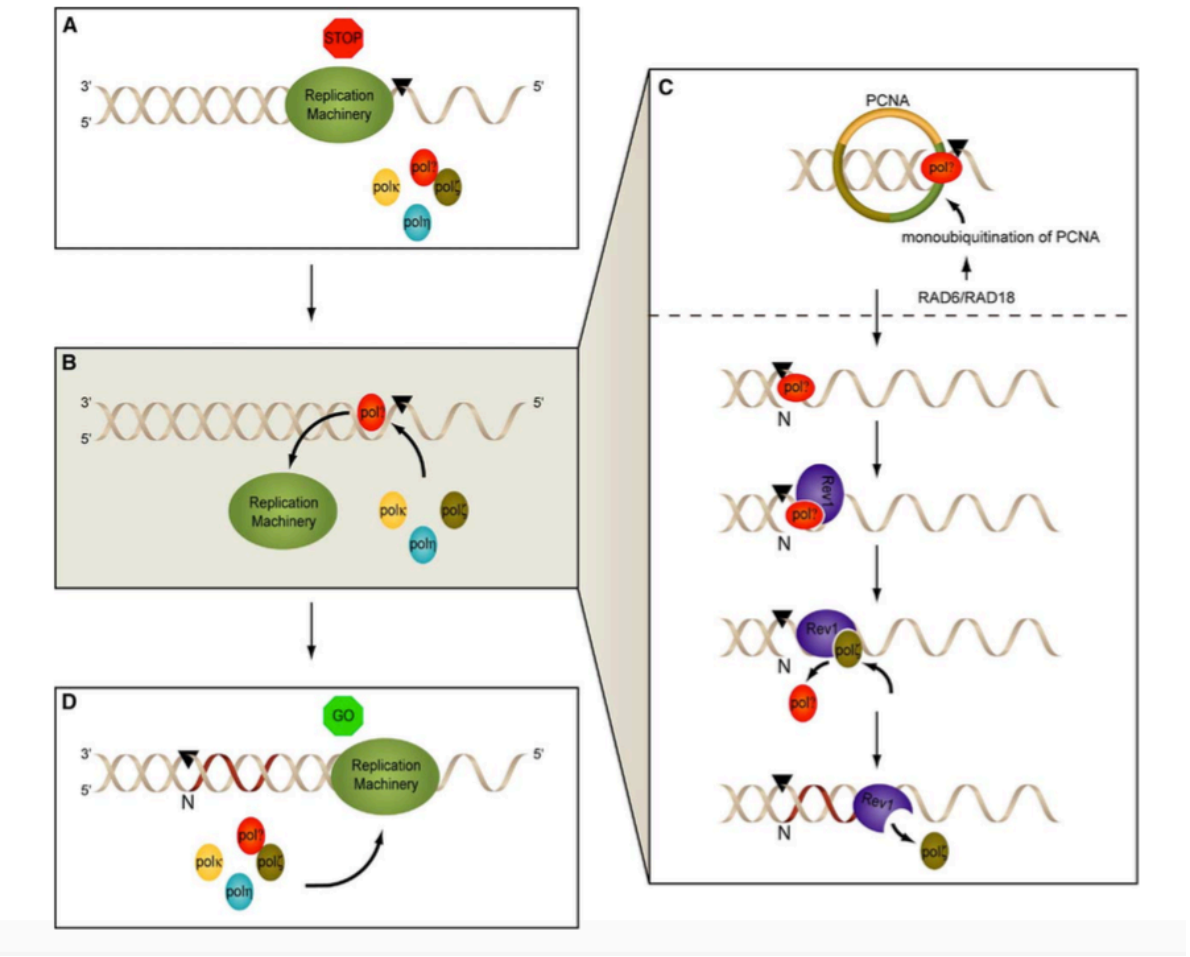

Figure 3: Model for Polymerase Switching during TLS in eukaryotes. A) Replication machinery encounters a lesion during replication B) Replication machinery is switched out for a TLS polymerase, here "pol?" since the specificity and choice of TLS polymerases at this step remains uncertain C) Mono-ubiquitination of PCNA causes pol? to localize at the site of the fork stalling. Pol? inserts a nucleotide (N) across from the lesion and Rev1 enters to facilitate the switch between the initial TLS polymerase and pol ζ. Rev1 may also be involved in sequestering pol ζ away from the replication fork after the lesion has been safely bypassed. (figure modified from Friedberg, Lehmann & Fuchs 2005)

As mentioned previously, TLS is signaled via a mono-ubiquitination of PCNA. Since PCNA must be mono-ubiquitinated before it can be poly-ubiquitinated, the TLS pathway is often thought to be the cell's first line of defense in bypassing a lesion. (Chang & Cimprich 2009). Current understanding of signaling for TLS indicates that Rad18, an E2 ubiquitin conjugating enzyme, may recognize and bind to the RPA-coated tracts of ssDNA characteristic of helicase and polymerase uncoupling. Rad18 then acts in complex with Rad6, an E3 ubiquitin ligase,

which will catalyze the addition of the ubiquitin to Lys164 on PCNA (Figure 5) (Branzei & Psakhye 2016). Interestingly, all the TLS polymerases have ubiquitin and PCNA interacting domains leading to the hypothesis that PCNA mono-ubiquitination may recruit or increase the affinity of the TLS polymerases for the replication machinery. The current model for the recruitment of TLS polymerases after ubiquitination assumes that the TLS pols are constantly sampling the DNA so that when PCNA is ubiquitinated, this random sampling interaction will then be secured via the ubiquitin binding domains on the TLS pols. This model explains how these damage tolerating polymerases are recruited to the replication fork in the context of DNA replication stress (Ghosal & Chen 2013).

There is also evidence that, in yeast, PCNA ubiquitination can occur after replication is complete, indicating that the TLS pathway may serve to fill in single stranded gaps left by the replication machinery. The current model for post-replicative TLS has the replication fork re-established slightly before the lesion and involves the same mechanism of polymerase switching mentioned previously. Similar to if the lesions were bypassed at the original replication fork, lesions are still left to be repaired later in the cell cycle. It has been proposed that waiting to bypass lesions until after the replication fork has passed may allow for the cell to take stock of the local environment and damage, allowing it to make a more informed decision about how to bypass and eventually repair these lesions (Choe & Moldovan 2017).

B. Template Switching

Template switching (TS) is considered the error-free counterpart of TLS in the series of DDT pathways. Though the principles behind the TS pathway make it theoretically error-free, there is also opportunity for this pathway to induce mutations even more catastrophic than the nucleotide mismatches of TLS. The actual mechanisms and intermediate structures of the TS

pathway are not well characterized. Evidence suggests that the TS pathway involves the movement of the stalled, nascent strand of DNA to the newly forming duplex that will eventually be the sister chromatid. The nascent, stalled strand will use the newly forming strand in the other duplex as a template for synthesis past the lesion (Figure 4) (Chang & Cimprich 2009). Alternatively, there is evidence that the replication fork could form a regressed or reversed structure in which the newly synthesized leading and lagging strands pair with one another for synthesis past the lesion. Whether these reversed-fork structures actually form *in vivo* remains controversial (Chang & Cimprich 2009), though recent evidence has shown Rad51-dependent formation of these structures in human cells (Zellweger et al. 2015). Regardless, the TS pathway strongly parallels the mechanisms and structures formed during Homologous Recombination (HR) repair of DSBs, especially the D-loop like structure formed during the template switching pathway. This analogy is supported by evidence that indicates that Rad51, the factor involved in the strand invasion and homology-search events of HR, is often recruited to sites of replication damage. (Branzei & Psakhye 2016). In fact, many HR-associated proteins have known roles in DSB repair during replication so it is possible that they are also acting in the TS pathway. Studies have shown that HR factors like BRCA2 and RPA co-localize with PCNA and form foci when damage is induced during S-phase, further confirming the presence of a homology-directed pathway of DDT (Kolinjivadi et al 2017).

Like in TLS, recent studies have indicated that the TS pathway may also be occurring behind the replication fork rather than solely in coordination with the replication machinery. A recent study in yeast solidified roles for some of the proposed players in this post-replicative TS mechanism. In their model, single stranded DNA is expanded past the post-replicative gaps by the Exo1 exonuclease and the newly generated ssDNA is coated with RPA. Addition of RPA

then recruits many homologous recombination factors, like Rad51 and Rad52, to the site of the gap, allowing for the formation of the recombination-like D loop. After formation of the D loop, the replicative polymerase, Pol δ synthesizes past the site of the lesion, using the sister chromatid as a template. After synthesis is sufficient to bypass the lesion, any X-shaped intermediates are resolved via the action of Sgs1 helicase and topoisomerase 3 (Vanoli et al. 2010) (Figure 4). These X-shaped intermediates have been visualized in yeast using 2D gel electrophoresis, further supporting a model of sister-chromatid strand invasion during TS (Branzei et al. 2008).

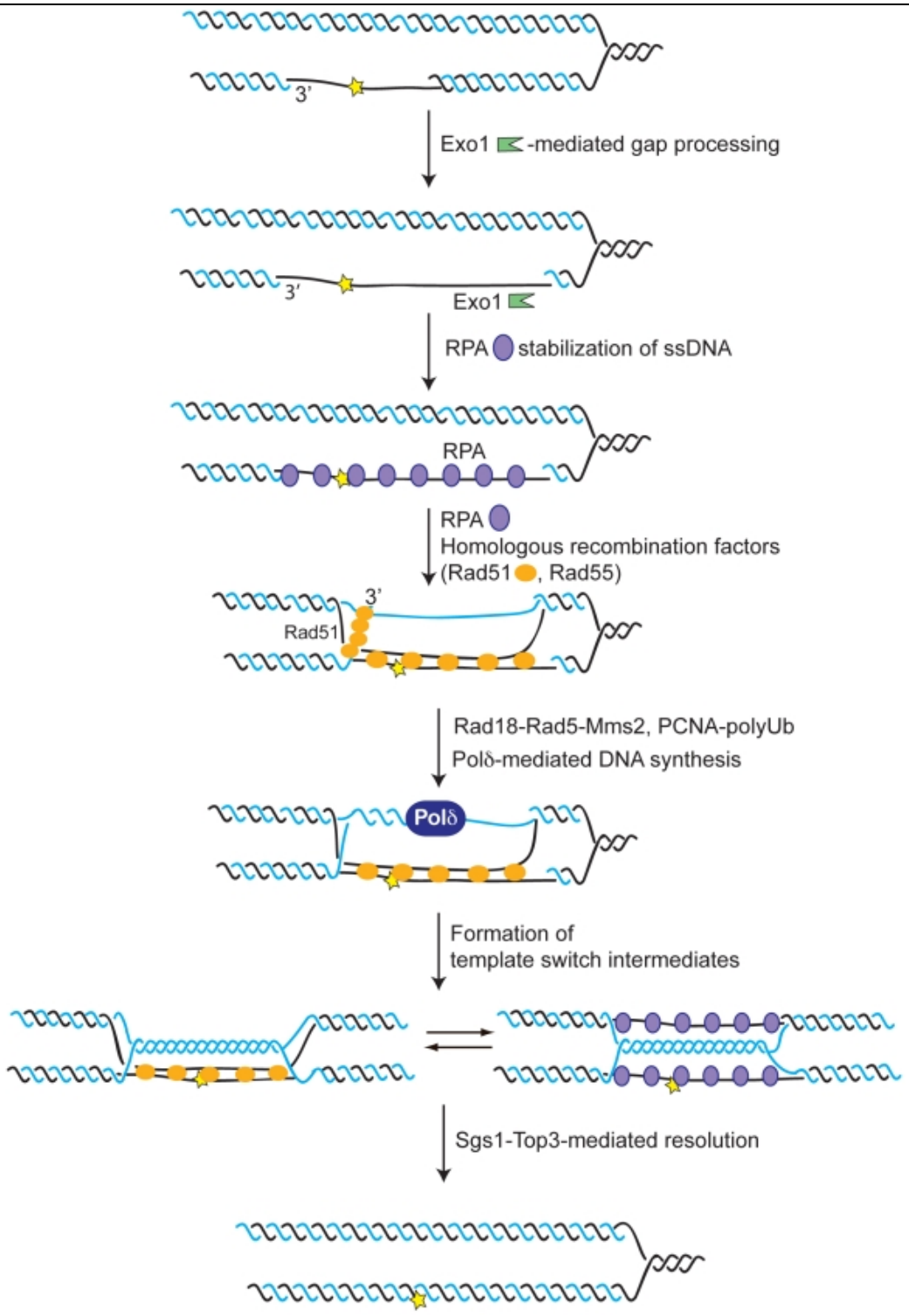

Figure 4: Model for Template Switching mechanism behind in replication fork in yeast. Exo 1 exonuclease extends the tracts of ssDNA surrounding the lesion. RPA coats the ssDNA and recruits HR factors like Rad51 and Rad52 to facilitate the formation of the D-loop. Pol δ enters at the D loop to synthesize past the lesion, using the sister chromatid as a template. The D-loop is resolved by the action of Sgs1 and Top3 (figure from Vannoli et al. 2010).

As discussed above, the TS pathway is signaled via poly-ubiquitination of PCNA. Since poly-ubiquitination can only come after mono-ubiquitination, it has been proposed that the poly-ubiquitin chain might prevent the TLS polymerases from accessing the DNA template or by binding and sequestering them away from the DNA (Branzei & Psakhye 2016). During poly-ubiquitination in *S. cerevisiae*, the pre-existing, single ubiquitin is extended via the Ubc13-Mms2 E2 ubiquitin conjugating heterodimer and Rad5 E3 ubiquitin ligase (Figure 5). In mammals the poly-ubiquitination of PCNA is mediated by two E3 ligases, SHPRH and HLTF; while humans have both SHPRH and HLTF, only the SHPRH gene has been found in *Drosophila.* Though SHPRH and HLTF have similar domain organization, their specific functions and poly-ubiquitination contexts have yet to be differentiated (Chang & Cimprich 2009). Though TS is generally thought to be an error free pathway because of its homology-directed mechanism, there is still potential for it to be deleterious, especially in areas of repeated sequence where misalignment during strand invasion could lead to expansions or deletions of sequence. Additionally, if there are short microhomologies at the ends of the TS repaired intermediates, large chromosomal translocations can occur (Kolinjivadi et al 2017).

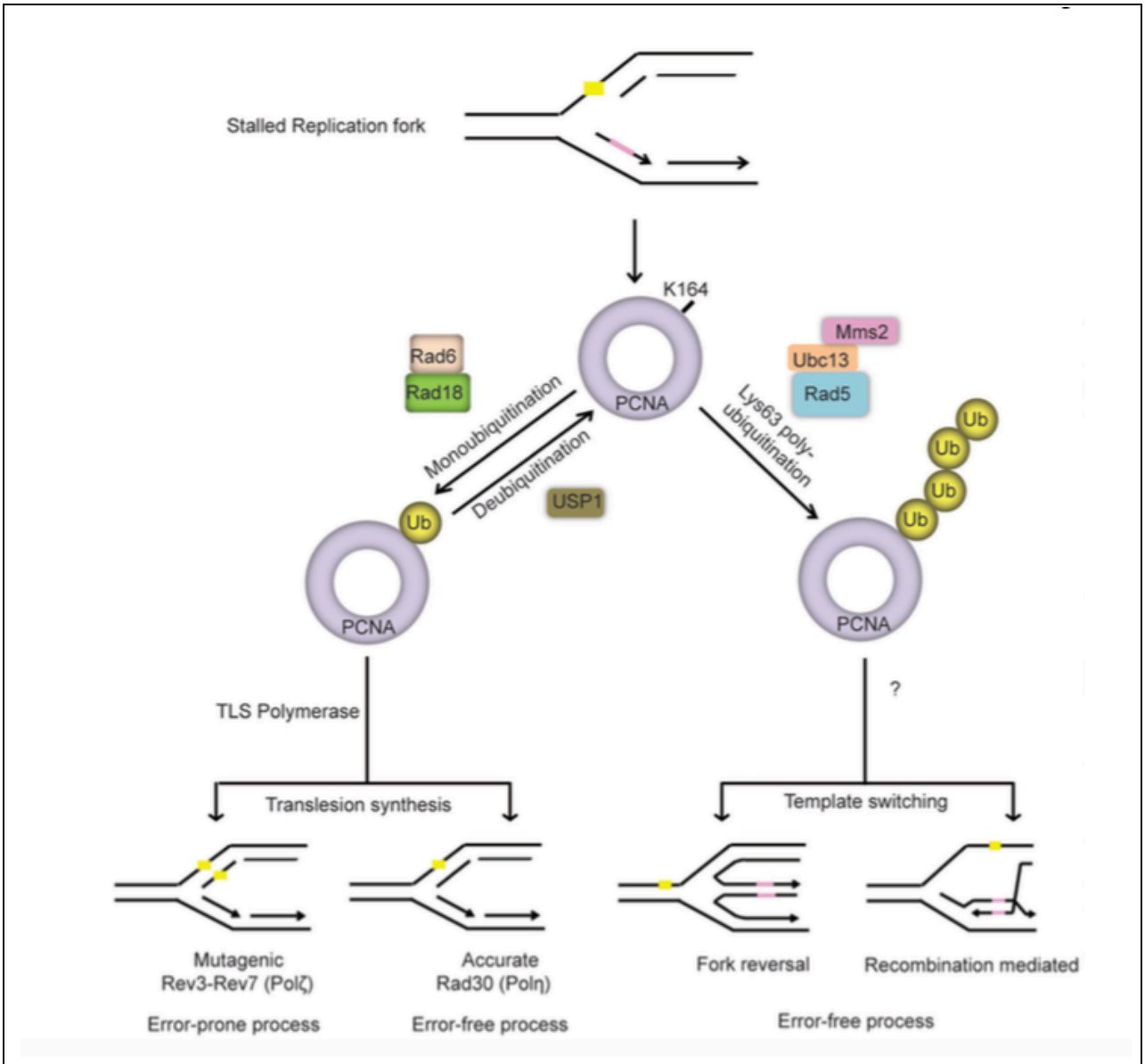

Figure 5: DNA Damage Tolerance (DDT) pathways and players. Here, the yellow square represents a fork stalling lesion. Upon encountering a lesion on the leading strand, PCNA is either mono-ubiquitinated at lysine 164, via the Rad6-Rad18 E2/E3 ubiquitin ligase system or poly-ubiquitinated via the Rad5-Ubc13-Mms2 E2/E3 ubiquitin ligase system. Mono-ubiquitination sends the stalled fork to the TLS pathway to either be repaired by the mutagenic TLS polymerase ζ or error-free polymerase η. Poly-ubiquitination likely shunts the stalled fork into the template switching pathway which could entail either a recombination-mediated strand invasion event or a reversed fork structure, both of which create an error-free lesion bypass (Ghosal & Chen 2013).

C. DDT Pathway Coordination, Choice and Timing

Though the general mechanisms of the two DDT pathways are clearly delineated, their contexts and coordination remain to be clearly understood. The necessity for two separate DDT pathways with different tendencies for mutagenesis may be explained by their dependence on timing and cell cycle progression. Two recent studies in yeast have indicated a cell cycle dependence for bypass of both alkylating and UV-induced nucleotide lesions (Huang, Piening & Paulovich 2013) (Callegari & Kelly 2016). When dividing yeast cells were exposed to very low doses of the alkylating agent, MMS, results indicated that the TS pathway may be used primarily during S phase to prevent the formation of ssDNA (Huang, Piening & Paulovich 2013). Similar results were seen with UV radiation, though this early lesion bypass mechanism was not directly characterized as template switching but more generally as a homology-directed form of bypass. Interestingly, though, this study indicated that early S phase bypass using homology was consistent with cells stalling at the G2/M transition, thereby providing the cell sufficient time to complete the slower, homology-directed bypass of the lesion (Callegari & Kelly 2016). Additionally, both studies indicated that the action of the TLS polymerases, specifically Rev1 and Pol ζ, were only essential to bypass lesions later in the cell cycle, and that Rev1 expression is only upregulated after the G2/M transition, implicating the TLS pathway might be used predominantly later in the cell cycle (Huang, Piening & Paulovich 2013) (Callegari & Kelly 2016). There is no evidence that the TLS polymerases are active before the G2/M transition, unless in a Rad51 mutant background, providing evidence for a role of this homologous recombination factor in preventing the more mutagenic TLS early in the cell cycle (Callegari & Kelly 2016). Furthermore, there is evidence that helicases specific for resolving TS intermediate structures, Mus81 and Mms4, are suppressed until the later G2 or M portions of the cell cycle (Szakal & Branzei 2013). Overall, the current model for the coordination of the two DDT

pathways involves the timing of the cell cycle and availability of a homologous template. Since sister chromatids are still paired early in the cell cycle, there are appropriate homologous templates available for repair via TS. Additionally, evidence regarding cell cycle arrest would indicate that the cell does need sufficient time to carry out a homology-directed lesion bypass, which is optimal when the cell cycle checkpoints are still an option, before the G2/M transition. It seems, then, that the TLS pathway is utilized primarily when the cell does not have a template for error-free repair nor time to halt the cell cycle and invade a homologous template.

III. Rev1 and its role in DDT

A. Rev1 structure and known functions

Rev1 was first discovered as a Y-family polymerase with deoxycytidl transferase activity that allows it to add deoxycytidl (dCMP) across from guanines and abasic sites in the ssDNA template. Early studies of Rev1 noted that a catalytically inactive form of the protein still promoted damage-induced mutagenesis in yeast, specifically mutagenesis associated with Rev3, the catalytic subunit of Pol ζ. This finding was the basis for the model of polymerase recruitment and switching in TLS, mentioned previously (Figure 3) (Sharma et al 2013). Rev1 interacts with Pol ζ, as well as other TLS polymerases like Pol η and Pol ι at its C-terminal domain (CTD). The Rev1- Pol ζ interaction is mediated by Rev 7, a subunit of Pol ζ which binds both the CTD of Rev1 and Rev 3; this interaction is consistent among yeast, *Drosophila* and *C. elegans* (D'Souza et al 2008). Between its catalytic and C-terminal domain, Rev1 has a ubiquitin-binding motif (UBM) allowing it to bind ubiquitin on other proteins. The presence of this domain is fitting with its role in TLS as it can not only bind the TLS polymerases but also other ubiquitinated molecules at the stalled fork (Sharma et al 2013). At its N-terminus, Rev1 has a BRCT domain, classically associated with protein-protein interactions. Studies in mammalian

cells show that Rev1 can bind directly to PCNA via this BRCT domain and that this binding is enhanced via ubiquitination of PCNA (Guo et al. 2006) (Figure 6).

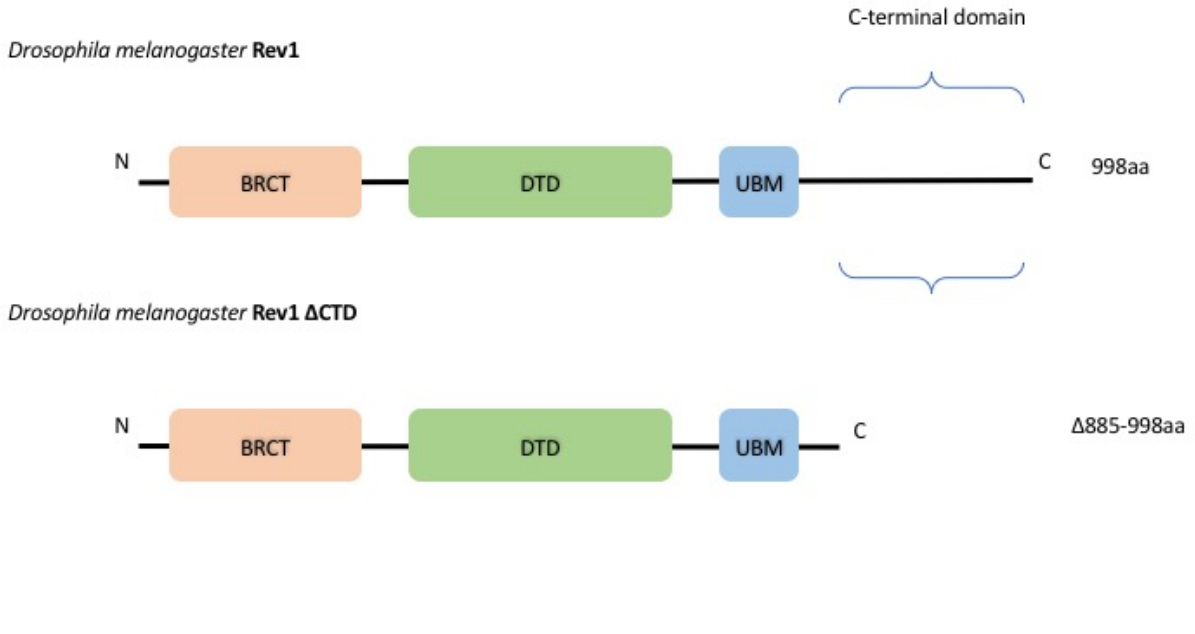

Figure 6: Rev1 and Rev1ΔCTD allele domain structure. In *Drosophila melanogaster* Rev1 is a 998 amino acid protein located on the left arm of the third chromosome. At its N terminus is a BRCT domain. Central to the amino acid sequence is its catalytic, deoxycitidl transferase domain (DTD) and a ubiquitin binding motif (UBM). The C-terminal domain is where Rev1 interacts with many TLS polymerases. In the ΔCTD allele, the coding sequence for the terminal 113 amino acids is deleted.

When considering the functions of the various Rev1 domains in the context of its known importance to TLS, a clearer model of its exact role in this bypass pathway begins to emerge. As one might expect of a classical polymerase, Rev1 has shown ssDNA binding ability and a preference for targeting a primer terminus *in vitro*. This functionality provides a potential mechanism for Rev1 recruiting and targeting the TLS polymerases to the site of a lesion during TLS (Masuda & Kamiya 2006). A recent study in yeast showed that Rev1's CTD interacts directly with Rad5 at its N terminus. This newfound interaction generates a model for Rev1 in

TLS where Rad5 enters after ubiquitination by Rad6-Rad18 and acts as a switch between the two DDT pathways. If Rad5 is bound to Rev1 TLS will occur and Rev1 will serve as a scaffold for the other TLS polymerases. If Rad5 interacts with Mms2-UBC13 it will shunt the cell into the TS pathway (Kuang et al. 2012).

The current consensus is that Rev1's main role in DDT is limited to the TLS pathway, but there is also evidence that connects it to a homology-directed mode of DNA double strand break repair. For example, in yeast, Rev1 and Pol ζ localize at sites of DNA double strand breaks (DSBs) and it seems that Rev1 serves to recruit Pol ζ to these sites of damage (Hirano & Suglmoto 2006). Also, in *Drosophila*, Rev1 has a role in Homologous Recombination (HR) of DSBs by recruiting Pol ζ to structures of early repair intermediates where it competes with the replicative polymerases for access to the DNA template (Kane et al. 2012). Since Rev1 seems to act in the HR repair pathway, it is not surprising that in mammalian cells loss of Rev1 decreases the frequency of gene conversion in the context of DNA replication (Yang et al. 2015). There is also evidence that Rev1 is involved in HR-mediated fork stabilization. It was proposed that when a DSB occurs during replication, Rad18 mediates ubiquitination of FANCD2 which recruits Rev1 to the break where it will help maintain fork stability by binding to Rad51 filaments on ssDNA (Yang et al 2015).

B. DDT hierarchy in *Drosophila* and novel role of Rev1 in mediating both pathways

Recent, unpublished data from our lab implicates a role for Rev1 in the Template Switching pathway of DDT. Our studies provide an interesting and novel insight into the coordination of DDT as they are all in the context of a whole, multi-cellular organism, *Drosophila melanogaster*, in contrast to much of the literature which focuses mainly on human cell lines and yeast. These studies originated as an investigation of Rev1's recruitment to and

involvement in repair of DSBs. To assess Rev1's role in DSB repair, *Drosophila melanogaster* with a deletion of the Rev1 coding sequence (*Δrev1*) were treated with various DNA damaging mutagens. Topotecan (TPT), Bleomycin and Ionizing radiation (IR) induce DSBs, Nitrogen Mustard (HN2) introduces inter-strand crosslinks, Hydroxyurea (HU) causes depletion of dNTPs and Methylmethane sulfate (MMS) methylates bases. Interestingly, Rev1 was not very sensitive to two of the DSB-inducing agents, TPT and Bleomycin yet was hypersensitive to MMS (Figure 7) (V. Khodaverdian, unpublished). The sensitivity of Rev1 to IR fits with the proposed role for Rev1 in DSB repair and its hypersensitivity to MMS could also be a result of defective repair of DSBs induced by replication fork collapse. Interestingly, though, Rev1 mutants are not sensitive to the DSB-inducing agents bleomycin and TPT, implying that their MMS sensitivity is likely also a result of a Rev1 defect outside of DSB repair. Since MMS is creating bulky adducts that block replication machinery, the observed hypersensitivity of Rev1 to MMS supports its essential role for lesion bypass during replication. The *Δrev1* mutant hypersensitivity to MMS is surprising since, according to the literature, Rev1 seems to only be involved in TLS and these mutants should still be able to use TS to bypass MMS induced lesions.

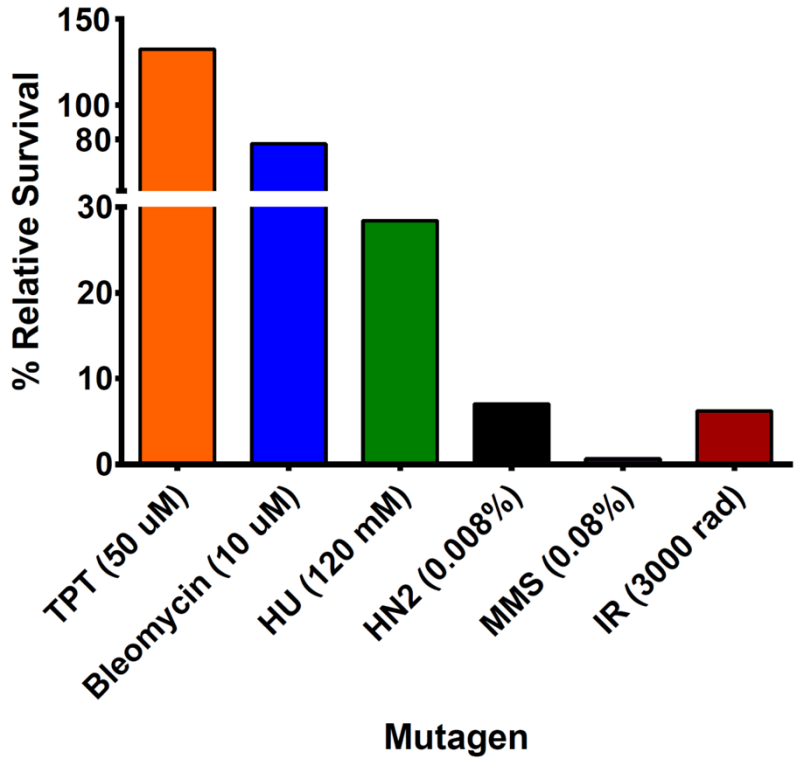

Figure 7: Sensitivity of Rev1 to various DNA damaging agents in *Drosophila*. Mutagen concentration/dosage used for treatment is listed after mutagen type. Relative % survival was measured by comparing number of heterozygous mutants that survived to adulthood to number of homozygous mutants that survived to adulthood after mutagen treatment at embryonic stage. (figure courtesy of V. Khodaverdian)

To further clarify these findings, the sensitivity of *Δrev1* mutants was compared to that of *Δrev3* mutants. In *Drosophila*, Rev3 is the catalytic subunit of pol ζ and therefore should be essential for the TLS pathway. Interestingly, the *Δrev1* mutants were significantly more sensitive to MMS than the *Δrev3* mutants, indicating that Rev1 may have a role in DDT outside of TLS (Figure 8) (V. Khodaverdian, unpublished). Since Rev1 and pol ζ are hypothesized to interact during TLS, specifically at Rev1's C-terminal domain, a C-terminal truncation of Rev1 was created (*Rev1ΔCTD*) and treated with MMS. The *Rev1ΔCTD* mutants phenocopied the *Δrev3* mutants at varying concentrations of MMS (Figure 8) (V. Khodaverdian, unpublished). Therefore, while Rev1 seems to have an essential role in recruiting pol ζ during TLS, it clearly also has a role

outside of TLS and outside of the functionality of its C-terminal domain. Based on the conventional classification of DDT into two distinct pathways, one possible explanation for these results is that Rev1 also functions in the alternate, TS pathway.

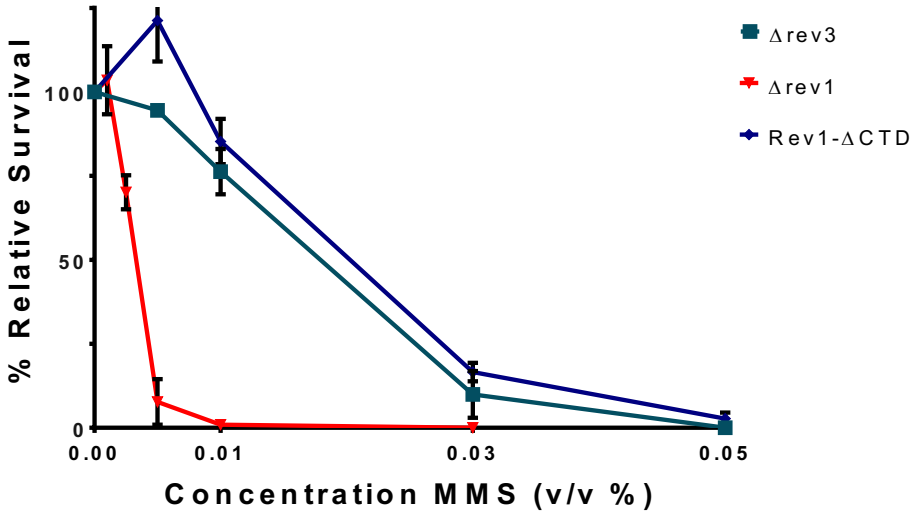

Figure 8: MMS Sensitivity of *Drosophila* Rev1 and Rev3 and BRCA2 single and double mutants. Sensitivity of *Drosophila* mutants at increasing concentrations of MMS. % relative survival measured by counting heterozygotes versus homozygotes of each mutant that survived to adulthood. Comparison of Rev1 knockout, Rev3 knockout and C-terminal truncation of Rev1 MMS sensitivity (V. Khodaverdian, unpublished) (figure courtesy of V. Khodaverdian)

To confirm that Rev1 was acting specifically in TS and not in some other DDT related function, the MMS sensitivity of a SHPRH knockout (*ΔSHPRH*) was tested both as a single mutant and in combination with other DDT-specific gene knockouts. Since SHPRH is believed to mediate the poly-ubiquitination of PCNA that signals the initiation of the TS pathway (Lin et al. 2011), a SHPRH knockout should prevent this mode of signaling for bypass of lesions via template switching, though it is possible that there are other E3 ubiquitin ligases that could compensate for loss of SHPRH function. Interestingly, *ΔSHPRH* mutants alone were not sensitive to MMS but when combined with the *Rev1ΔCTD* mutants which are defective in their ability to do TLS, the

sensitivity phenocopied that of the complete Rev1 knockout, further supporting the hypothesis that Rev1 has a role outside of TLS in the TS pathway (Figure 9) (A. Schmidt, unpublished)

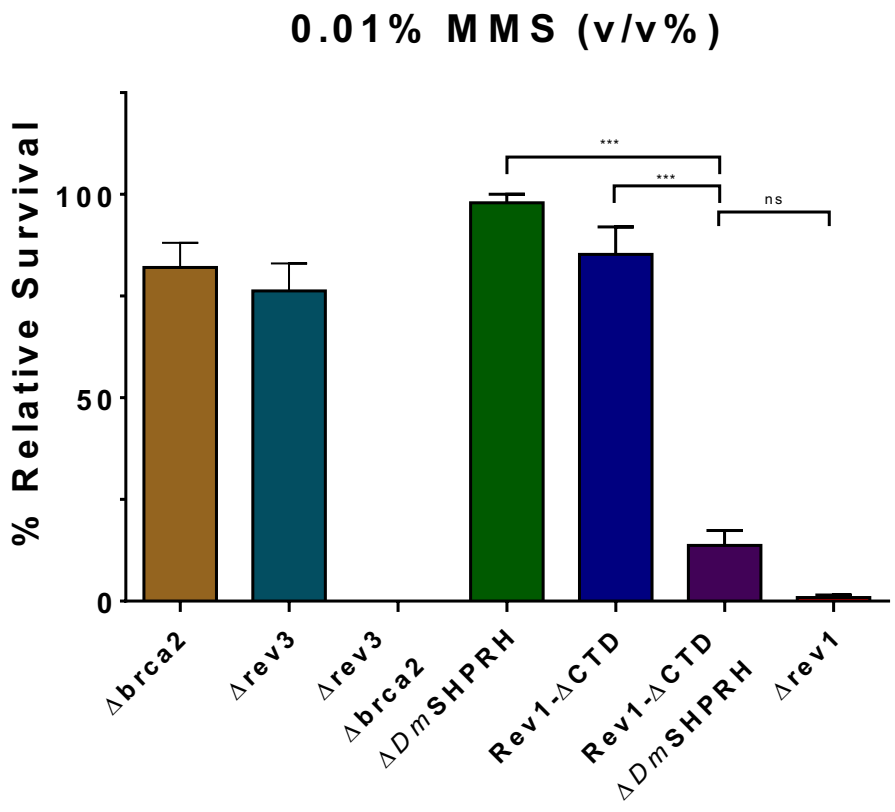

Figure 9: Sensitivity of *Drosophila* Rev1, SHPRH and other DDT factors to 0.01% MMS. Percent relative survival of *Drosophila* mutants measured by comparing survival of heterozygoes and homozygotes. All mutants treated in embryonic stage with 0.01% MMS. *** = $p<0.0001$: One way ANOVA with Tukey's multiple comparison test (A. Schmidt, unpublished) (figure courtesy of V. Khodaverdian).

These findings also indicated a hierarchy in DDT pathway choice in *Drosophila*. The *ΔSHPRH* mutants were not sensitive to MMS until combined with a TLS-deficient Rev1 mutant (*Rev1ΔCTD*), implicating that TS serves primarily as a back-up to TLS during DDT. This observation was confirmed using other TS and TLS specific mutants both alone and in combination. *Drosophila* missing the BRCA2 or Rad51 genes, essential for the strand invasion step during homology-directed repair, were not sensitive to MMS on their own (Figure 10 top),

yet when combined with the *Δrev3* mutation, BRCA2 became hypersensitive at all concentrations (Figure 10, bottom).

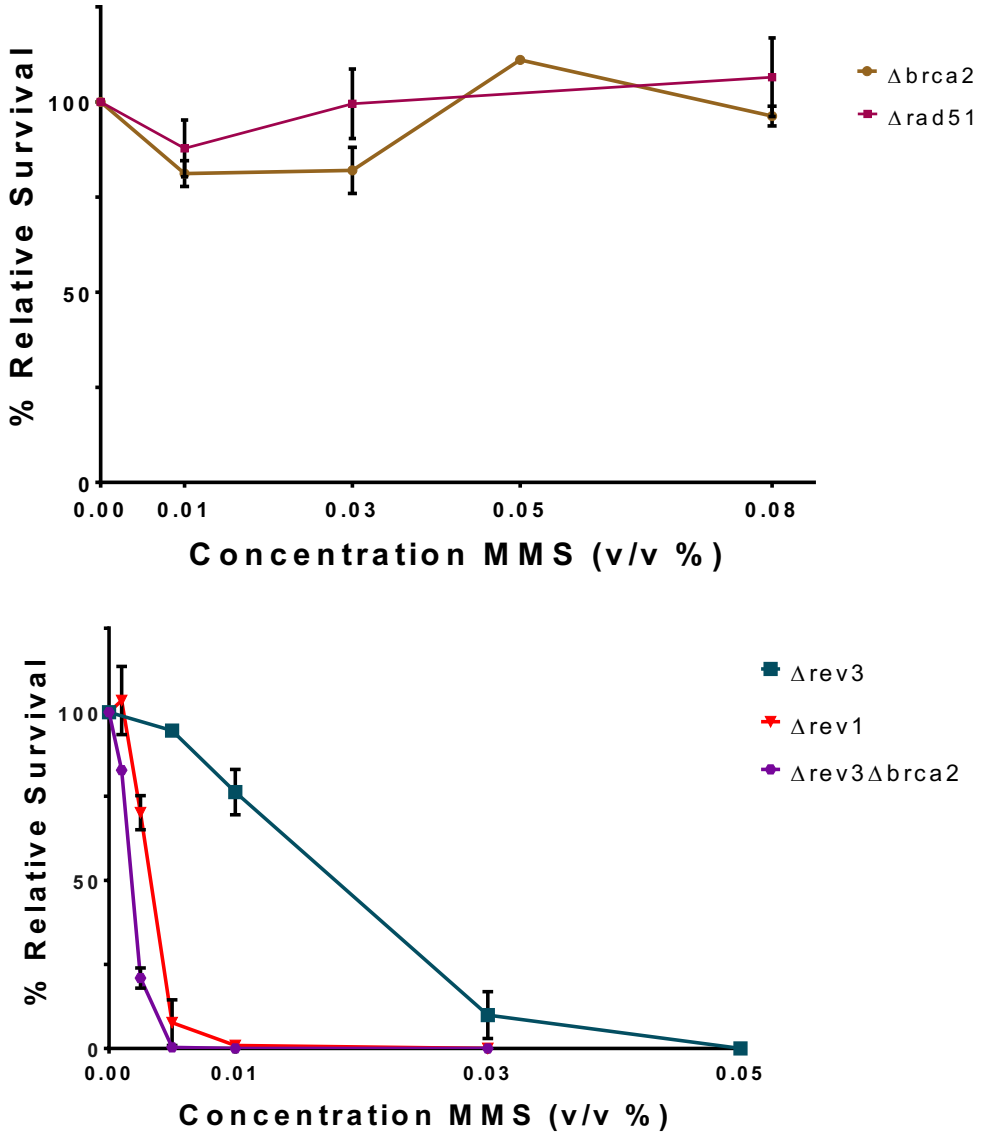

Figure 10: HR-mediated TS is likely the backup pathway of DDT. Relative % survival measured by comparing number of heterozygous and homozygous adults that survived to adulthood after embryonic treatment with varying concentrations of MMS. Top: sensitivity of HR-associated BRCA2 and Rad51 knockouts. Bottom: sensitivity of DDT deficient Rev3, BRCA2 double knockout in comparison to complete Rev1 knockout and Rev3 knockout (V. Khodaverdian, unpublished) (figure courtesy of V. Khodaverdian).

From these findings, we have generated a model for coordination of DDT and the involvement of Rev1 in both TLS and TS. After a replication fork has stalled, the initial signaling mechanism will be the mono-ubiquitination of PNCA by the Rad6-Rad18 ubiquitin conjugating enzymes. After mono-ubiquitination of PCNA, Rev1 localizes to the site of the fork stalling and recruits pol ζ to perform lesion bypass. Alternatively, if the cell is unable or conditions are unfavorable, the SHPRH-associated ubiquitin conjugating machinery will facilitate the poly-ubiquitination of PCNA again causing Rev1 to localize at the site of the replication fork stalling (Figure 11).

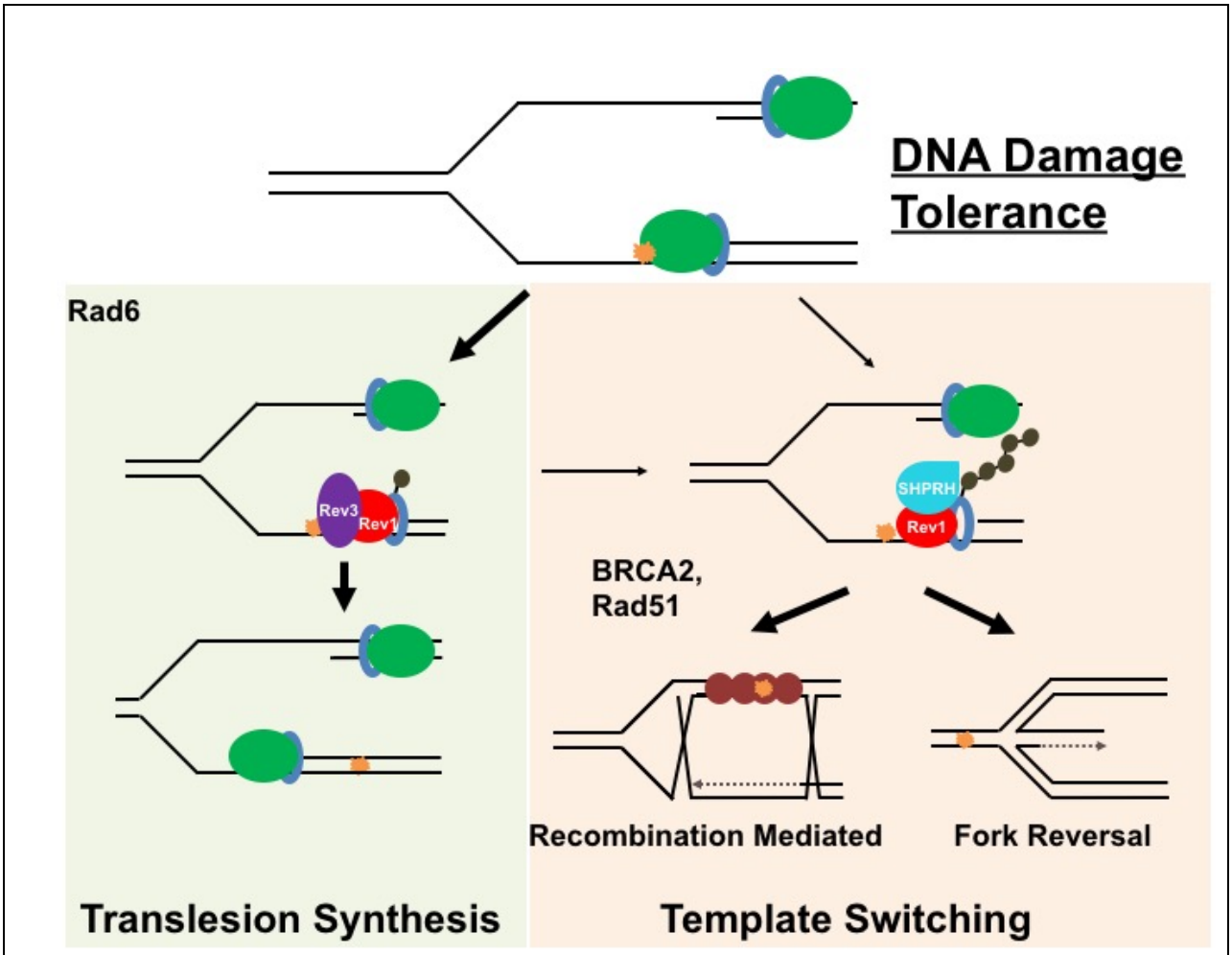

Figure 11: Model for the coordination of DDT and role of Rev1 in both pathways in *Drosophila* Top: DNA lesion, in yellow, encountered by replication machinery on leading strand. Bottom left: PCNA is mono-ubiquitinated via action of Rad6-Rad18 ubiquitin ligase complex, recruiting Rev1 and Pol ζ to bypass the lesion. Bottom right: SHPRH and ubiquitin-

conjugating complex extend the ubiquitin chain, recruiting Rev1 to the fork. Lesion is bypassed via a BRAC2, Rad51 dependent recombination mechanism or a reversed fork structure (figure courtesy of V. Khodaverdian).

Though this previous work from our lab provides an exciting and novel framework for the coordination of the DDT pathway and players involved in *Drosophila*, much remains to be understood. The most pressing question to be addressed is determining the exact role of Rev1 in the template switching pathway. As this phenomenon has not yet been seen in the literature, the first step to understanding this mechanism would be clarifying the specific interacting partners of Rev1 in the context of TS. With this idea in mind, this study involves the design, creation and utilization of a genetic construct that will allow for the identification of Rev1 interacting partners during both pathways of DDT. The ultimate goal of this endeavor is the development of a more specific model of Rev1 function in the template switching pathway of DDT. We are also hoping to understand the coordination in DDT pathway choice in cultured cells in order to determine if the phenomenon we have uncovered is specific to regulation of an entire organism.

Materials and Methods

Generation of Epitope-tag Gateway vector for integration into *Drosophila* genome

To stably integrate a Rev1-tagged transgene into the genome of *Drosophila melanogaster* a modified form of the pattB genome integration plasmid was created. The attB site on this plasmid is part of the PhiC31 integrase-mediated system for creating transgenic lines used by BestGene Inc. In this system, the bacteriophage PhiC31 integrase will facilitate sequence-specific and irreversible integration of sequence. This integration occurs between a bacterial attachment site sequence on a plasmid (attB) and a phage attachment site sequence (attP) within the genome of *Drosophila*. The pattB vector contains the *w+* gene for red eye color so stable integration of target sequence can be tracked phenotypically (BestGene Inc). Segments of an

epitope tag-containing Gateway vector were added to a pattB backbone to create a universal vector for integrating a tagged sequence into the *Drosophila* genome. Gateway vectors were products of the Drosophila Gateway Vector Collection (Carnegie Science). Segments of the pPWF and pPFMW vectors from this collection were added into the pattB backbone. The pPWF vector contains a C-terminal 3xFLAG while the pPFMW contains a N terminal 3xFLAG6xMYC tag (see Fig. 14 for plasmid maps). The Gateway vectors have two attR sites flanking the sequence of ccdB, which codes for a compound that is toxic to *E. coli*. The Gateway vector can react with another plasmid containing attL recombination sites (Gateway entry vector) so that the att sites recombine, switching the coding sequences between the att sites in each vector. In addition to the traditional antibiotic resistance selectable markers, the Ccdb gene serves as an additional selectable marker that is lost upon successful recombination between these two sites. To build the combined pattB-gateway vector, primers flanking the desired sequence on the Gateway vector were designed with restriction sites at their ends (see Supplementary for primer sequence details). These restriction sites corresponded to sites also present on the pattB plasmid. The sequence amplified from the Gateway vector included the UASp promoter, both selectable markers, att sites, ccdB, chloramphenicol resistance and transcriptional termination sequence (Figure 12).

Primer set NsiI-UASpF and BglII-pPFMGWR was used to amplify the N-terminal tag vector and BglII-UASpF and Acc65I-pPGWR to amplify the C-terminal tag vector. Midi-prep purified pPFMW and pPWF vectors were used as a template with corresponding primer sets in a 50μL Q5 PCR reaction (New England Biolabs). PCR reactions were verified by gel electrophoresis and PCR purified using the Nucleo-Spin Gel and PCR Clean-up Kit and protocol (Macherey-Nagel). PCR products were digested with restriction enzymes corresponding to the

sequences added by the primer sets; pPWF PCR product was cut with BglII and Acc65I and the pPFMW PCR product was cut with BglII and NsiI. Digestions were carried out with appropriate NEB enzyme buffers at 37°C for 1 hour. Digested PCR products were purified again using the Nucleo-Spin Gel and PCR Clean-up Kit. The pattB vector was purified via standard minprep protocol from laboratory stocks and digested with either one of the enzyme pairs (BglII and Acc65I, BglII and NsiI). Purified pattB DNA was digested with each enzyme set at 37°C overnight and digestion was visualized via gel electrophoresis. Digested pattB vector bands were excised from the gel and purified using the Nucleo-Spin Gel and PCR Clean-up Kit and gel purification protocol. The digested vector was phosphatase treated with Antarctic phosphatase (New England Biolabs) at 37°C for 20 min. The reaction was stopped by heating to 65°C for 6 minutes.

Ligations of digested vector and insert were set up at 4°C overnight in ratios of 1:1, 3:1 and 5:1 (insert: vector). The ligations were halted through heat inactivation at 65°C for 6 minutes. 1.5 µl of each ligation reaction was transformed into 50µl of chemically competent cells resistant to ccdb (T1R cells, Invitrogen). 1.5µl of ligation reaction was added to the competent cells and then placed on ice for 30 minutes, heat shocked for 30 seconds at 42°C and put on ice for 1 minute. 250µl of SOC media was added to the cells and they were spun at 37°C for 1 hour before being plated on agar containing both ampicillin and chloramphenicol. Plates were left at 37°C overnight. Colonies were grown up in overnight cultures containing 2mL of LB broth, ampicillin and chloramphenicol at 37°C overnight. DNA was extracted using standard miniprep protocol. To ensure that the ligation was successful, both a diagnostic digest and PCR reaction were performed on DNA purified from each colony. At least one successful isolate from both the

N and C terminal tag vector reactions was obtained. These samples were then sequenced by Sanger sequencing (Eton Biosciences).

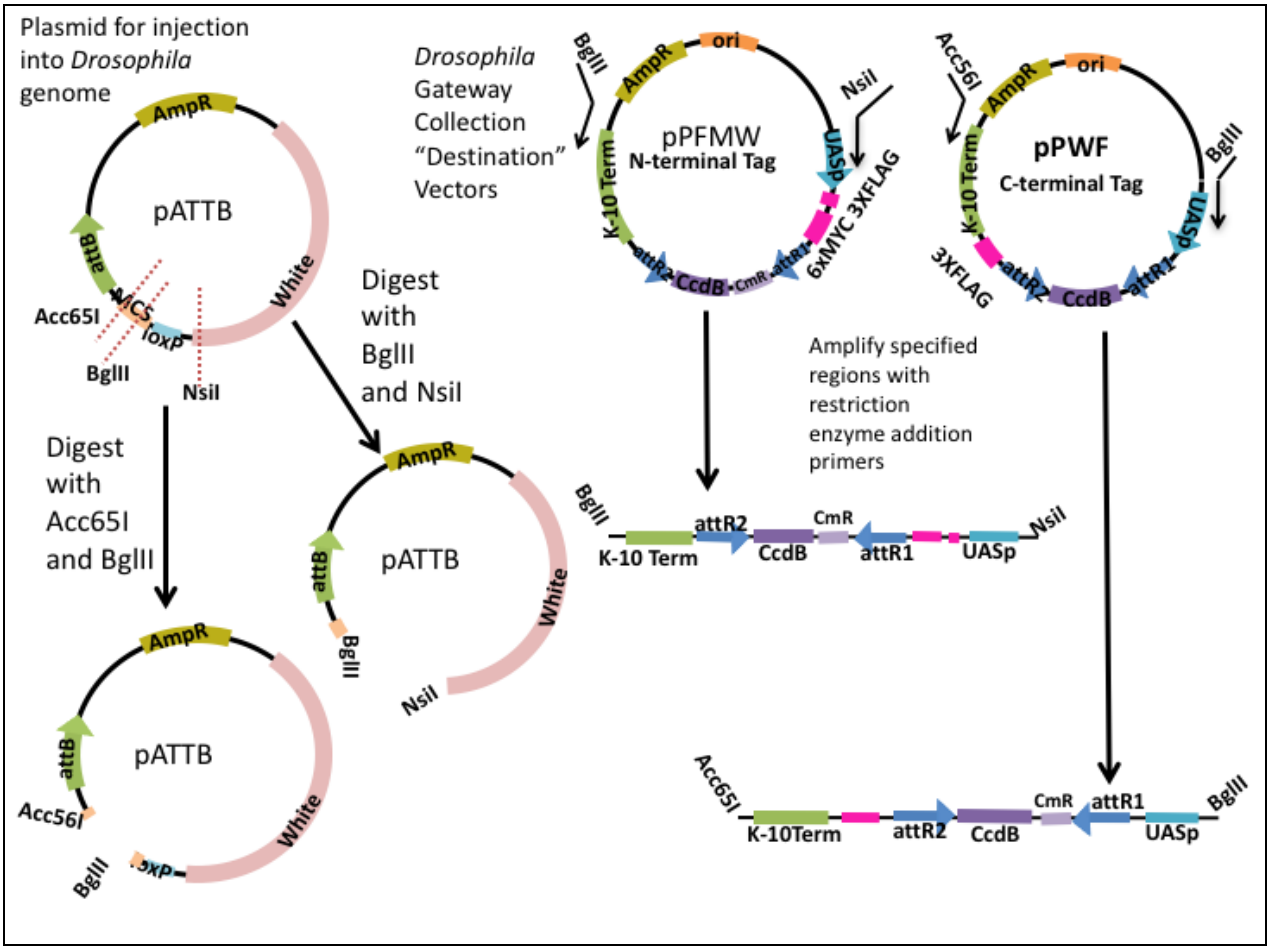

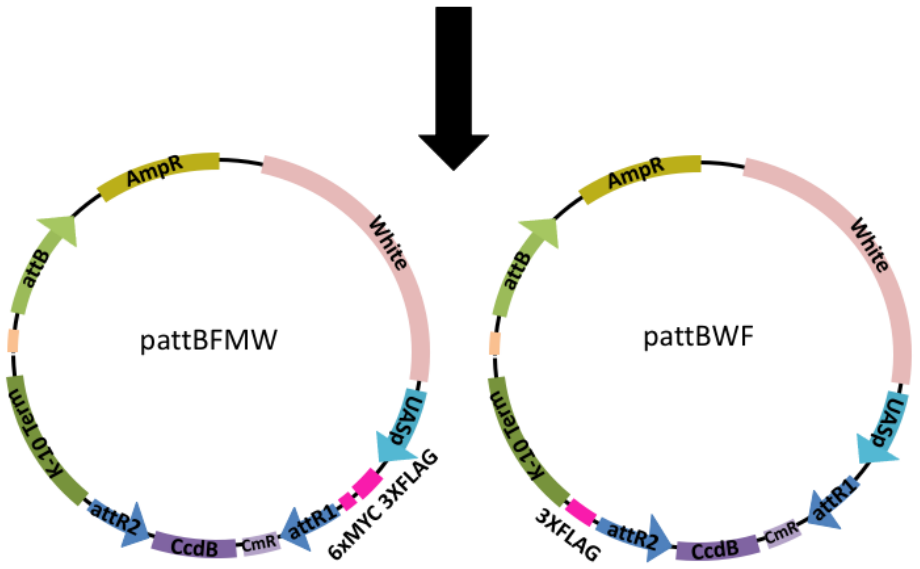

Figure 12: Schematic for creation of Gateway integration vector and plasmids for injection into *Drosophila* genome. pattB vector contains an ampicillin resistance gene, an attB integration site, a multiple cloning site (MCS), a loxP recombination site and a copy of the *Drosophila white* gene. To generate the pattBWF vector, pattB was digested with Acc65I and BglII for ligation of Gateway vector insert. Primers Acc65I_pPGW_R and BglII-UASpF were used to amplify desired region of the pPWF vector while adding the corresponding restriction sites. Digested pattB vector and digested pPWF insert were ligated using T4 ligase. Similarly, to generate the pattBFMW vector, pattB was digested with BglII and NsiI. Primers Nsil-UASpF and BglII-pPFMGW R were used to amplify desired region of pPFMW vector. Digested vector and insert were combined using T4 ligase.

Generation of pCR8 [Rev1] Gateway Entry vectors

To generate Rev1 sequence for insertion into a Gateway entry vector, a Q5 PCR reaction (New England Biolabs) was used to amplify from plasmid pTV [Rev1] (V. Khodaverdian). Primers were designed to amplify either the complete wild type sequence or a C-terminal domain truncation of the sequence (ΔCTD). All PCR reactions were performed using the same forward primer, Rev1_79F. To amplify the wild type Rev1 sequence Rev1_3432R was used to add a stop codon to the end of the sequence and Rev1_3429R was used to create sequence without a stop codon. To create the ΔCTD sequence with a stop codon Rev1_3236R was used and without a

stop codon, Rev1_3233R was used (Supplementary Table 1 for primer details). The PCR products that included the stop codon were used for combination with the N-terminal tag while the products without the stop codons were used for combination with the C-terminal tag. Each PCR product was verified via gel electrophoresis and purified using the Nucleospin Gel and PCR clean up kit, PCR purification protocol. Single stranded adenine overhangs were added to the end of the PCR products; each PCR product was mixed with Taq polymerase, dNTPs and buffer and incubated at 37°C for 1 hour. 4 µL of the PCR product with A-overhang was added to 1µL of linearized pCR8 Gateway entry vector along with 1µL of salt solution and incubated at room temperature for 1 hour (Figure 13). 4µL of this reaction was then added to 50µL of One-shot Top10 chemically competent cells (Thermo Fisher). After addition of the vector reaction, the cells were placed on ice for 30 minutes, at 42°C for 30 seconds and back to ice for 1 minute. 250µL of SOC media was added to the transformed cells and they were spun at 37°C for 1 hour. 100µL of transformed cells were plated on LB agar with spectinomycin to select for successful transformants and left at 37°C overnight. Single colonies were selected and grown in overnight cultures of LB broth and spectinomycin. DNA was extracted using standard miniprep protocol. Successful integration of the Rev1 sequence into the pCR8 vectors was confirmed via restriction digest. The Rev1 coding sequence of each isolate confirmed by Sanger sequencing. Two isolates of each correct clone were used to create a glycerol stock and stored at -80°C.

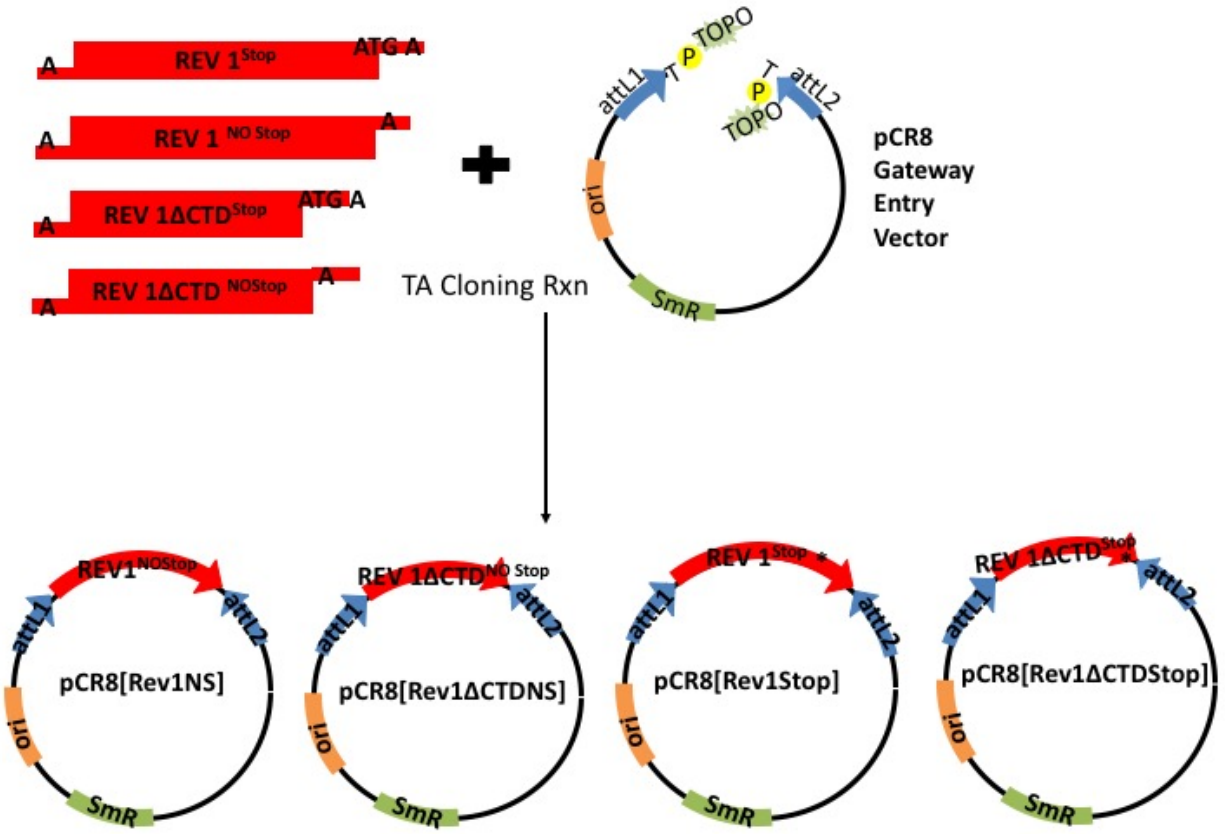

Figure 13: Schematic of cloning scheme for Gateway Entry vector. The pCR8 vector contains a spectinomycin resistance gene, an origin of replication and two attL sites. The ends of the linearized plasmid are bound by a topoisomerse enzyme at a single-stranded T overhang which will react with the single stranded A overhang on the PCR products, facilitating integration into the entry vector. 4 constructs were created at this step: pCR8[Rev1^{stop}], pCR8 [Rev1$^{No\ Stop}$], pCR8 [Rev1ΔCTD^{stop}], pCR8[Rev1ΔCTD$^{No\ stop}$]. Vectors containing Rev1 with a stop codon were used along with the N terminal tag while those without the stop codon were used for the C terminal tag.

Gateway Cloning of pCR8-Rev1 entry vectors into Epitope-tag integration vectors.

To add the Rev1 sequence to the Gateway integration vector, pattBFMW or pattBWF vectors and appropriate Rev1-containing pCR8 vectors were combined with TE buffer (pH 8) and 2µL of clonase II enzyme mix (Thermo Fisher) and incubated at 25°C for 1 hour (Figure 14). The reaction was stopped by incubating at 37°C with 1µl of proteinase K. 4µL of each Gateway reaction was added to 50µL of Top10 One-shock chemically competent cells (Thermo Fisher)

and incubated on ice for 30 minutes. To transform the cells they were heat shocked at 42°C for 30 seconds and put on ice for 1 minute. 250µL of SOC media was added to each transformation before spinning at 37°C for 1 hour. Cells were plated on LB agar with ampicillin and left at 37°C overnight. Colonies were grown overnight in LB broth with ampicillin and then DNA was extracted using standard miniprep protocol. Clones were then verified using restriction digest and PCR amplification of vector and insert junction regions. Plasmid DNA was verified via Sanger sequencing (Eton Biosciences).

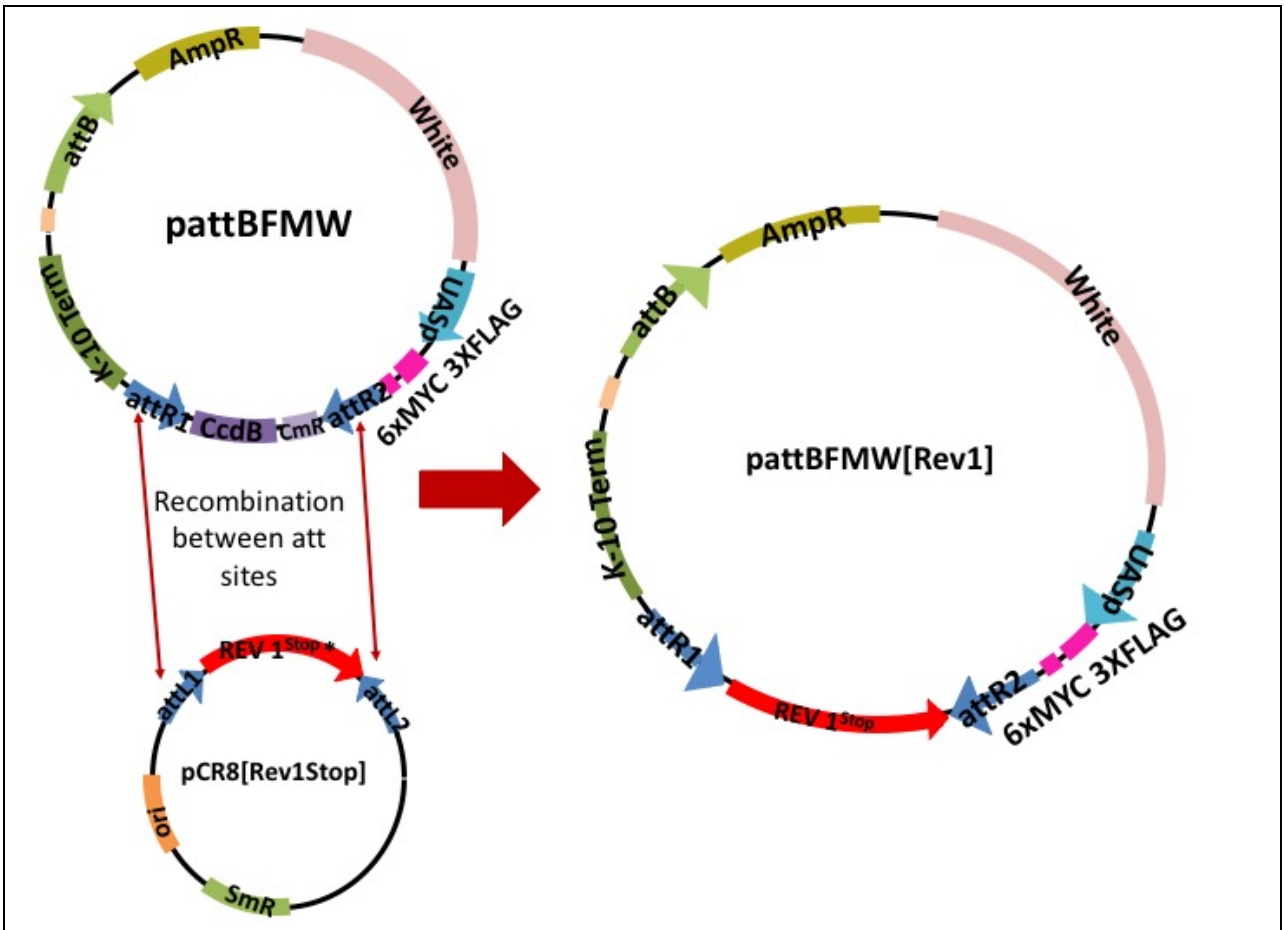

Figure 14: Gateway reaction to create Rev1-tag integration vectors. The final step in the generation of the Rev1-tag integration construct was the combination of the generated pCR8 entry vectors with the pattBPWF or pattBPFMW integration-Gateway vectors. This reaction was facilitated by a Gateway-specific clonase enzyme that mediates recombination between the att sites. This recombination essentially switches the coding sequence between the two sites in each vector and the ccdB should prevent any pCR8 vectors that have successfully recombined or any

pattBFMW vectors that have unsuccessfully recombined from growing, making the selection of clones after this reaction very efficient.

Integration of Rev1 tagged sequence into *Drosophila* genome.

The cloned Rev1 tag sequence was injected into *Drosophila* embryos by BestGene Inc. Confirmed cloned plasmids were prepared via standard midiprep protocol and sent to BestGene for injection. The constructs were inserted into *Drosophila* embryos of genotype y^1 w^{1118}; PBac{y^+-attP-9A}VK00005 allowing for the integration of the construct on the right arm of the third chromosome at cytological location 75(A10). Successful integration at this locus confers orange eye color as a selectable marker.

Fly DNA preparation

Single flies from desired samples were collected in 0.5 mL tubes and put at -20°C for 15 minutes. Frozen flies were then mashed using a pipette tip containing a mix of 50 μL of squishing buffer (SB) and 1μL of Proteinase K (10 mg/mL). SB is 10 mM Tris-Cl with a pH of 8.2, 1mM EDTA, and 25mM NaCl. The mashed fly and solution are incubated at 37°C for 30 minutes. To deactivate the Proteinase K, the samples are incubated at 95°C for 1-2 minutes.

***Drosophila* stocks**

This study used a stock of *Drosophila,* y^1 w^**; P{Act5C-GAL4}25FO1/CyO,* y^+ (Bloomington) as the source of Gal4. A stock of *Δrev1 Drosophila* created by our lab (V. Khodaverdian), *rev1*^{5}*/TM3, ser, w+* was used throughout. Stocks of double balancer flies, *TM3, Ser, w+ / TM6B, Tb, Hu* (Bloomington) were also used.

PCR amplification of injected transgenes

Primers specific to each tag sequence were designed and used in PCR amplification of injected constructs, specifically the junction of Rev1 and tag coding sequence. To amplify the

3xFLAG-6xMYC-Rev1 sequence, primer FLAG_MYC_expressF was paired with Rev1_363 R to produce a 698 bp product in the full length Rev1 and ΔCTD variants. To amplify the Rev1-3xFLAG sequence, primer 3xFLAG express R was paired with Rev1_2023 F to produce a 946 bp product in the ΔCTD variants and a 1391bp product in the full-length variants.

RNA isolation and RT-PCR

All RNA extractions were performed using a Nucleospin RNA extraction kit and protocol (Machery Nagle). For RNA extraction on Kc167 cells, cells were first collected in 1.5mL Eppendorf tubes and spun at 3,000 rcf for 3 minutes. Supernatant was removed and cells were stored at -80°C until ready for use. For RNA preparation from whole *Drosophila*, 4 flies were collected and frozen at -20°C. The frozen flies were pulverized using liquid nitrogen and a pestle. The RNA extraction was then completed following the kit protocol. cDNA was made from each RNA sample using the ProtoScript First Strand cDNA Synthesis Kit and protocol (New England Biolabs). From each cDNA sample, a PCR reaction was performed with primers specific to transcripts of interest.

Western Blotting

All western blotting was performed on samples prepared from whole flies. All flies were frozen at -20°C before preparation. Samples were prepared one of two ways, disruption via sonication or via mashing with liquid nitrogen. For purification via sonication, flies were first mashed with a pestle in 100 μL of 20% TCA and then sonicated for 5 cycles of 30 seconds of sonication and 30 seconds to cool. Samples were then spun at 3000 rcf for 10 min at 4°C and supernatant was then removed. The remaining protein pellet was combined with 100μl of 1X Laemmli buffer (50% 2X Laemmli buffer, 5% β-Mercaptoethanol) and 25μL of 2M Tris.

Samples were then boiled for 5 minutes and stored at -20°C until use. Alternatively, samples were mashed in the presence of liquid nitrogen creating a fine powder before the addition of 20% TCA. These samples were not sonicated but then spun at 3000 rcf for 10 minutes at 4°C. Supernatant was removed and the pellet was resuspended in 1X Laemmli buffer and 2M Tris, as described previously. Samples were either run on either 8% or 6% polyacrylamide gels. To prepare the gels, 16 mL of solution was prepared (8mL per gel). 8% polyacrylamide was 6.5 mL water, 6 mL of 1M Tris at pH 8.8, 3.2 mL of 40% polyacrylamide, 160 μL of 10% SDS, 160 μL of 10 X ammonium persulfate (APS) and 16 μL TEMED. 6% polyacrylamide was 7.3 mL water, 2.2 mL of 40% polyacrylamide, 6mL of 1M Tris pH 8.8, 160 μL of 10% SDS, 160 μL of 10X APS and 16 μL TEMED. After polyacrylamide gel was solidified, staking gel was added to the top of the gel. Stacking gel was 5.8 mL water, 1.5 mL 40% acrylamide, 2.5 mL Tris pH 6.7, 100μL 10% SDS, 100μL 10X APS and 10μL of TEMED. For 8% polyacrylamide gels, 15 μL of sample was run for 3 hours while for 6% polyacrylamide gels, 30 μL of sample was run for 2 hours, both at 100 volts and in 1X Laemmli buffer. 10X Laemmli buffer was 30.24g Tris base, 144.2g glycine, 10g of SDS and water to 1L. Samples were transferred from the polyacrylamide gel to a nitrocellulose membrane using 1X transfer buffer for 1 hour at 0.4 A. 10X transfer buffer was made with 1L of water, 33.5g Tris base and 144g glycine. After membrane transfer, membrane was blocked for 1 hour with 5% milk in 1X TBS. 10X TBS (Tris-buffered saline) was 24g of Tris base and 88g NaCl in 1L of distilled water. Membranes were then incubated with 1:2000 anti-FLAG primary antibody (Sigma) in BSA overnight. After incubation with primary antibody, the membrane was washed 4 times with 1X TBST, 5 minutes for each wash. 1X TBST was 50mL 10X TBS, 447.5 mL water and 2.5 mL Tween 20. After washes, membrane was incubated with secondary antibody anti-rabbit-HRP (Promethius Protein Biology Products) in

5% milk in TBS. 2uL of anti-HRP was added to 40mL of 5% milk in TBS. Membranes were rocked in secondary antibody for 1 hour. ProSignal Pico Chemiluminiscent HRP Substrate (Promethius Protein Biology Products) kit was used to visualize the blot.

To strip blots and re-probe with anti-MYC antibody (abcam), membrane was covered in mild stripping buffer (for 1L, 15g glycine, 1g SDS, 10ml Tween 20 with pH 2.2 in water) and incubated for 5-10 minutes. Buffer was discarded and incubated for another 5-10 minutes in fresh stripping buffer. Membrane was then washed twice with 1X PBS for 10 minutes each wash and the twice with 1X TBST for 5 minutes each wash. The membrane was blocked in 5% milk in TBS for 1 hour and then incubated with primary antibody anti-MYC (abcam) at 1:1000 in 5% milk in 1X TBS overnight. The next morning, the membrane was washed four times with 1X TBST for 5 minutes each wash and then incubated with secondary antibody anti-rabbit-HRP at 1:20000 in 5% milk in 1X TBS. The membrane was washed 4 times in 1X TBST and then imaged using the ProSignal Pico kit as described above.

Generation of *Rev1-tag, Δrev1* mutants

To create Rev1-tag, *Δrev1* double mutants, males homozygous for the Rev1-tag transgene were crossed to females with the Rev1 deletion (*Δrev1*). The Rev1-tag allele was phenotypically tracked via its orange eye color. The *Δrev1* flies were heterozygous as they also had a phenotypically-marked balancer chromosome, *TM3, Ser, w+* which gives them red eyes and a serrated wing phenotype. From this cross, females with one Rev1-tag allele and one *Δrev1* allele were collected; these flies were selected from all the possible progeny based on their orange eye phenotype and normal wing phenotype. These females were then crossed to males with two balancer chromosomes *TM3, ser, w+* and *TM6B, Tb, Hu*. From this cross, males with orange eyes were selected and each male was crossed separately to double balancer females

(*TM3, Ser, w+ / TM6B, Tb, Hu)*. Each single male was removed from its respective cross after 5 days and prepared as detailed in the Fly DNA Preparation section. PCR reactions were performed on each single male with two different primer sets corresponding to the Rev1 deletion. Rev1 -250F and Rev1 5438R both flank the deletion and should give an approximately 2kb product if the deletion is present and should not amplify in absence of the deletion. Rev1_del5pF and Rev1_5438 R should amplify an approximately 750bp product if the deletion is present. Progeny of the single male crosses with the Rev1-tag, *Δrev1* allele were selected for the *TM3, Ser, w+* balancer chromosome and were crossed to one another to maintain a stock of these mutants.

The standard process for setting up and maintaining *Drosophila* crosses like the ones described above is as follows. To cross *Drosophila* of differing genotypes, males of one genotype and virgin females of the other genotype were collected and combined in vials containing food. Female *Drosophila* are unable to reproduce until approximately 8 hours after they eclose so if bottles are sorted every 8 hours, all females collected can be assumed to be virgins. Anywhere from 5 to 20 total flies are combined in a vial of food and left in a 25°C, humidity and light controlled environmental room. After approximately 3 days, the mated flies are transferred into another vial where the females will continue to lay eggs in the food. This process is repeated approximately 5 times until the females' reproductive capabilities have been exhausted. 10 days after the initial cross or after transferring the parental generation into a new vial, the next generation of progeny will begin to eclose and can be screened based on phenotypic markers.

Kc167 Cell Lines

In this study, the *Drosophila* Kc167 embryonic cell line was utilized. Cells were provided courtesy of Dr. Irene Chiolo at University of Southern California. Cells were cultured in TNM-FH media with 5% FBS and grown in 250 mL tissue culture flasks. Cells were passaged every 5 days and resuspended as 3 $x10^6$ cells.

Kc167 cells RNAi

To prepare RNA for Kc167 cell knockdown, a Q5 PCR reaction was used to amplify actively transcribed regions of each gene to be knocked down. These regions were chosen based on information provided by the Drosophila Genome Resource center (DGRC). Primers with T7 transcription start site flaps were designed to flank these regions and were used to amplify them in a Q5 PCR reaction using *Drosophila* genomic DNA as the template sequence. See primer table in supplementary figures for primer specifics. Primers were designed to create knockdown of transcript of Rev1, BRCA2, mus205 (Rev3), SHPRH, spnA and Brown. For Rev1, BRCA2 and SHPRH, two primer sets were designed. The products of the Q5 PCR were first confirmed via gel electrophoresis and then used in the MEGAscript Kit for generation of RNA (ambion) protocol. 1-8μL of PCR reaction was used for each RNA-generating reaction. RNA was stored at -20°C until ready for use.

RNAi was performed on Kc167 cells in either 24, 48 or 96 well plates. Cells were at optimal confluence for treatment with RNA 2 days after being passaged. For 24 well plates, the total volume of each well was 250 μL with a concentration of $2x10^6$ cells/mL, for 48 well plates the total volume was 125 μL with a concentration of $2x10^6$ cells/mL, for 96 well plates, total volume was 100 μL with a concentration of $5x10^5$ cells/mL. Cells were removed from the bottom of the culture flasks with a single sharp tap of the flask against a hard surface. Once most cells had been removed from the bottom of the flask and were suspended in the media, the

contents of the flask were spun down for approximately 10 minutes at no more than 2,500 ω until a large pellet was visible. Media above the pellet was removed until approximately 5mL remained and the pellet was re-suspended in the remaining media. 10μL of these resuspended cells were added to 190μL of Trypan blue and placed into a hemocytometer where living cells were counted and used to calculate the corresponding concentration of cells in the sample. An appropriate volume of the measured sample of cells was added to enough media to fill the desired number of wells in the plate. Once aliquoted into individual wells, the cells in media were left to adhere to the bottom of the plate for 20 minutes before adding RNA.

For 24 well plates, 15μg of RNA was added to each well, and 30μg was added for 48 and 96 well plates. Appropriate amounts of RNA, based on concentration of stock solutions, were added to 2X HBS to bring the reaction to 35-37μL. Additionally, in a separate tube, DOTAP was added to 2X HBS so that the volume of DOTAP would be 3% of the total well volume and, after addition of HBS, the mixture would be 5% of the total well volume. The RNA and 2X HBS were then mixed with the DOTAP solution. This mixture would serve as the master mix for all wells receiving that type of interfering RNA. From every well that was receiving a specific RNA treatment, half of the volume of cells was removed and added to the appropriate RNA, DOTAP and HBS mixture. The mixture was mixed vigorously via pipetting and an appropriate amount of the RNA mixture was added back to the wells, so that each well received the same volume of cells and RNA. Plates were incubated until ready to be collected, treated or analyzed.

RNAi and MMS Sensitivity Assays in Kc167 Cells

For this study, all RNAi assays were set up in 96 well plates (see above). Three days after initial RNA knockdown, cells were treated with varying concentrations of MMS (0.005%, 001%

and 0.03% or 0.003%, 0.005% and 0.01%). MMS solutions were made from 1% MMS stock solution and 12.5µL of MMS solution in sterile, pico-pure water was added to each well. For each 96 well plate three wells of each knockdown type were treated with each MMS concentration and three wells were given 12.5µL of media as a control. 3 days after MMS treatment, cell survival was measured using an MTS Cell Proliferation Kit and protocol (abcam). 15µL of MTS reagent was added to each well and the plate was incubated at 37°C for 1 hour after which the optical density of each well was measured at 490nm. As a control for background optical density of the media itself, 15 µL of MTS reagent was also added to a well with just media. Before any calculations were performed the background optical density of the media was subtracted from measured optical density values. The relative percent survival was calculated by comparing survival of cells treated with MMS to the untreated wells within RNA knockdown type (Figure 15).

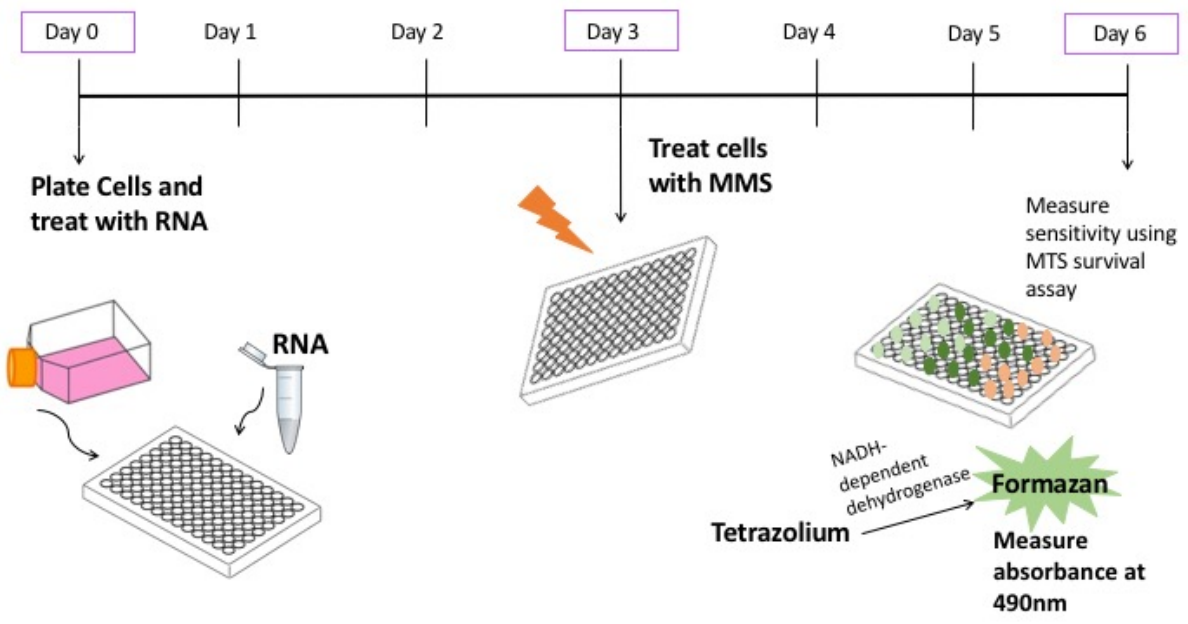

Figure 15: Protocol for determining MMS sensitivity of Kc167 cells after RNA knockdown. Two days before cells were plated in a 96-well plate they were passaged into a new tissue culture

flask. On day 0 they were treated with 15μg of RNA and incubated until day 3 when they were treated with varying concentrations of MMS. On Day 6 MTS reagent was added to each well and optical density was measured to assess survival post treatment.

Results:

Establishing a protocol for RNAi knockdown in Kc167 Cells

Our work with Drosophila tissue culture was primarily driven by our interest in determining DDT pathway hierarchy, as our previous work with MMS sensitivity in whole *Drosophila* provided evidence that TLS serves as the primary DDT mechanism and TS as the back-up (Figure 10). Also, since our previous work in whole *Drosophila* indicates that Rev1 is involved in the TS pathway of DDT, a phenomenon not seen amongst the other single-cellular systems, we were interested in determining if this role of Rev1 was specific to the more complex regulatory systems of a whole organism. In order to answer these questions, we used *Drosophila* cell lines in MMS sensitivity assays after knocking down genes of interest via RNAi. Specifically, we were interested in comparing the sensitivity of cell lines to MMS after knocking down genes that had been tested for sensitivity in the whole fly, notably mus205 (Rev3), BRCA2, SHPRH, SpnA and Rev1.

In order to establish the appropriate timing of Kc167 cell MMS treatment post RNA knockdown, we set up a time-course knockdown experiment. Using the protocol described in materials and methods, we set up 24-well plates of Kc167 cells; each row represented a different knockdown type and each column a different day post RNA treatment. Starting one day post initial RNA treatment, we removed and froze down cells from one column of each RNA treatment type. 6 days post RNA treatment, all samples were collected and we performed a RT-PCR on each knockdown type for each day post-treatment. Our initial trial of this assay was with only mus205 (Rev3) knockdown. Results indicated that knockdown was complete enough to

treat cells with MMS 3 days post-initial RNA treatment but that knockdown was no longer complete after day 4 (Figure 26) as the m205-specific PCR amplified bands in the samples from days 4 and 5 post knockdown. We would expect to see m205 RNA on day 1 post knockdown as this is likely not enough time for complete knockdown of endogenous transcript, but the absence of amplification here is likely not due to failed PCR or lack of RNA used in the reverse-transcriptase reaction as the corresponding positive control reaction (Figure 27, left) produced noticeable amplification of the cDNA sample. This could be explained by low levels of mus205 transcript in the cell on day 0, though if this were the case, it may also make it difficult to determine if knockdown on days 1-3 is efficient.

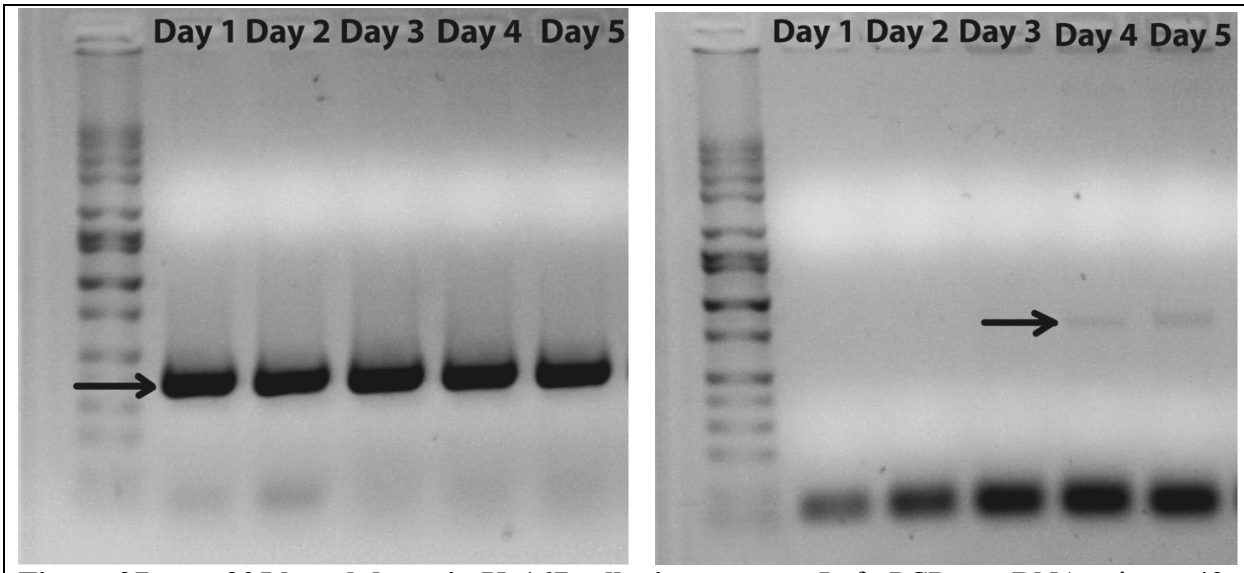

Figure 27: mus205 knockdown in Kc167 cells time-course. Left: PCR on cDNA using rp49 primers. These reactions serve as positive controls for the corresponding m205 reactions; banding in these samples indicates that there is an appropriate amount of cDNA present. Right: Each lane represents the RT-PCR performed from RNA samples extracted each day after initial RNA treatment, as described in materials and methods.

After this trial, we felt comfortable doing MMS sensitivity assays on the Kc167 cells as described in materials and methods, with MMS treatment coming 3 days after initial RNA knockdown.

In order to determine if the other RNA types had a similar knockdown efficiency to mus205, a time-course knockdown was performed with all RNA types (Rev1, BRCA2, mus205, SHPRH, spnA, Brown). In this trial, though, only the RNA extracted from the Rev1 knockdown was sufficient to complete a RT-PCR (Figure 28). From this trial, it appears that Rev1 is not knocked down at all until 4 days after RNA treatment and even then some trace amounts of Rev1 transcript remain.

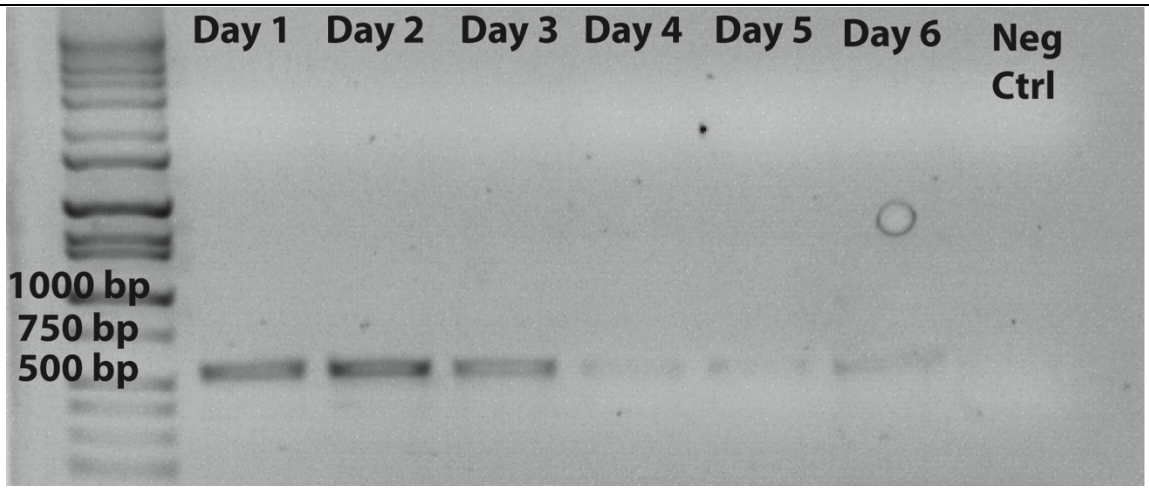

Figure 28: Rev1 knockdown in Kc167 cells time-course. Each lane represents the RT-PCR performed from RNA samples extracted each day after initial RNA treatment, as described in materials and methods.

After these separate trials, it appears that RNA knockdown efficiency varies between the different RNA types and that the ideal time for MMS treatment may therefore vary depending on what is being knocked down.

Kc167 cells exhibit no specific sensitivity to MMS after RNA knockdown

We measured the sensitivity of Kc167 cells to MMS after RNA knockdown in two separate trials, using slightly different concentrations of MMS for each trial. In our initial trial, we treated cells with 0.003%, 0.001% or 0.01% MMS (Figure 29**).** After this trial, no noticable pattern in sensitivity of Kc167 cells post knockdown was apparent, with little variation from the

control, Brown, at all MMS concentrations. As Brown is an eye color gene and therefore not involved in lesion bypass, it was expected that the other knockdown types would display noticably more sensitivity at all concentrations of MMS. In our second trial of this assay, we used higher concentrations of MMS, in an attempt to distinguish differential sensitivities of the knockdown types not seen at lower doses (Figure 30). This trial was consistent with the previous trial, except for the BRCA2,m205 knockdown which appears to have moderately increased sensitivity at all conentrations of MMS. Though these results may indicate that DDT regulation and pathway choice in response to MMS differs from that seen in whole *Drosophila*, it is more likely that issues with the RNA knockdown protocol, discussed above, are confounding these findings. It sems that a more refined RNA knockdown protocol and more trials of the MMS sensitivity assay are necessary before a definitive conclusion can be made about DDT heirarchy in *Drosophila* Kc167 cells.

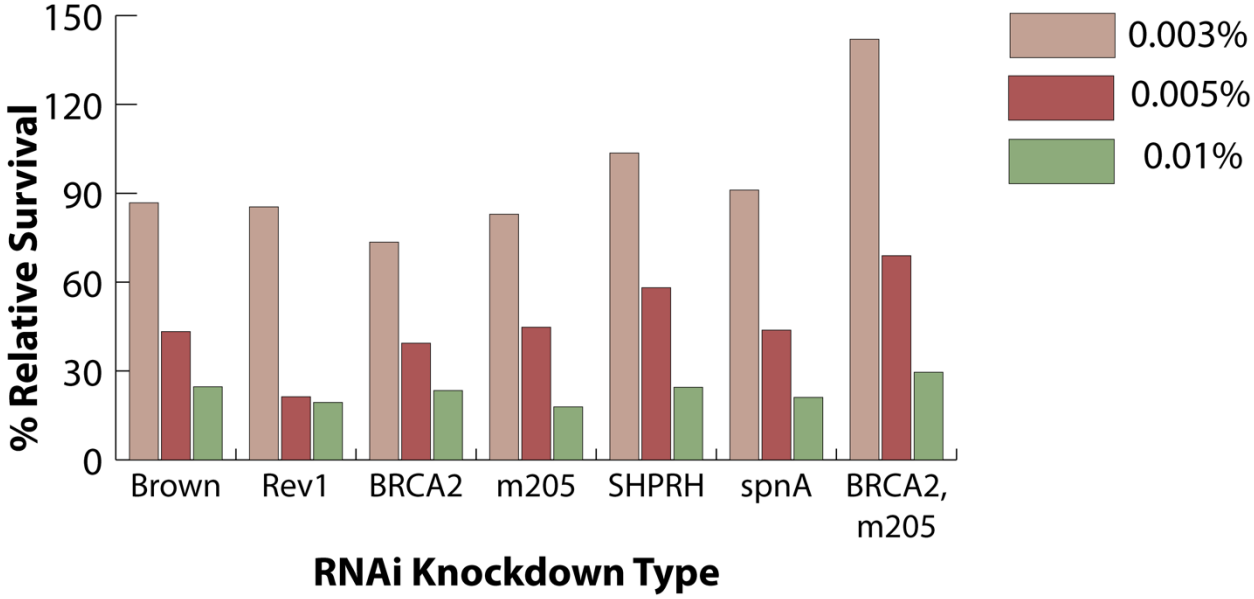

Figure 29: Kc167 cell sensitivity to MMS post RNA knockdown at 0.003%, 0.005% and 0.01% MMS. Kc167 cells were treated with the varying concentrations of MMS 3 days after initial RNA knockdown. Cell surivial was measured 3 days after MMS treatment via the MTS proliferation assay and surivial was based on the optical density of each well after addition of MTS reagent.

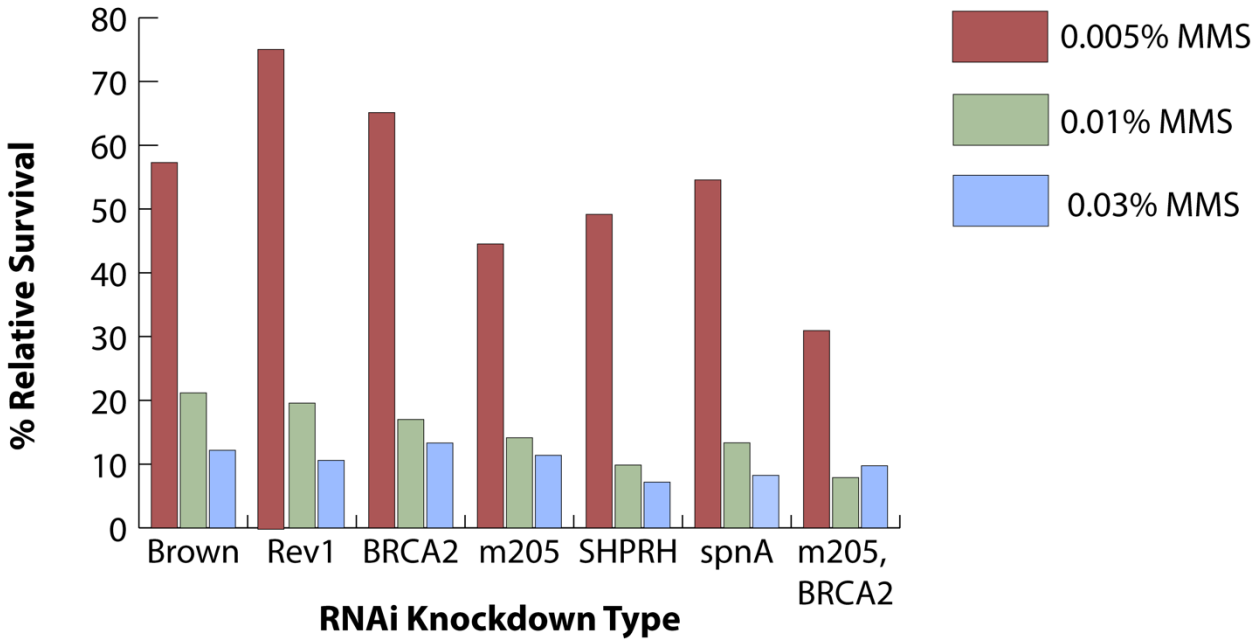

Figure 30: Kc167 cell sensitivity to MMS post RNA knockdown at 0.005%, 0.01%, and 0.03% MMS. Kc167 cells were treated with the varying concentrations of MMS 3 days after initial RNA knockdown. Cell surivial was measured 3 days after MMS treatment via the MTS proliferation assay and surivial was based on the optical density of each well after addition of MTS reagent.

***Drosophila* Gateway-integration tag vectors: pattBFMW and pattBWF**

As part of our efforts to clone an epitope-tagged version of Rev1 into the pattB integration vector, we built a universal tool for easily generating epitope tagged proteins to be integrated into the genome of *Drosophila*. Once the pattBWF and pattBFMW epitope tag Gateway integration vectors were generated, the process of integrating our gene of interest involved a simple topo-TA cloning reaction into the pCR8 entry vector and then a Gateway reaction into the final integration vector. There are no other vectors like the pattBWF and pattBFMW plasmids created in this study so we now have a unique and simple tool for others to use to quickly generate tagged proteins *in vitro*.

Creation of Rev1-tag transgenic *Drosophila* line

Since our previous work with *Drosophila* MMS sensitivity unveiled a potential role for Rev1 in the TS pathway, we were interested in more clearly developing a model for its function

in TS. Until now, evidence of Rev1's function in has been limited to TLS, so our first step in building a model for its action in TS was to identify its unique interacting partners in this role. To do this, we built four Rev1 constructs, all with an epitope tag that would facilitate pull-down assays for potential interacting partners. While two of these constructs include the full length Rev1, two have the C-terminal truncation and therefore preclude Rev1 from performing any TLS function. A comparison of the proteins pulled down in the full length versus the C-terminal truncation variants will help clarify which interacting partners are TS-specific. We generated these constructs via molecular cloning, as described in materials and methods. The constructs are full length Rev1 with an N-terminal 3xFLAG 6xMYC tag or a C-terminal 3xFLAG tag and Rev1ΔCTD with an N-terminal 3xFLAG 6xMYC tag or a C-terminal 3xFLAG tag. Throughout this rest of this study, the terminology FM-Rev1, and Rev1-F will be used for the N and C-terminally tagged full length Rev1 transcripts, respectively. FM-CTD and CTD-F will be used to refer to the N and C-terminally tagged Rev1ΔCTD transgenes, respectively. A schematic of this nomenclature can be found in Figure 16 A.

All four Rev1-tag constructs were successfully injected into the genome of *Drosophila* via embryo injection by BestGene Inc. Multiple isolates of each transformant were recovered for each construct. For both the N and C-terminally tagged Rev1ΔCTD transgenes, we recovered 5 individual isolates (FM-CTD 1-5, CTD -1-5). We recovered 3 isolates of the C-terminally tagged wild-type Rev1 transgene (Rev1-F 1-3) and 5 isolates of the N-terminally tagged wild type Rev1 transgene (FM-Rev1 1-5). When we first received these stocks, they were heterozygous for the injected transgene and exhibited a faint orange eye color phenotype. Male and female heterozygotes were crossed to each other in attempts to create and maintain a homozygous stock

of each isolate. Upon homozygosing, the orange eye-color phenotype of the transgene became much more pronounced, especially in males (Figure 16 B).

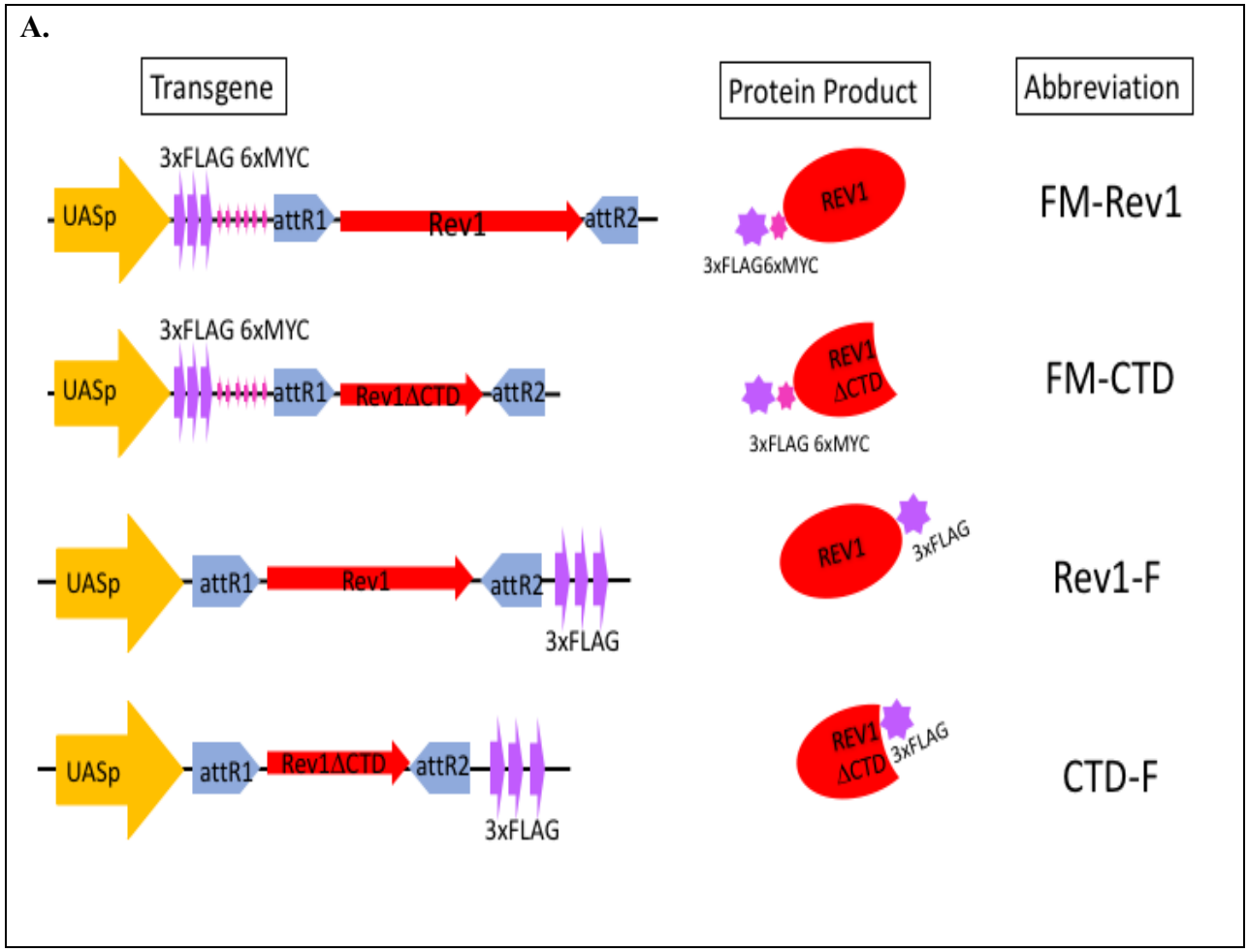

B.

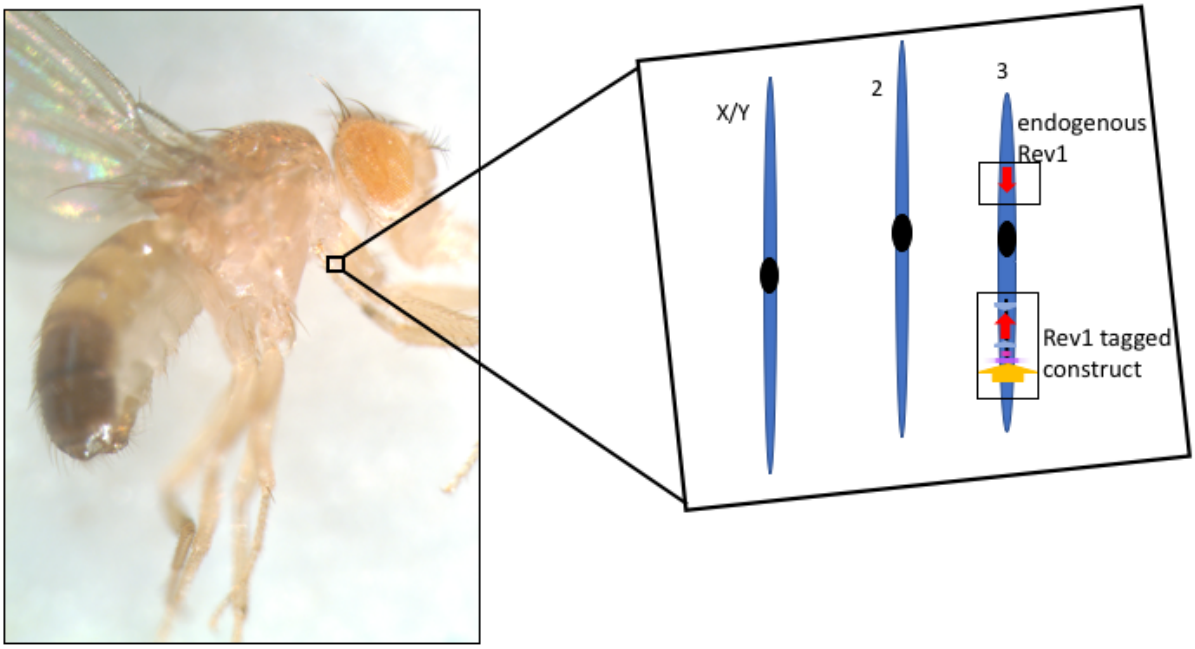

Figure 16: Rev1-tag construct nomenclature and transgenic *Drosophila* eye color phenotype. A) The FM-Rev1 transgene is the coding sequence for the 3xFLAG6xMYC epitope tag followed by a full length Rev1 transcript. This translates into an N-terminally tagged Rev1. The FM-CTD transgene is the coding sequence for the 3xFLAG6xMYC epitope tag followed by the C-terminal truncation of Rev1. This translates into an N-terminally tagged Rev1ΔCTD. The Rev1-F transgene is the wild-type Rev1 sequence followed by the 3xFLAG coding sequence. This translates into a C-terminally tagged Rev1. The CTD-F transgene is the C-terminally truncated Rev1 sequence followed by the 3xFLAG coding sequence. This translates into a C-terminally tagged Rev1ΔCTD. The abbreviation nomenclature seen here will be used throughout. B) Shown here is the orange eye color phenotype of a male Rev1-tag transgenic fly homozygous for the Rev1-tag construct on the third chromosome.

Confirmation of Rev1-tag construct sequence in whole *Drosophila*

To confirm the presence of the Rev1-tag transgene coding sequence in our homozygous stocks, we collected two homozygous males from each isolate of each transgene and prepared their DNA as described in materials and methods. To identify the transgene coding sequence, we used PCR with specialized primers that recognized the epitope tag coding sequence, each paired with a primer specific to Rev1 coding sequence. All samples produced a visible band of expected size (Figure 17 &18) except the FM-Rev1 isolate 3 bands which were slightly smaller than

expected (Figure 18). It is possible that in this isolate, some sequence may be missing in the Rev1-tag junction amplified by this PCR reaction or that sequence rearrangement caused primers to anneal at different locations in the sequence. These sequence deletions or alterations likely occurred during the initial integration of the construct. Each PCR reaction was performed with a negative control fly prep of genotype $y^1\ w^*;\ P\{Act5C\text{-}GAL4\}25FO1/CyO,\ y^+$, and none of these controls produced the band seen in the transgenic flies though there were some non-specific bands seen in these preps. There was also a noticeable amount of non-specific banding in the PCR reactions from the transgenic preps, especially with the C-terminal 3xFLAG primer set (Figure 17). Since this non-specific banding was consistent among the isolates and was not as prominent as expected bands, we concluded that this was likely a result of off-target annealing of the primers.

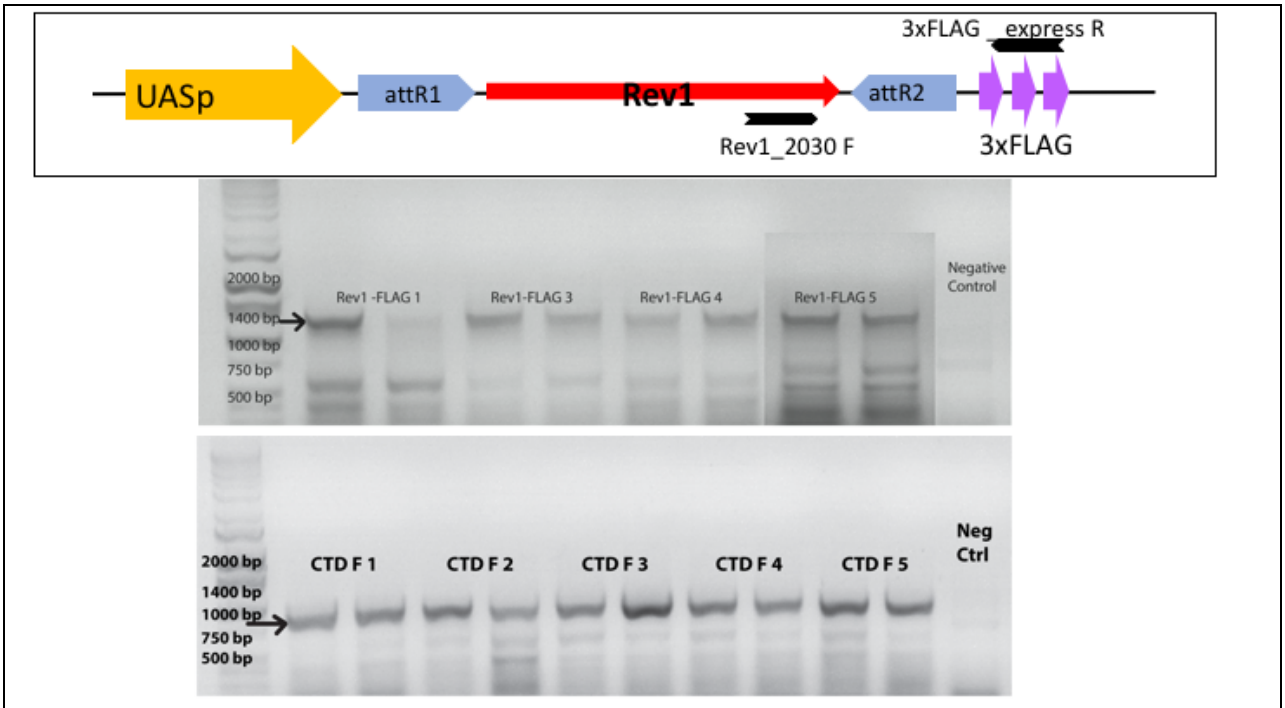

Figure 17: Verification of C-terminal 3xFLAG-tagged constructs via PCR amplification. Preps of males homozygous for the 3xFLAG transgenes were amplified using primer 3xFLAG_express R which targets the FLAG coding sequence and Rev1_2030 F which lies upstream of the C-terminal domain of Rev1 coding sequence. On the full length Rev1 constructs,

this primer set should amplify a 1391bp product and 946bp product in the ΔCTD construct. All reactions were performed in duplicate.

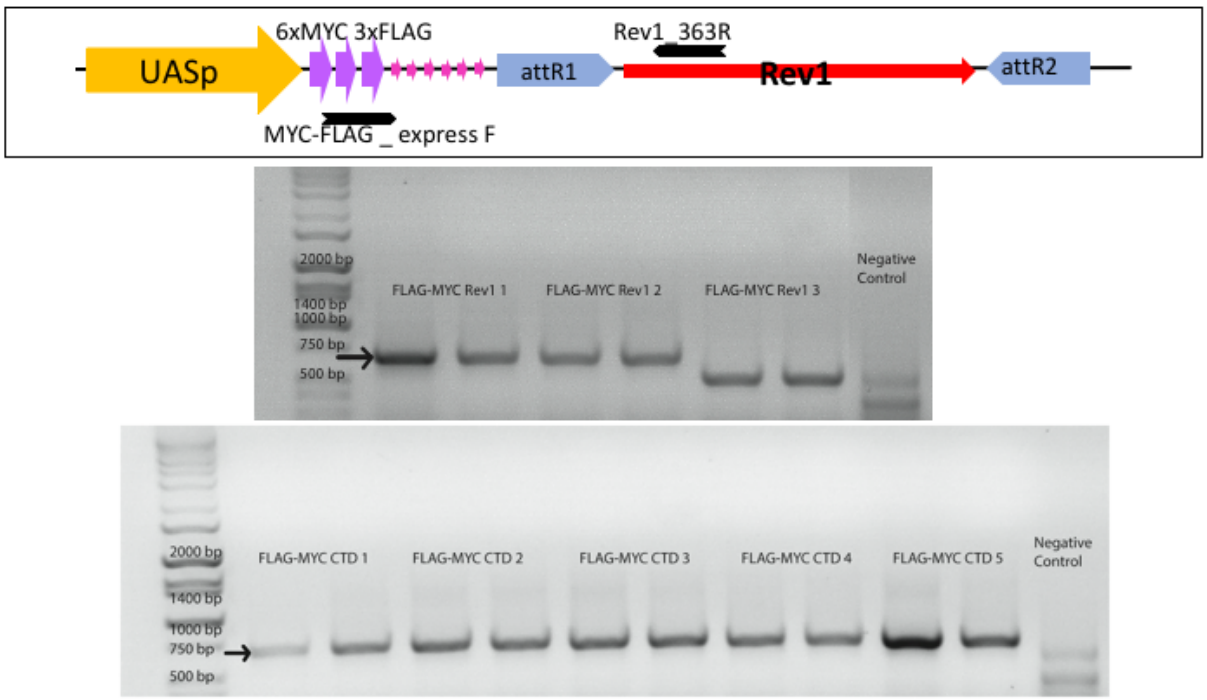

Figure 18: Verification of N-terminal 3xFLAG-6xMYC-tagged constructs via PCR amplification. Preps of males homozygous for the 3xFLAG-6xMYC-tagged transgenes were amplified using primer MYC-FLAG_express F which targets the FLAG coding sequence of the epitope tag and Rev1_363 R which lies at the N-terminus of the Rev1 coding sequence. This primer set should amplify a 698 bp product (arrows) in both the full-length and ΔCTD constructs. All reactions were performed in duplicate.

Gal4/UAS Expression System

The Rev1-tag constructs are all under control of the UASp promoter. This promoter is part of the Gal4/UAS system commonly used in *Drosophila* to drive the expression of transgenes in a tissue-specific manner. There are two gene-promoter sets required for the functionality of this system: the gene to be conditionally expressed under control of the UASp promoter and the Gal4 gene under control of a tissue-specific promoter. Gal4 is a transactivator of the UASp promoter which contains seven consecutive Gal4 recognition sites. When Gal4 is present in a

cell, it will activate and drive the expression of the gene regulated by the UASp promoter. Gal4 expression itself can be paired with tissue-specific promoters thereby also controlling where the transgene of interest is expressed (Rorth, 1998) (Figure 19). For this study, a stock of Drosophila with Gal4 expression under control of the Actin 5c promoter was used to drive expression of our transgenes (stock specifics found in materials and methods). This promoter is active in all tissues, so overexpression of the transgene should be ubiquitous and uniform throughout the fly. This specific *Drosophila* line has the Actin5c-Gal4 system on the second chromosome while the UASp-Rev1-tag system is on the third chromosome. To drive expression of the Rev1-tag constructs, males homozygous for the Rev1-tag alleles were crossed to virgin females with the Act5c-Gal4 allele on their second chromosome. Specifically, 2 isolates of each of the 4 transgenes was crossed to these Act5c-Gal4 flies and the progeny of these crosses were used for various components of the study.

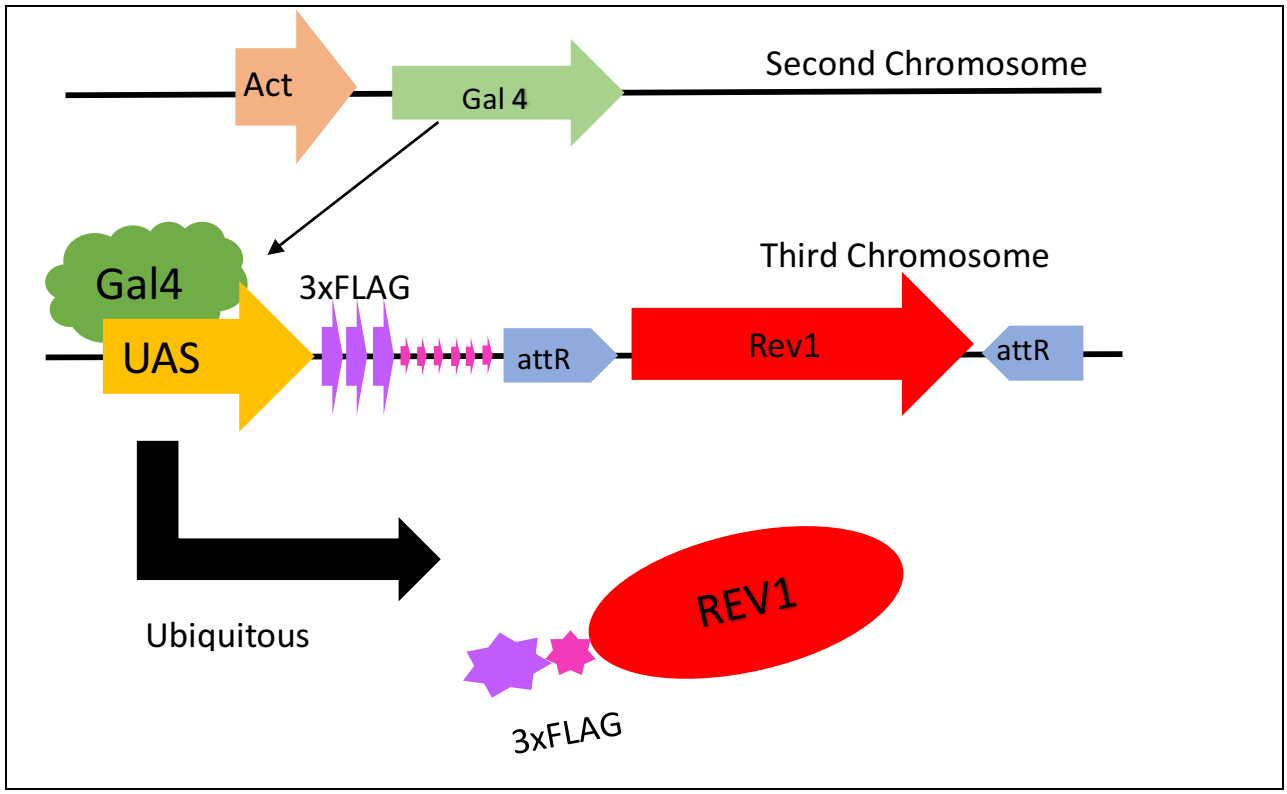

Figure 19: Gal4/UASp expression system used for Rev1-tag constructs. In this study, Gal4 expression was driven by the ubiquitous Actin 5c promoter, present in all tissues of *Drosophila*. Stocks of *Drosophila* with the Actin5c-Gal4 construct on the second chromosome were crossed to stocks with the UASp-Rev1-tag on the third chromosome. The ubiquitously expressed Gal4 protein will bind to the Gal4 recognition sequences on the UASp promoter and drive expression of the Rev1-tag sequence.

Confirmation of Rev1-tag construct RNA expression in whole *Drosophila*

To confirm that the Actin-driven Gal4 expression system was inducing expression of the Rev1-tag transgenes *in vitro*, we performed an RT-PCR assay, as described in materials and methods. For this assay, we collected the appropriate progeny of a cross between Rev1-tag homozygous males and females with the Actin 5c-Gal4 system on their second chromosomes. We chose to sample only two isolates of each Rev1-tag transgene variant, FM-Rev1 isolates 2 and 3, Rev1-F isolates 3 and 5, FM-CTD isolates 2 and 3 and CTD-F isolates 1 and 3. From each cross, 4 flies with the transgene and the Actin-Gal4 system (Act) and 4 flies with the transgene but no Actin-Gal4 (CyO; they inherited the *CyO* second chromosome balancer instead of the Actin-Gal4 system) were collected and RNA was extracted as described above. cDNA was made from each RNA extraction and primer set Rev1_1188 F and Rev1_1731 R were used to amplify the cDNA, producing a 542 bp genomic product and 489 bp product if introns were removed. Based on the relative intensity of the bands produced, we were able to assess the relative expression levels of Rev1 mRNA transcript. Based on the size of each band we could detect if it was an amplification of cDNA or genomic DNA. It is important to note that primers specific to Rev1 and not the Rev1-tag transgene sequence were used in this assay. Though these primers will amplify some endogenous Rev1 transcript, we still expected to see differences in expression levels between the Actin and CyO controls as the Gal4-UASp system should drive transgene expression to levels far above those of endogenous Rev1.

The results of this assay indicate that in all four transgenes, both isolates tested express elevated levels of Rev1 transcript, likely from Gal4-induced expression of the Rev1-tag sequence. This can be deduced from the noticeable banding pattern seen in Figure 20 A-D (left panel). In the Rev1-specific amplification there is a notably darker band of appropriate size in the Act lanes when compared to the corresponding CyO lanes of the RT+ reactions. Interestingly, this contrast in band intensity seems more intense in both Rev1ΔCTD constructs (Figure 20 B & C left) though it is still noticeable in the full length Rev1 constructs (Figure 20 A & D left).

Our results also indicated that there was likely some genomic contamination in our cDNA samples, but because of our controls, we were able to prevent this from confounding our confirmation of Gal4 induced Rev1-tag expression. In the Rev1 specific reactions for all transgenes tested, there appears to be a faint band in all RT- reactions, which is not expected since these reactions were performed without the reverse-transcriptase enzyme (Figure 20A-D, right). But, upon closer examination, these bands appear to be running slightly higher than the corresponding RT+ bands, indicating that any amplification in the RT- reactions is likely templated from trace amounts of genomic DNA that were present in the initial RNA samples. This is confirmed when examining the trends in the positive control reactions (Figure 20 A-D, right). Here, the banding in the RT+ lanes is very intense, while in the RT- lanes it is faint and running at a noticeably larger size. The banding seen in the positive control RT- lanes matches the size of the genomic DNA control reaction, performed with the same primer set (Figure 20 B, right-most panel), confirming that the RT- bands are a result of genomic contamination. We considered this genomic contamination to be relatively negligible, though, because of the relative intensity of the banding in the RT+ lanes, a sign that the cDNA concentrations are much higher than that of the genomic DNA. Since the cDNA concentrations were significantly greater than

the genomic DNA, we remained confident that the difference in expression seen in the Rev1 specific reactions is a result of Gal4-induced transgene expression.

A.

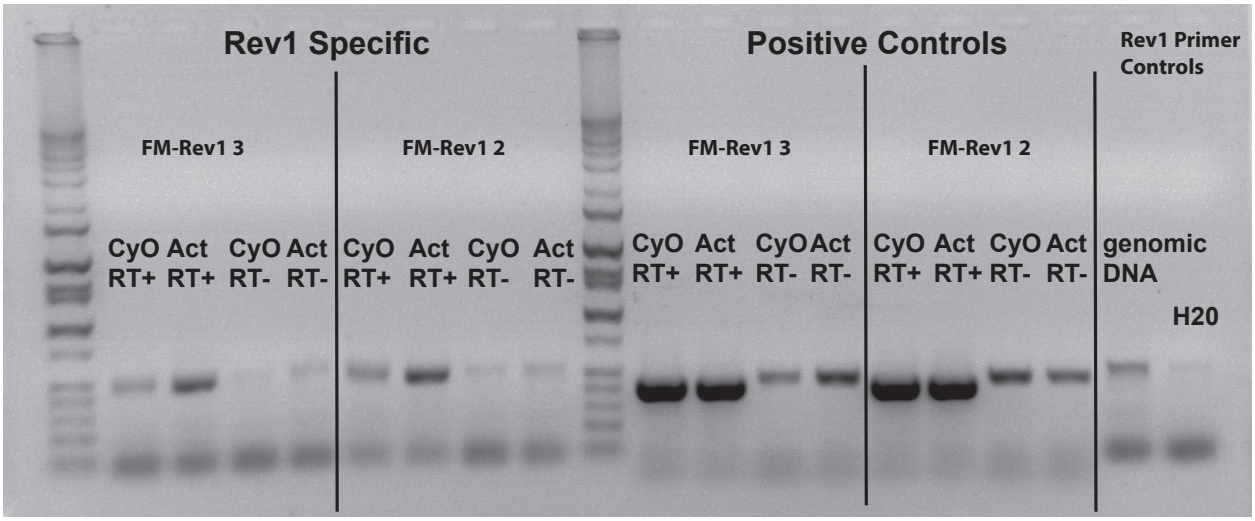

B.

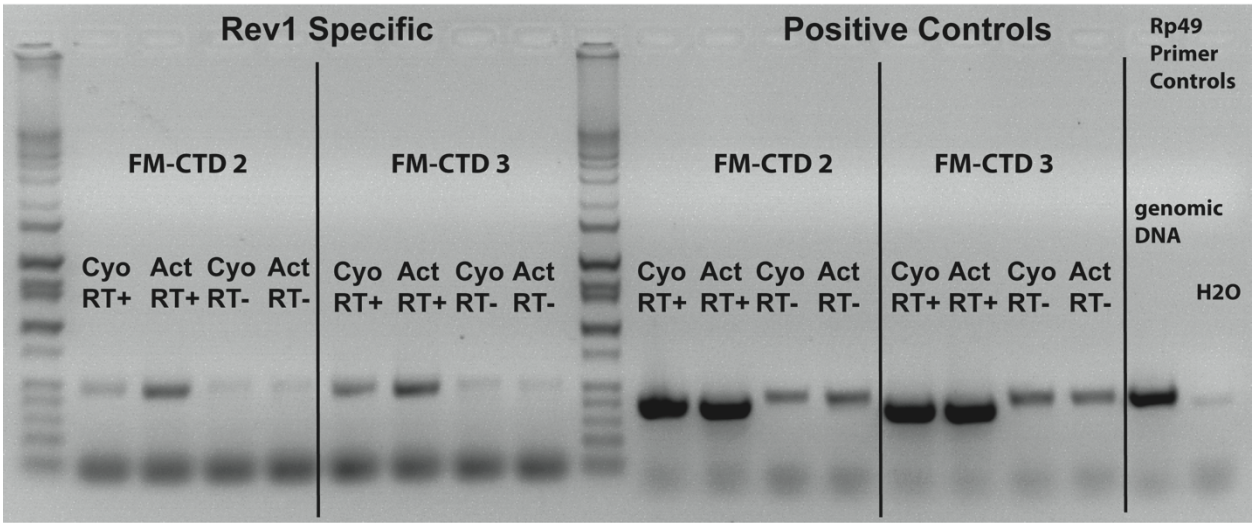

C.

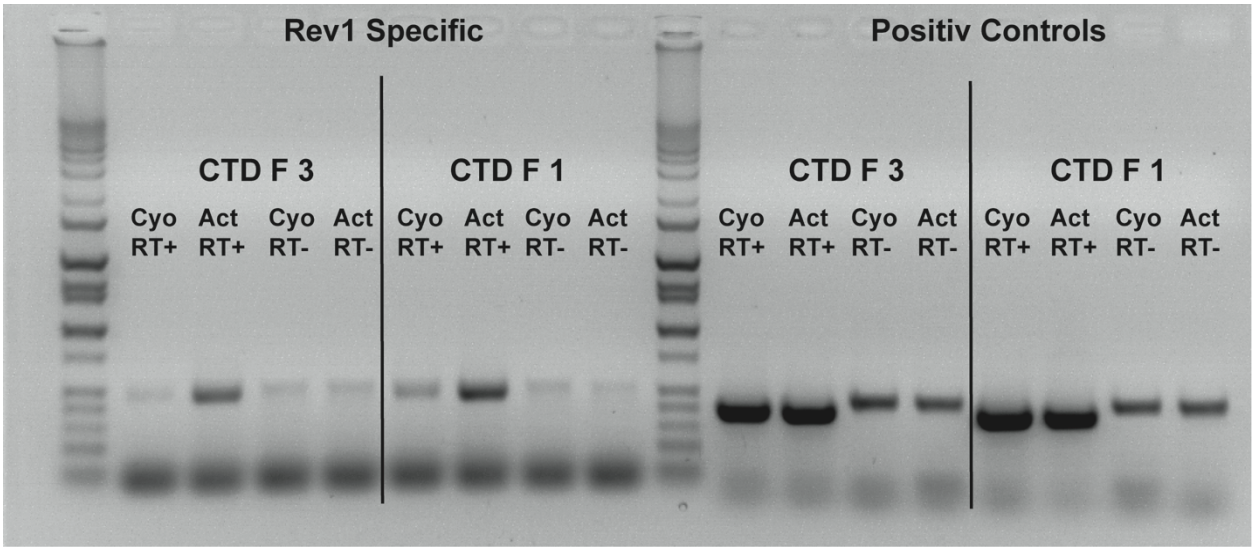

D.

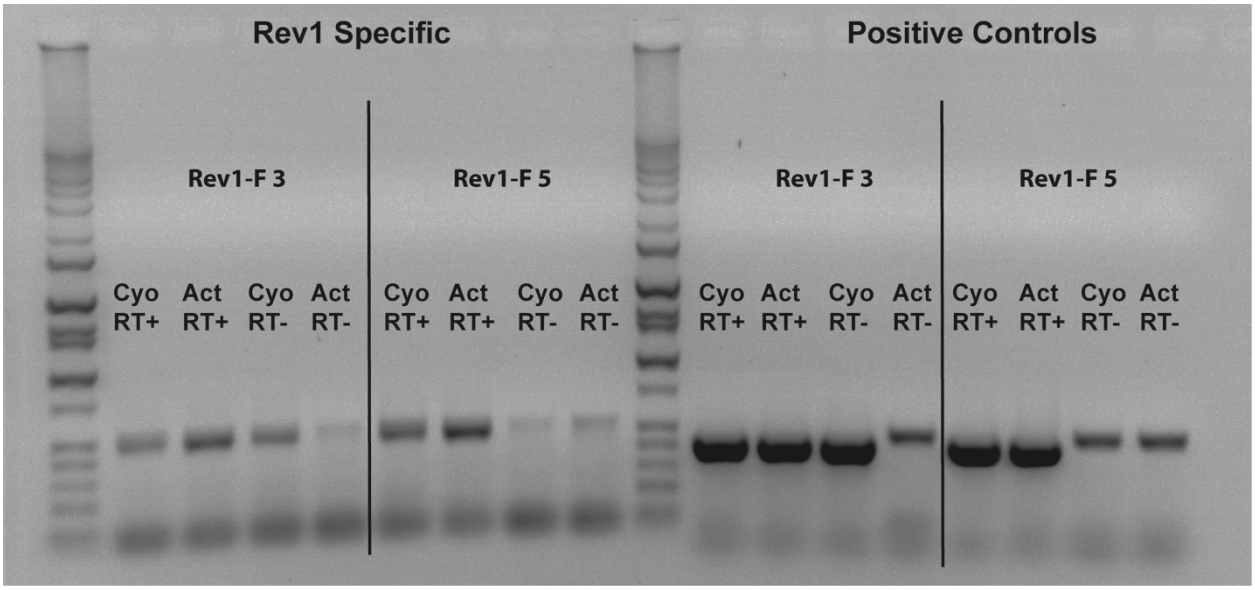

Figure 20: rtPCR of Rev1-tag transgene expression from whole *Drosophila*. For each RT-PCR reaction, 4 flies with the transgene and the Gal4 system (Act) and 4 flies with the transgene but not the Gal4 system (CyO) were collected and prepared as described in the RNA isolation and RT-PCR section. RT+ reactions were prepared using reverse-transcriptase enzyme while RT- reactions used an appropriate volume of water in place of the enzyme. The positive control reactions used Rp49 primers. These reactions were a positive control for the presence of cDNA. A) FM-Rev1 isolates 3 and 5 B) FM-CTD isolates 2 and 3 C) CTD-F isolates 1 and 3 D) Rev1-F isolates 3 and 5

Confirmation of Rev1-tag construct protein expression in whole *Drosophila*

To confirm that the Rev1-tag constructs were being expressed and translated appropriately, western blot analysis was used to probe for the FLAG epitope tag on all four construct variants, as described in materials and methods. In total, two isolates of each construct were used as samples for this assay to ensure that there was consistency amongst the various isolates of each construct. From each transgenic isolate, we prepared samples of flies with the Gal4 expression system (Actin) and without (CyO). Pronounced bands of appropriate size in the Actin lanes but not in the CyO lanes, would indicate that the transgenes were being properly expressed and translated *in vivo*. The calculated molecular weight of the FM-Rev1 constructs is 128 kDa, the Rev1-F constructs is 117 kDa, the FM-CTD constructs is112 kDa and the CTD-F constructs is 102 kDa. Endogenous Rev1 is approximately 112 kDa. Though we did expect the bands to run at roughly the correct molecular weight, we expected to see some variation from calculated molecular weight. For our first trial, we prepared samples from CTF-F isolate 1 (CTD-F 1), FM-CTD isolate 2 (FM CTD 2), Rev1-F isolate 3 (Rev1 F 3), and FM-Rev1 isolate 3 (FM Rev1 3) and a negative control (*OregonR*, wild type flies).

In our first trial, we confidently confirmed the proper expression and translation of the FM-Rev1 transgene in isolate 3 and the CTD-F transgene in isolate 1. Despite the consistent off-products observed, there is a noticeable and unique band in the Actin-Gal4 sample for FM-Rev1 3 (Figure 21, lane 8) and CTD F 1 (Fig. 21, lane 2) that is not seen in the corresponding CyO lanes (lanes 7 & 1 respectively). The FM-Rev1 3 specific band appears to run slightly above 135 kDa (Figure 21, lane 8) and the CTD F 1 specific band appears to run at approximately 110 kDa (Fig. 21, lane 2). Though both of these bands are larger than expected from molecular weight calculations (see above), they are not outside of normal variation seen in western blotting in our

lab and this is supported by the fact that *both* samples are running at a slightly higher molecular weight than expected. It is interesting that the FM-Rev1 isolate 3 sample produced a band of expected size as this isolate seemed to be missing some coding sequence when verified via PCR (Figure 18). Since the band seen here is of approximately appropriate size, and indicates that the 3xFLAG epitope is being properly transcribed, we can conclude that the rest of the Rev1 sequence is likely also being successfully transcribed, despite apparent complications with the original transgene sequence.

After more careful inspection of our results, there is also evidence that the Rev1-F 3 and FM-CTD 2 isolates are also being translated and expressed properly. In the FM-CTD 2 Actin-Gal4 expression lane (Fig. 21, lane 4), there is a faint band running at approximately the same weight as the CTD-F 1 band. This band is also not present in the CyO, un-induced expression lane (lane 5) nor the negative control (lane 9). We would expect a FM-CTD band to be slightly larger than a CTD F band, though, as the 6xMYC also present on this construct should make it slightly heavier. It may be possible that the differential in weight between the 3xFLAG and 3xFLAG 6xMYC tags is not large enough to be differentiated with a polyacrylamide gel protocol. In the Rev1-F 3 Actin expression lane (lane 6), there is a noticeable band running slightly below 135 kDa that is not present in the negative control lane. This band very likely represents the Rev1-F 3 protein product. Interestingly, this band is noticeably smaller than the FM-Rev1 band, as we would expect since it is lacking the 6xMYC epitope, though this is not necessarily consistent with the apparent equivalent sizes of the FM-CTD and CTD-F constructs. Though we were confident in our identification of the FLAG epitope on the FM-Rev1 and CTD-F isolates tested in this trial, our Rev1-F and FM-CTD results warranted another trial of this assay.

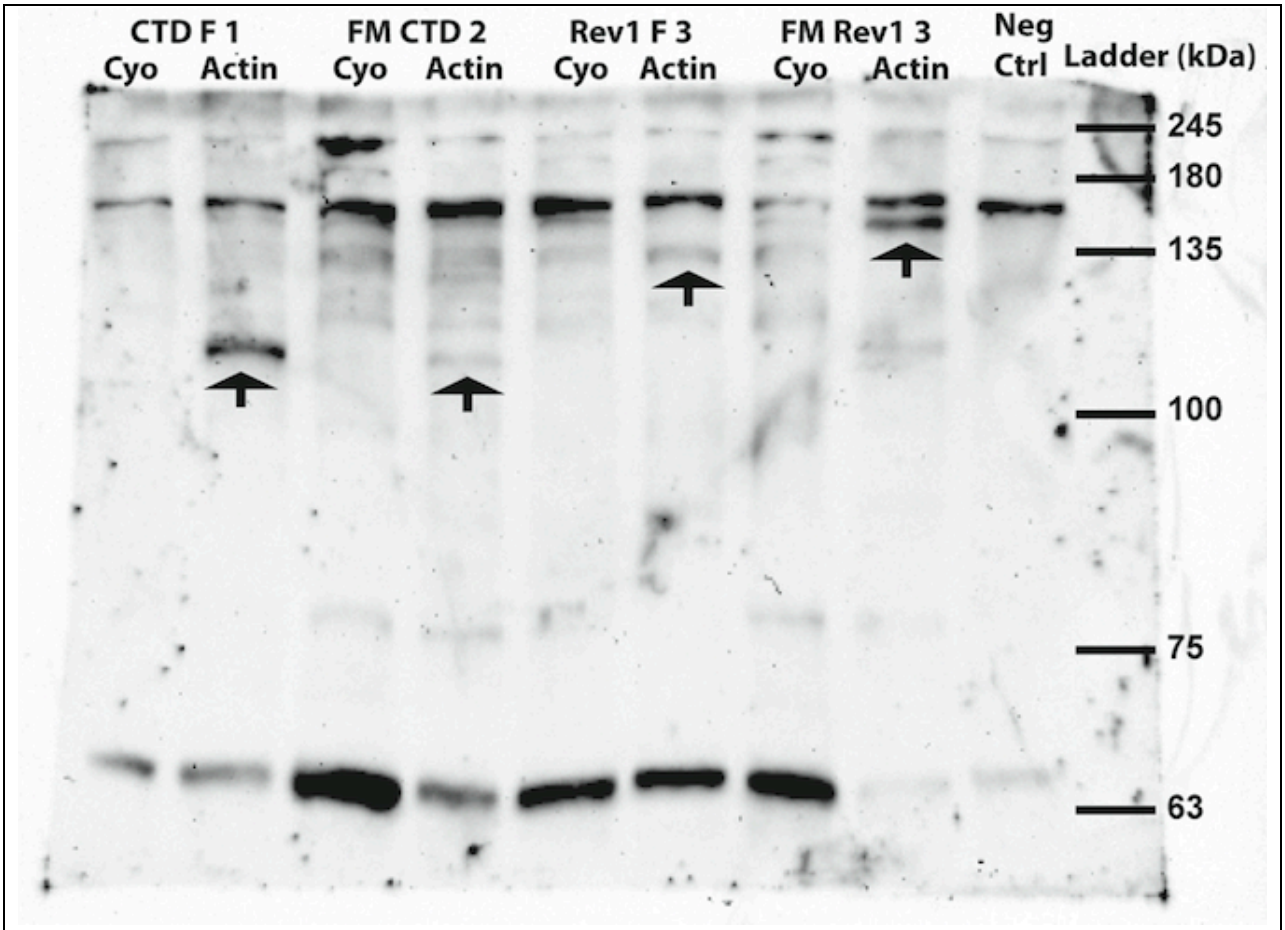

Figure 21: Western blot for FLAG peptide from whole Rev1-tag transgenic flies. Samples for this blot were prepared via sonication (see materials and methods) and run on an 8% polyacrylamide gel for 3 hours before membrane transfer. This image is a 960 second exposure. Arrows refer to bands of translated transgenes.

The results of our second trial of FLAG detection via western blot analysis again confirmed the proper translation and expression of all four constructs, this time from different isolates of each. The goal was to determine if there was consistency in successful protein expression amongst construct type or if there was any variation in protein expression between different isolates of each construct type. For this trial, isolates CTD-F 3, FM-CTD 3, Rev1-F 5, and FM-Rev1 2 were used. In order to generate consistently cleaner samples, protein extracts from these isolates were prepared using liquid nitrogen and run on a lower percentage polyacrylamide gel (Figure 22). Similar to the first trial, our western blot provided clean, positive results for the FM-Rev1 and CTD-F isolates tested. A prominent band, running slightly above

the 135 kDa marker can be seen in the FM Rev1 isolate 2 samples and is only present in the Actin5c-Gal4 induced sample (Fig. 22, lane 9) and an approximately 110 kDa band is seen in the CTD F isolate (Fig. 22, lane 3) that is not present in the un-induced sample (lane 2) nor the negative control (lane 1). Again, there are some distinct, non-specific bands present in all samples, including the negative control. After a much longer exposure of our blot, we were able to confirm the proper transcription and expression of the FM-CTD and Rev1-F constructs in the isolates sampled. With this exposure, in the FM-CTD 3 Actin expression lane (Figure 23, lane 5) there is a light band running just below 135 kDa that is not present in the corresponding un-induced control (Figure 23, lane 4), though this band is not the same size as the proposed FM-CTD band seen in the first blot (Figure 21, lane 4). Also, after a longer exposure, we can now see a faint band at approximately 135 kDa in the Rev1-F 5 expression lane (Fig. 23 lane 7), that is not present in the corresponding CyO lane (6) nor the negative control (lane 1). Like in the first trial, the FM-Rev1 and Rev1-F bands seem to be running at approximately the same size, despite the predicted differential in molecular weight. Though we remained confident in the proper transcription and expression of our transgenes, the sizing discrepancies between the two trials left room for further validation of these results.

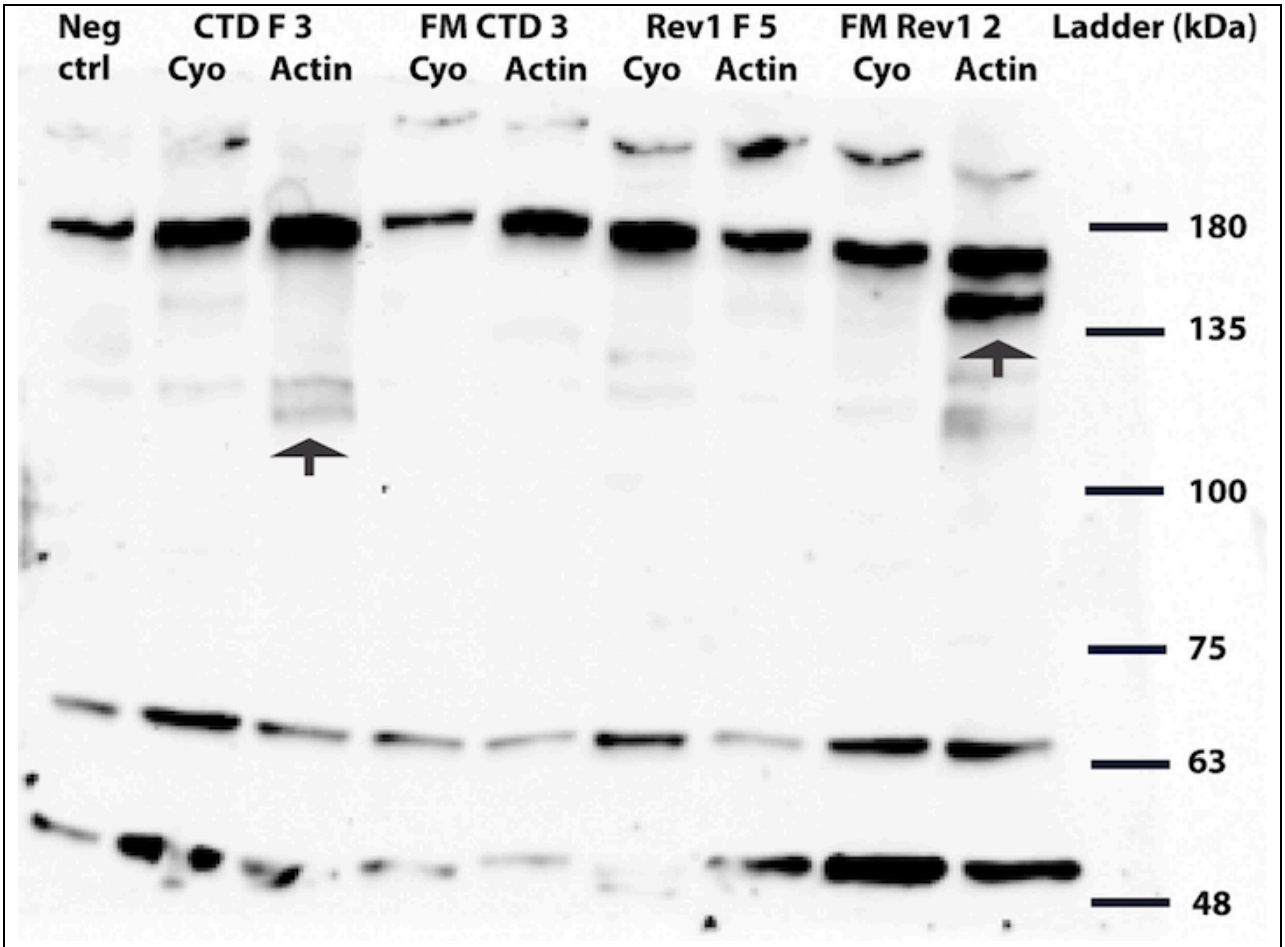

Figure 22: Adjusted protocol western blot for FLAG peptide from whole Rev1-tag transgenic flies, short exposure. These samples were prepared via liquid nitrogen mashing (see methods) and run on a 6% polyacrylamide gel for 2 hours, in attempts to generate more consistent, clean samples with greater separation of the high molecular weight regions. This blot is a 360 second exposure. Arrows refer to bands of translated transgenes.

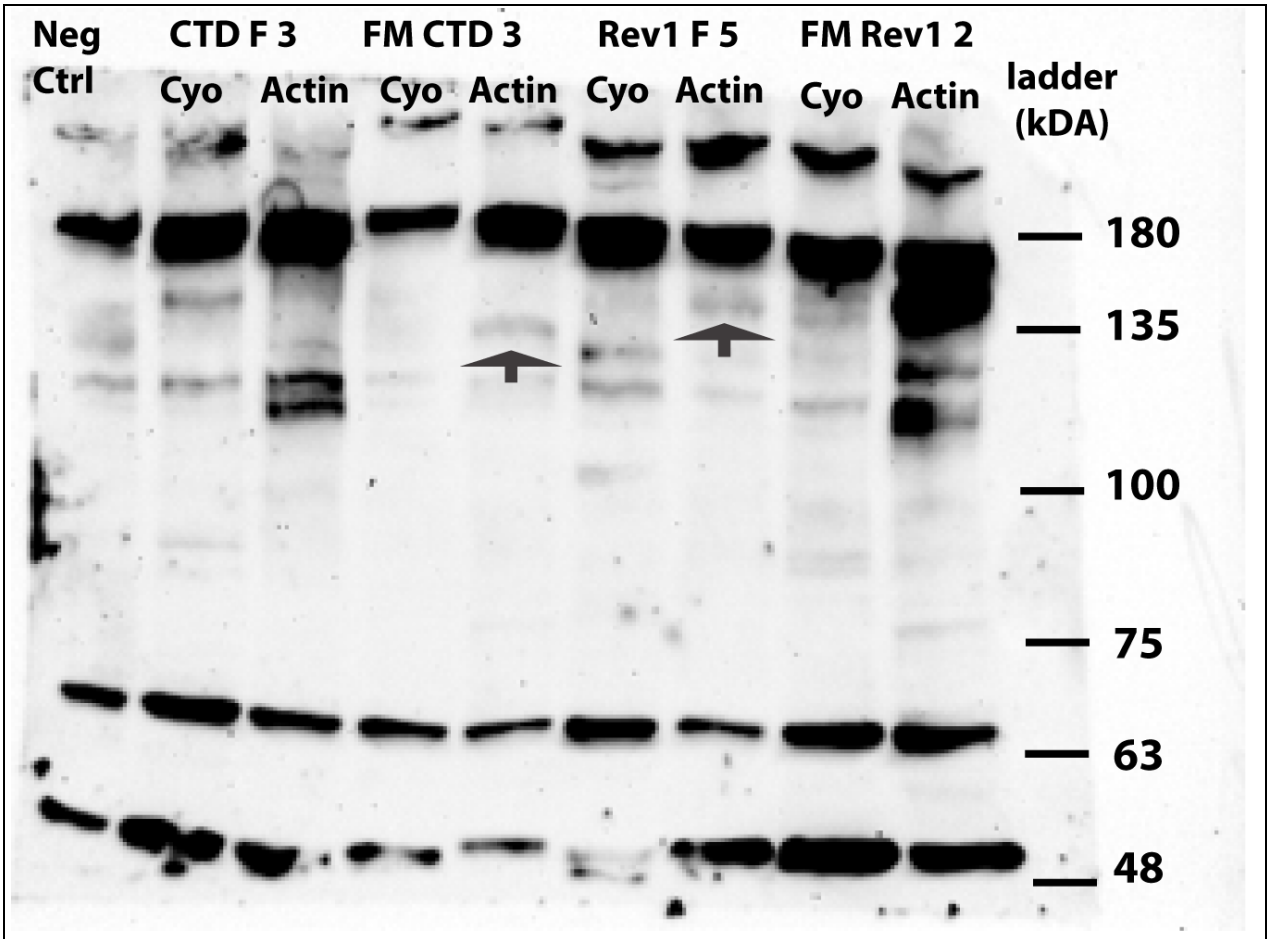

Figure 23: Adjusted protocol western blot for FLAG peptide from whole Rev1-tag transgenic flies, short exposure. This is a 1790 second exposure of the blot seen in Figure 23. This blot was over-exposed in attempts to visualize any faint bands in the Rev1-F and FM CTD samples that could not be visualized after 360 seconds. Arrows refer to bands of translated transgenes not seen in Figure 22

After stripping and re-probing our second blot with an anti-MYC antibody, we validated our original conclusions about the FM-Rev1 and FM-CTD isolates sampled in this trial. The anti-MYC antibody is known to be much more stringent than the anti-FLAG antibody so we hypothesized that this re-probe would clarify the identity of some of the faint bands in the FM-CTD samples and further validate the FM-Rev1 product. As can be seen in Figure 24, this blot provided clear confirmation of the FM-Rev1 2 product, as the band seen in the Actin expression lane (Figure 24, lane 9) is approximately the same size as when probed for FLAG. Interestingly, there is a faint band of equal size seen in the corresponding un-induced expression samples

(Figure 24, lane 8) indicating that UASp expression of the FM-Rev1 constructs may be leaky. In the FM-CTD 3 samples, there is a distinct band in the Actin expression lane (5) that is not present in the corresponding, un-induced expression sample (4). This band is running at approximately 130 kDa which is higher than the expected 112 kDa expected product, but consistent with the size of the FM-CTD band seen when probed with the anti-FLAG antibody (Figure 23, lane 5).

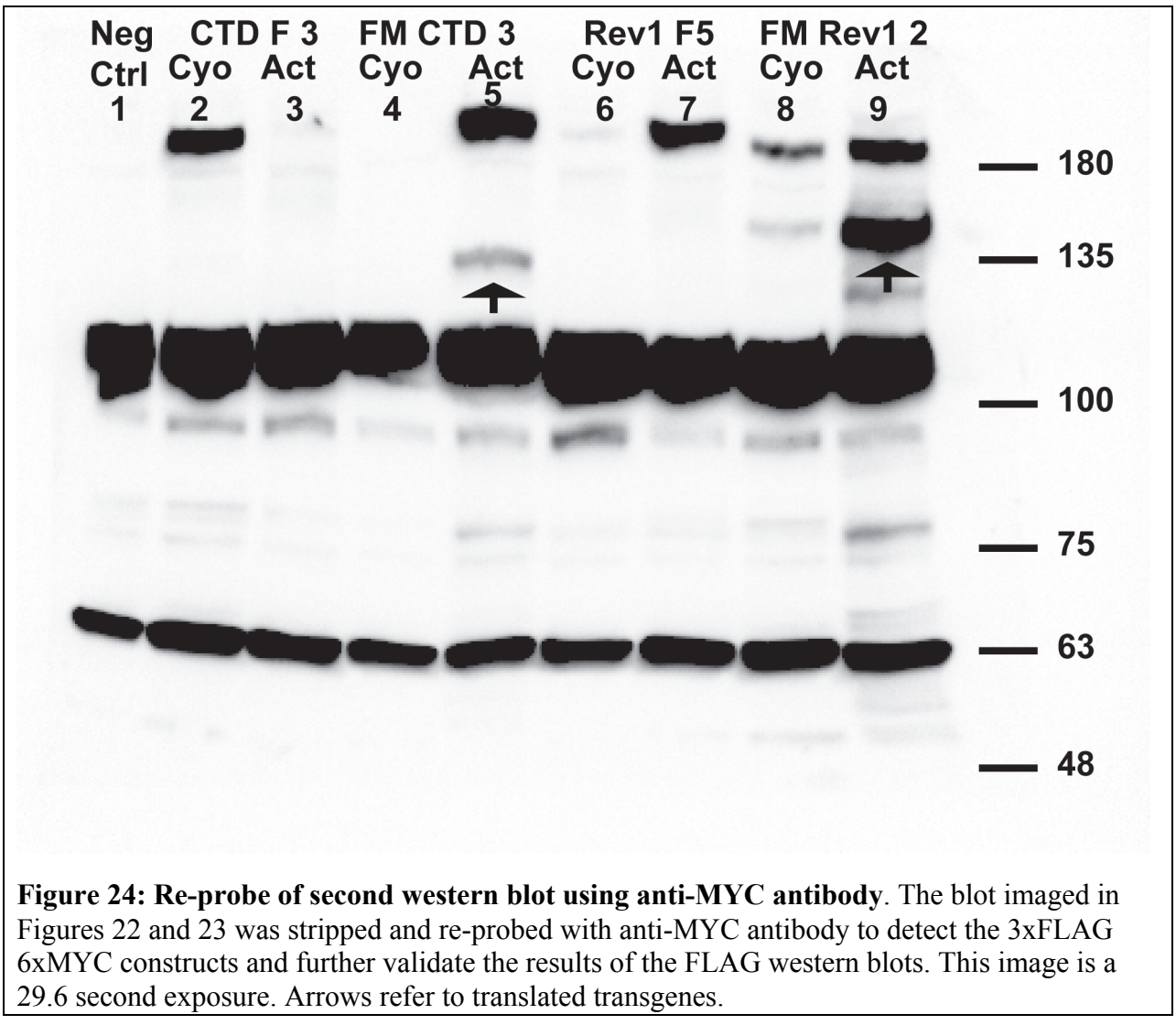

Figure 24: Re-probe of second western blot using anti-MYC antibody. The blot imaged in Figures 22 and 23 was stripped and re-probed with anti-MYC antibody to detect the 3xFLAG 6xMYC constructs and further validate the results of the FLAG western blots. This image is a 29.6 second exposure. Arrows refer to translated transgenes.

***Rev1-tag, Δrev1* mutants**

In order to use the Rev1-tag transgenes in experiments without interference from endogenous Rev1 expression, they were combined with the Rev1 deletion allele, *Δrev1*. This was done using a *Drosophila* cross scheme which takes advantage of crossing over between homologous chromosomes in the female germline (Figure 25). The location of Rev1-tag transgene integration was strategically chosen to be far from Rev1's endogenous locus, thereby increasing the frequency of crossing over between the two alleles. The first step in generating these double mutants was to generate females with a Rev1-tag allele on one chromosome and a *Δrev1* allele on the other chromosome. Since there is crossing over between homologous chromosomes in the female germline, there is potential for both the deletion and the transgene alleles to end up on a single chromosome in the germline of these females. Each potentially recombined chromosome was recovered in the male progeny, where no recombination can occur in the germline, ensuring that the two alleles will not recombine back onto separate chromosomes. The males selected at this stage were heterozygous for the potentially recombined chromosome, carrying it over the *TM6B, Tb, Hu* balancer chromosome. Each individual male was separately crossed to females with the *TM3, Ser, w+* / *TM6B, Tb, Hu* double balancer genotype. Since balancer chromosomes cannot recombine, there was no risk of losing any Rev1-tag, *Δrev1* cross-on events at this point. After these males had sufficient time to fertilize females, they were removed from the cross and any potential recombination events were verified via PCR. Specifically, since males were selected based on the orange eye color phenotype of the Rev1-tag alleles, PCR was used to check for the presence of the *Δrev1* allele. Two separate primer sets were used to amplify the Rev1 deletion in these males because initial tests showed some inconsistency in amplification of positive controls (Figure 26). In total 5 FM-Rev1, 6

Rev1-F, 3 FM-CTD and 10 CTD-F, *Δrev1* double mutants were created. Any future experiments involving the Rev1-tag transgenes will use these Rev1-tag, *Δrev1* double mutant stocks. Since the epitope tag on the Rev1 transgenes will help us answer questions about Rev1 protein interactors, we want to avoid endogenous Rev1 competition for binding with these partners.

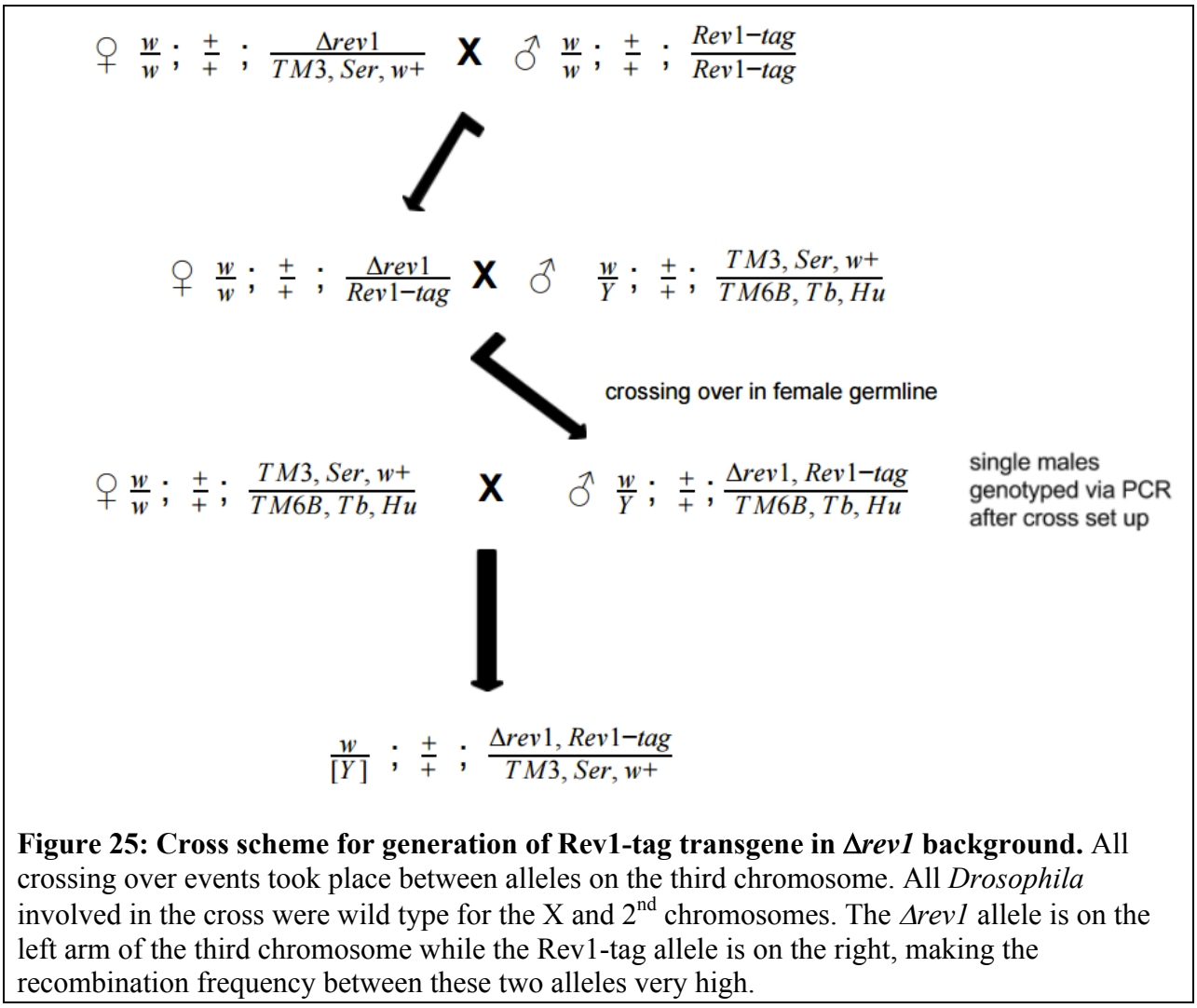

Figure 25: Cross scheme for generation of Rev1-tag transgene in Δ*rev1* background. All crossing over events took place between alleles on the third chromosome. All *Drosophila* involved in the cross were wild type for the X and 2nd chromosomes. The *Δrev1* allele is on the left arm of the third chromosome while the Rev1-tag allele is on the right, making the recombination frequency between these two alleles very high.

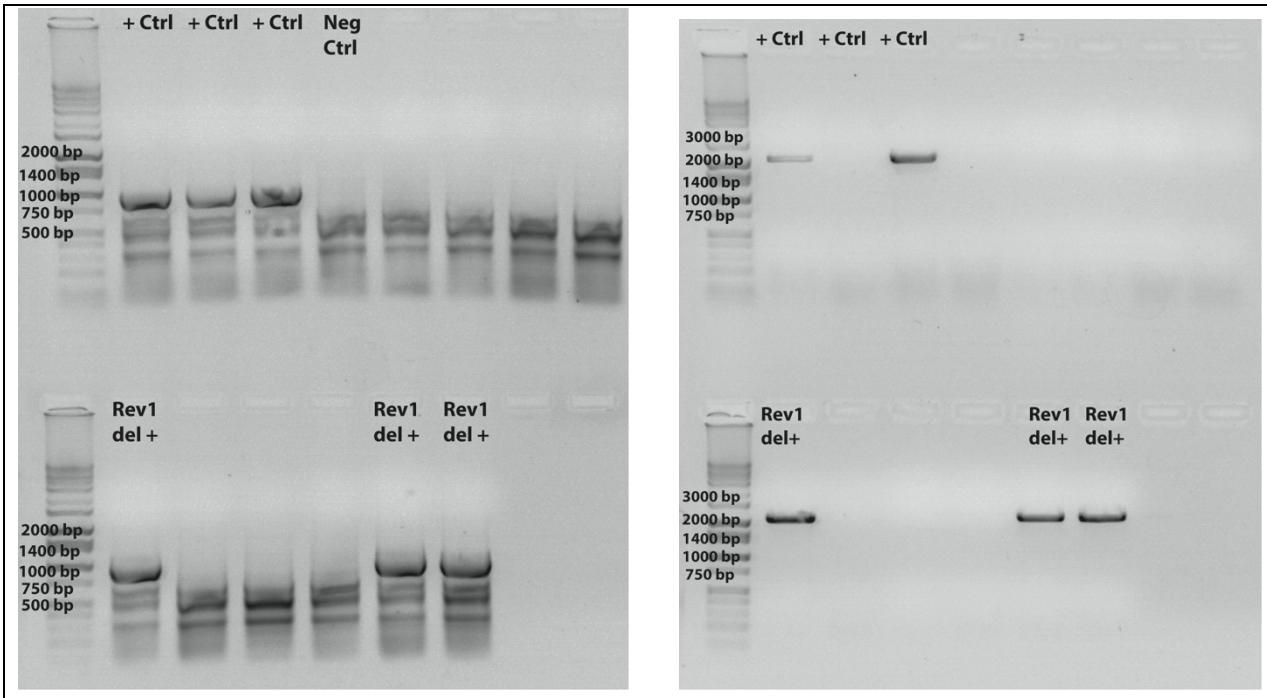

Figure 26: Verification of Rev1 deletion in generation of *Rev1-tag, Δrev* double mutants. Sample of *Δrev1* allele verification in potential double mutants. On the left, amplification with primer set Rev1_del5P F and Rev1_5438R on the right, amplification with primer set Rev1_-250F and Rev1_5438R. Since there was significant non-specific banding in the reaction on the left and failure to amplify one of the positive controls on the right, both reactions were performed on each isolate to ensure accurate verification.

Discussion

Kc167 cell sensitivity to MMS remains uncertain

Unfortunately, after considering the data presented above, it seems that the RNAi-MMS protocol for Kc167 cells needs to be further refined before we can glean any truly meaningful results from this assay. Based on the results of both Kc167 cell MMS sensitivity assays, there is no noticeable sensitivity to MMS at a wide variety of concentrations. Interestingly, at the highest concentration tested, 0.03% the mus205, BRCA2 double knockdown did exhibit increased sensitivity to MMS (Figure 30). This result is expected, as knocking down mus205 (Rev3) and BRCA2 should inhibit both TLS and TS therefore rendering cells unable to carry out either DDT pathway. The fact that we do see knockdown but only at the highest dose of MMS and in the

double knockdown context indicates that we may be having issues with RNA knockdown efficiency. Though our initial time-course analysis of RNA knockdown with mus205 (Rev3) indicated that there was successful knockdown until day 4 post treatment (Figure 27, right), this result may not be accurate as there is no mus205 transcript seen on day 1 post treatment and it is unlikely that all transcript present at the time of knockdown had been degraded after only 1 day. This reaction was run with a control primer set, Rp49, which should amplify if there is sufficient cDNA sample present (Figure 27, left). Since there are bright bands seen with the Rp49 primers in each day post knockdown, this indicates that the RNA extraction and generation of cDNA were successful reactions. Since there was no sample taken on day 0, from which to compare the day 1 levels of transcript, it is makes it difficult to draw conclusions from this initial test.

In order to gain a clearer picture of the knockdown efficiency of each RNA type, a RNAi time-course was set up with all RNA types but unfortunately, complications with RNA extraction only allowed us to quantify knockdown in the Rev1 treatment. As is seen in Figure 28, Rev1 does not appear to be effectively knocked down until day 4 at which point some transcript still remains. This indicates that it is very likely that our initial quantification of RNA knockdown was not accurate, and could possibly explain the failure to notice any sensitivity in our MMS treated cells. When considering the noticeable sensitivity of the mus205, BRCA2 knockdown at 0.03%, we are confident that with further modifications to our knockdown protocol, we will be able to answer our questions about coordination of DDT and function of Rev1 in cells versus whole *Drosophila*.

The goal of our Kc167 MMS sensitivity assays was twofold. First, we were interested in looking at how DDT pathway choice was coordinated in single cells versus whole organisms. There is evidence in yeast that the coordination of DDT pathway choice is cell cycle dependent

and that TS is preferred in cycles in which a homologous template for lesion bypass is available (Callegari & Kelly 2016). Following this logic, it seems that the TLS pathway may be preferentially used in rapidly-dividing cells that are competing for resources during development because it facilitates a more rapid lesion bypass, and cell cycling is less likely to stall. For this reason, we were interested to see if there might be a difference between MMS sensitivities in whole flies and cells in culture. If TLS is preferred in contexts of rapid cell cycling and competition, we would not expect to see the same hierarchy of DDT pathway choice that was observed in whole *Drosophila*, evidenced specifically by the lack of MMS sensitivity of the BRCA2 and *spnA* mutants (Figure 11). Since cells in culture are not competing for resources and dividing at the rapid rate of developing tissues, they may not need to use the mutation-prone yet rapid TLS pathway and can afford to pause the cell cycle to bypass lesions via TS. Interestingly, this same study in yeast noted that Rev1 function was only necessary later in the cell cycle, when TLS should be predominating. Our second question was then, is the essential function of Rev1 in the TS pathway a *Drosophila* specific phenomenon? If our cell line Rev1 MMS sensitivity is similar to that of whole *Drosophila*, this is further support for our proposed role of Rev1 in TS and indicates that it is likely a *Drosophila*-specific phenomenon.

Rev1-tag construct is properly transcribed and translated in transgenic *Drosophila*

We were successful in generating four variants of an epitope tagged Rev1 transgene for further studies of Rev1 function in DDT. Specifically, we will be using these transgenes to generate a model of Rev1 function in the TS pathway of DDT as this is a previously unstudied function of the protein and there is no pre-existing framework for potential protein interactors in this mechanism. The goal of creating an epitope tagged Rev1 was for completion of pull down assays to identify interacting partners. Our rationale for building four different constructs was

twofold. We wanted to be able to compare the interacting partners of the wild type versus the TLS deficient C-terminal truncation to narrow down interacting partners that are specific to Rev1's role in TS. Also, we chose to create a N and C terminal tag for each Rev1 variant to control for the potential of the tag itself disrupting protein interactions at either terminus.

Based on the results of our genotyping via PCR (Figure 17&18) and verification of expression via RT-PCR (Figure 20), we are confident that the Rev1-tag coding sequences were successfully integrated and are properly transcribed in the sampled isolates of each construct. Also, via western blot analysis, we are confident that at least one isolate of all four constructs is properly expressing its epitope tag *in vivo*. Much of our confidence in confirming the proper expression of our constructs comes from the western blot analysis not only because it is the most specific to formation of an actual protein but also because this assay involves reactivity with the anti-FLAG and anti-MYC antibodies which will continue to be essential when we use these constructs for pull down assays.

We are most confident in the FM-Rev1 and CTD-F transgenes, specifically FM-Rev1 isolate 2 and CTD-F isolates 1 and 3. In both western blots for the FLAG epitope, the FM-Rev1 isolates produced a clear band slightly above the 135 kDa marker in the Actin-Gal4 driven expression lanes but not in the un-induced lanes (CyO) (Figures 21 and 22). Further support for the presence of the FM-Rev1 construct came from re-probing our second blot with an anti-MYC antibody and detection of an identical band in the FM Rev1 Actin lane (Figure 24, lane 9). Though the FM-Rev1 isolate 3 sample did show a slightly lower than expected band in PCR amplification (Figure 18), it showed appropriate expression on the RNA and protein levels and formed a FLAG epitope recognizable by the very specific anti-FLAG antibody (Figure 21). Also, since the other FM-Rev1 isolate tested (2) showed virtually identical results in terms of RNA

expression, protein expression and size, we are confident that both isolates are producing a 3xFLAG 6xMYC-Rev1 protein, though we will likely only use isolate 2 in any further studies to avoid any unidentified confounding effects of the potential isolate 3 sequence deletion. It is important to note that though the protein sizes mentioned here are slightly larger than the expected size based on molecular weight calculations, we saw all our samples run slightly higher than predicted and have concluded that this variation it is likely a result of the polyacrylamide gel conditions. Similar to the FM-Rev1 isolates, both CTD-F isolates samples produced a noticeable band in the Actin-Gal4 driven lanes (Fig 21, lane 3 & Fig. 22 lane 2). These bands were both approximately 110 kDa, again slightly larger than the 102 kDa expected from calculations but consistent between trials and with the variation seen in all the samples. Since these constructs only contained the FLAG epitope, we could not detect any banding when probing for MYC, which also helps support the conclusion that the bands we predicted to be the CTD-F construct were specific, despite the various non-specific bands in the FLAG western blots.

Initially, we were less certain about the successful translation of the Rev1-F and FM-CTD isolates tested. Though the PCR and RT-PCR analyses indicate that the transgene sequence was successfully integrated and is properly transcribed and expressed (Figure 17, 18, 20) western blots for the FLAG epitope were somewhat less conclusive. In our first western blot analysis, both Rev1-F 3 and FM-CTD 2 showed faint bands in the Actin-Gal4 driven samples (Figure 21 lanes 6 & 4). The Rev1-F 3 specific band was smaller than the FM-Rev1 3 band, as expected, running just below the 135 kDa marker. In our second attempt to detect the Rev1-F construct, this time from isolate 2, the approximately 135 kDa band did not appear until after a lengthy blot exposure (Figure 23). Since the banding was consistent with expected expression of the UASp-

Gal4 system and band sizes were consistent between trials and isolates, we can comfortably say that this construct is forming properly *in vivo* but note that its reactivity with the anti-FLAG antibody is weak. Both FM-CTD isolate results also proved doubtful after the FLAG-specific western blots. Though there was a very faint band in FM-CTD Gal4-expression lanes in both isolates tested (Figure 21, lane 4 & Figure 23, lane 5), the second isolate could only be visualized after a lengthy exposure of the blot and was clustered amongst many other non-specific bands (Figure 23). When this blot was stripped and re-probed with an anti-MYC antibody, a similarly sized band in the same lane became predominant and clear after only 30 seconds of exposure, making us confident that the proposed bands in the FLAG westerns were, in fact, the FM-CTD constructs (Figure 24).

It is important to note that while the anti-FLAG and anti-MYC antibodies are specific to the Rev1 constructs, they also seem to have some consistent and non-specific cross reactivity which could prove to be a hindrance when completing pull down assays. Interestingly, the anti-MYC antibody seems to be more specific than the anti-FLAG antibody, though both blots did produce noticeable non-specific banding. The specificity of each antibody may become important when determining which antibodies to use in which steps of the pull-down assays. Since we have confirmed at least one isolate of both the FM-Rev1 and FM-CTD transgenes, we will likely focus our future work on these two constructs.

Rev1-tag, *Δrev1* double mutants provide an important foundation for future Rev1 studies

The Rev1-tag, *Δrev1 Drosophila* stocks will be essential to further studies involving the Rev1-tag transgenes, as the *Δrev1* allele will insure that there is no competition with endogenous Rev1 for interacting partners during pull down assays and will prevent confounding the effects of the Rev1ΔCTD mutants. These stocks are also essential to confirming the functionality of the

Rev1-tag transgene protein products. Though we have confirmed the proper translation of all four Rev1-tag constructs via western blotting, further trials are necessary to conclude that the presence of the epitope tag is not interfering with Rev1 function in DDT. To do this, we will be crossing the Rev1-tag, *Δrev1* flies to a stock of flies ubiquitously expressing Gal4 (also in the *Δrev1* background) and treating with MMS. If the transgenes can rescue the previously measured MMS sensitivity of the *Δrev1* and *Rev1ΔCTD* mutants, then we can be confident that these Rev1 transgenes are functional.

Continuing work and future directions

We plan to continue with our studies of Kc167 cell MMS sensitivity after RNA knockdown. Our primary objective is to develop an efficient and prolonged RNA knockdown protocol that we can then use to measure the MMS sensitivities of various genes of interest. Once we understand how *Drosophila* cell lines might be coordinating DDT, we may also use our Rev1-tag plasmids in the Kc167 cells to do a pull down and compare Rev1 interacting partners *in vivo* and in cell culture.

The pattBWF and pattBFMW Gateway integration vectors generated in this study open the door to similar studies of identifying protein interacting partners *in vivo*. Next, we plan to use the same general cloning scheme to generate a GFP variant of the gateway integration vector, so we can also visually track localization of genes of interest.

This study was also successful in building and validating four variants of an epitope-tagged Rev1 that are now stably integrated into flies and ready to be utilized in experiments. As mentioned above, the last step in validating the Rev1-tag constructs and first step after the completion of this study, will be to confirm that the Rev1-tag transgenes rescue MMS sensitivity

and are therefore able to perform normal Rev1 function in the context of DDT. Once this is confirmed, we can begin using the Rev1-tag flies in a pull-down assay to identify novel interacting partners in DDT. With this assay, we expect to be able to confirm Rev1's role in TLS, as we should be able to pull-down TLS polymerases, specifically Pol ζ, with the full length Rev1 transgenes but not with the C-terminal truncations. There would be a few, known DDT players that, if pulled down, would provide clear support and insight into our current model of Rev1 action in TS, namely SHPRH or any of the notable HR proteins. A newly developed model for Rev1 action in HR-mediated fork stabilization has it binding to and stabilizing Rad51 filaments, implying that Rev1 may bind to and or recruit Rad 51 or BRCA2, therefore serving as a mediator of strand-invasion (Yang et al. 2015). Interaction of Rev1 with SHPRH, on the other hand, would characterize its role during TS as a mediator of pathway choice, helping to recruit or regulate factors necessary for poly-ubiquitination of PCNA. This interaction is not unlikely as in yeast, the SHPRH ortholog, Rad5, is known to interact with Rev1's C-terminal domain (Kuang et al. 2012) Also, since there is evidence that SUMOylation of PCNA is preventing HR-like events during replication, we have speculated that Rev1 could be interacting with or recruiting a de-SUMOylase enzyme (Chang & Cimprich 2009). This enzyme would remove the HR-inhibiting SUMO from PCNA thereby facilitating TS, but this model is purely speculative at this point.

Our questions about DDT coordination and pathway choice have led us to speculate about a tissue or developmental stage specific requirement for a specific DDT pathway or Rev1 function. We have recently acquired some tissue-specific Gal4 drivers that will allow us to direct expression of tagged Rev1 and compare its interacting partners in various tissue-specific contexts. Specifically, we have acquired Gal4 drivers specific to either the wing imaginal disks

or to all tissues except the wing disks. If our hypothesis that Rev1-directed TLS is important specifically to rapidly proliferating tissues, we might expect to pull-down more interacting partners consistent with TLS in the rapidly dividing wing-disk tissues (extracted during larval stages) and more partners consistent with TS in the other tissues, which divide less rapidly. If Rev1 is interacting with different partners in different tissues, this may provide more insight into Rev1's role in coordinating DDT and DDT pathway choice in general.

Supplementary Table 1: List of primers used, sequences and appropriate templates

Primer Name	***Primer Sequence***	***Template***
NsiI-UASpF	NNNNNNATGCATTACTAGAATTGGCGC	pPFMW
BglII-pPFMGW R	NNNNNNAGATCTGATGAGAATGGCCAGA	pPFMW
BglII-UASpF	NNNNNNAGATCTTACTAGAATTGGCCGC	pPWF
Acc651-pPGW R	NNNNNNGGTACCGATGAGAATGGCCAGA	pPWF
Rev1_79F	ATGACCCGCGATGAGGATAAT	pTV[rev1]
Rev1_3432R	TTAGGAGCACTTTATGCAACGAATG	pTV[rev1]
Rev1_3429R	GGAGCACTTTATGCAACGAATGTA	pTV[rev1]
Rev1_3233R	TGCCACAATCTGATCCGATCG	pTV[rev1]
Rev1_3236R	TTATGCCACAATCTGATCCGATCG	pTV[rev1]
Rev1 -250 F	aacgctgaaactgtatgctcg	Rev1-tag, *deltaRev1* single males
Rev1_5438 R	ctgttgttcgttcggctgact	Rev1-tag, *deltaRev1* single males
Rev1_del5P F		Rev1-tag, *deltaRev1* single males
FLAGMYCexpress F	ACGATGACAAGCACCGGTTG	3xFLAG-6xMYC-Rev1 males
Rev1_363R	TTGGCGCTGATGAACTTGCTGAG	3xFLAG-6xMYC-Rev1 males

3xFLAG expressR	CTTTGTAGTCCAGGTGGCGG	Rev1-3xFLAG males
Rev1 2023 rt F	CAGTCGAAACCTCCAAGTACATGG	Rev1-3xFLAG males
T7 Rev1-12189 F	TAATACGACTCACTATAGGGATTTGTGAACGGCCGGACTGA	Genomic DNA - for making RNA
T7 Rev1-12189 R	TAATACGACTCACTATAGGGTGCGAGCGGTGGTGGAGGTAT	Genomic DNA - for making RNA
T7 BRCA2-04220R	TAATACGACTCACTATAGGGTTGCATGCAAATAGG	Genomic DNA - for making RNA
T7 BRCA2-04220F	TAATACGACTCACTATAGGGCCAACCAACTGTGATCTCTG	Genomic DNA - for making RNA
T7 m20506800 F	TAATACGACTCACTATAGGGTGGCCTGGCAATGT	Genomic DNA - for making RNA
T7 m20506800 R	TAATACGACTCACTATAGGGACTGGCGCAGAAAGGAAC	Genomic DNA - for making RNA
T7 BW 04005 F	TAATACGACTCACTATAGGGCTATGGCGTGACGTATATATTT	Genomic DNA - for making RNA
T7 BW 04005 R	TAATACGACTCACTATAGGGGATATTATCGATGTCGATCCAAG	Genomic DNA - for making RNA
T7 spnA-16812 F	TAATACGACTCACTATAGGGCTCGCACCTTCTATCAAATG	Genomic DNA - for making RNA
T7 spnA-16812 R	TAATACGACTCACTATAGGGCATCGGCCAGGCGTTG	Genomic DNA - for making RNA
T7 SHPRH 38315F	TAATACGACTCACTATAGGGACCGAAACGATTACTGGCAC	Genomic DNA - for making RNA
T7 SHPRH 38315R	TAATACGACTCACTATAGGGAGAGTTGGGACGCATGTACC	Genomic DNA - for making RNA
T7 REV1 08624 F	TAATACGACTCACTATAGGGCCGTCCTGAGCCTCGTC	Genomic DNA - for making RNA
T7 REV1 08624 F	TAATACGACTCACTATAGGGTCCTGCTGAGCACGGAC	Genomic DNA - for making RNA
T7 BRCA2-042119F	TAATACGACTCACTATAGGGcgacggaatggccaaaata	Genomic DNA - for making RNA
T7 BRCA2-042119R	TAATACGACTCACTATAGGGCCTCCCTTGCTTCGGTT	Genomic DNA - for making RNA

mus205 rt F	GCAGTTCACCGSTTTGGATGTGG	KC167 Cell time-course rtPCR
mus205 rt R	ACGTGTCCTTATGGAGCTTCATCG	KC167 Cell time-course rtPCR
Rev1_1188F	ACAAGAAAATGTCGCTCTCGGA	KC167 Cell time-course rtPCR
Rev1_1731R	TTTGAGCTTATGGCTTATGCTGCT	KC167 Cell time-course rtPCR

Literature Cited

Branzei, D., & Foiani, M. (2010). Maintaining genome stability at the replication fork. *Nature Reviews Molecular Cell Biology*, *11*(3), 208–219. https://doi.org/10.1038/nrm2852

Branzei, D., & Psakhye, I. (2016). DNA damage tolerance. *Current Opinion in Cell Biology*, *40*, 137–144. https://doi.org/10.1016/j.ceb.2016.03.015

Branzei, D., & Szakal, B. (2016). DNA damage tolerance by recombination: Molecular pathways and DNA structures. *DNA Repair*, *44*, 68–75. https://doi.org/10.1016/j.dnarep.2016.05.008

Branzei, D., Vanoli, F., & Foiani, M. (2008). SUMOylation regulates Rad18-mediated template switch. *Nature*, *456*(7224), 915–920. https://doi.org/10.1038/nature07587

Callegari, A. J., & Kelly, T. J. (2016). Coordination of DNA damage tolerance mechanisms with cell cycle progression in fission yeast. *Cell Cycle (Georgetown, Tex.)*, *15*(2), 261–273. https://doi.org/10.1080/15384101.2015.1121353

Chang, D. J., & Cimprich, K. A. (2009). DNA Damage Tolerance: When It's OK to Make Mistakes. *Nature Chemical Biology*, *5*(2), 82–90. https://doi.org/10.1038/nchembio.139

Choe, K. N., & Moldovan, G.-L. (2017). Forging Ahead through Darkness: PCNA, Still the Principal Conductor at the Replication Fork. *Molecular Cell*, *65*(3), 380–392. https://doi.org/10.1016/j.molcel.2016.12.020

Cimprich, K. A., & Cortez, D. (2008). ATR: an essential regulator of genome integrity. *Nature Reviews. Molecular Cell Biology*, *9*(8), 616–627. https://doi.org/10.1038/nrm2450

D'Souza, S., Waters, L. S., & Walker, G. C. (2008). Novel conserved motifs in Rev1 C-terminus are required for mutagenic DNA damage tolerance. *DNA Repair*, *7*(9), 1455–1470. https://doi.org/10.1016/j.dnarep.2008.05.009

Friedberg, E. C., Lehmann, A. R., & Fuchs, R. P. P. (2005). Trading Places: How Do DNA Polymerases Switch during Translesion DNA Synthesis? *Molecular Cell*, *18*(5), 499–505. https://doi.org/10.1016/j.molcel.2005.03.032

Ghosal, G., & Chen, J. (2013). DNA damage tolerance: a double-edged sword guarding the genome. *Translational Cancer Research*, *2*(3), 107–129. https://doi.org/10.3978/j.issn.2218-676X.2013.04.01

Guo, C., Sonoda, E., Tang, T.-S., Parker, J. L., Bielen, A. B., Takeda, S., … Friedberg, E. C. (2006). REV1 Protein Interacts with PCNA: Significance of the REV1 BRCT Domain In

Vitro and In Vivo. *Molecular Cell*, *23*(2), 265–271. https://doi.org/10.1016/j.molcel.2006.05.038
Heller, R. C., & Marians, K. J. (2006). Replication fork reactivation downstream of a blocked nascent leading strand. *Nature*, *439*(7076), 557–562. https://doi.org/10.1038/nature04329
Hirano, Y., & Sugimoto, K. (2006). ATR Homolog Mec1 Controls Association of DNA Polymerase ζ-Rev1 Complex with Regions near a Double-Strand Break. *Current Biology*, *16*(6), 586–590. https://doi.org/10.1016/j.cub.2006.01.063
Huang, D., Piening, B. D., & Paulovich, A. G. (2013). The Preference for Error-Free or Error-Prone Postreplication Repair in Saccharomyces cerevisiae Exposed to Low-Dose Methyl Methanesulfonate Is Cell Cycle Dependent. *Molecular and Cellular Biology*, *33*(8), 1515–1527. https://doi.org/10.1128/MCB.01392-12
Jena, N. R. (2012). DNA damage by reactive species: Mechanisms, mutation and repair. *Journal of Biosciences*, *37*(3), 503–517.
Kane, D. P., Shusterman, M., Rong, Y., & McVey, M. (2012). Competition between Replicative and Translesion Polymerases during Homologous Recombination Repair in Drosophila. *PLoS Genetics*, *8*(4). https://doi.org/10.1371/journal.pgen.1002659
Kolinjivadi, A. M., Sannino, V., de Antoni, A., Técher, H., Baldi, G., & Costanzo, V. (2017). Moonlighting at replication forks: a new life for homologous recombination proteins BRCA1, BRCA2 and RAD51. *FEBS Letters*, n/a–n/a. https://doi.org/10.1002/1873-3468.12556
Kuang, L., Kou, H., Xie, Z., Zhou, Y., Feng, X., Wang, L., & Wang, Z. (2013). A non-catalytic function of Rev1 in translesion DNA synthesis and mutagenesis is mediated by its stable interaction with Rad5. *DNA Repair*, *12*(1), 27–37. https://doi.org/10.1016/j.dnarep.2012.10.003
Leman, A. R., & Noguchi, E. (2013). The Replication Fork: Understanding the Eukaryotic Replication Machinery and the Challenges to Genome Duplication. *Genes*, *4*(1), 1–32. https://doi.org/10.3390/genes4010001
Lin, J.-R., Zeman, M. K., Chen, J.-Y., Yee, M.-C., & Cimprich, K. A. (2011). SHPRH and HLTF Act in a Damage-Specific Manner to Coordinate Different Forms of Postreplication Repair and Prevent Mutagenesis. *Molecular Cell*, *42*(2), 237–249. https://doi.org/10.1016/j.molcel.2011.02.026
Masuda, Y., & Kamiya, K. (2006). Role of Single-stranded DNA in Targeting REV1 to Primer Termini. *Journal of Biological Chemistry*, *281*(34), 24314–24321. https://doi.org/10.1074/jbc.M602967200
Mazouzi, A., Velimezi, G., & Loizou, J. I. (2014). DNA replication stress: Causes, resolution and disease. *Experimental Cell Research*, *329*(1), 85–93. https://doi.org/10.1016/j.yexcr.2014.09.030
Moldovan, G.-L., Pfander, B., & Jentsch, S. (2007). PCNA, the Maestro of the Replication Fork. *Cell*, *129*(4), 665–679. https://doi.org/10.1016/j.cell.2007.05.003
Rørth, P. (1998). Gal4 in the Drosophila female germline. *Mechanisms of Development*, *78*(1–2), 113–118. https://doi.org/10.1016/S0925-4773(98)00157-9
Sale, J. E. (2013). Translesion DNA synthesis and mutagenesis in eukaryotes. *Cold Spring Harbor Perspectives in Biology*, *5*(3), a012708. https://doi.org/10.1101/cshperspect.a012708

Sharma, S., Helchowski, C. M., & Canman, C. E. (2013). The roles of DNA polymerase ζ and the Y family DNA polymerases in promoting or preventing genome instability. *Mutation Research*, *0*, 97–110. https://doi.org/10.1016/j.mrfmmm.2012.11.002

Szakal, B., & Branzei, D. (2013). Premature Cdk1/Cdc5/Mus81 pathway activation induces aberrant replication and deleterious crossover. *The EMBO Journal*, *32*(8), 1155–1167. https://doi.org/10.1038/emboj.2013.67

Vanoli, F., Fumasoni, M., Szakal, B., Maloisel, L., & Branzei, D. (2010). Replication and Recombination Factors Contributing to Recombination-Dependent Bypass of DNA Lesions by Template Switch. *PLoS Genetics*, *6*(11). https://doi.org/10.1371/journal.pgen.1001205

Waters, L. S., Minesinger, B. K., Wiltrout, M. E., D'Souza, S., Woodruff, R. V., & Walker, G. C. (2009). Eukaryotic Translesion Polymerases and Their Roles and Regulation in DNA Damage Tolerance. *Microbiology and Molecular Biology Reviews*, *73*(1), 134–154. https://doi.org/10.1128/MMBR.00034-08

Yang, Y., Liu, Z., Wang, F., Temviriyanukul, P., Ma, X., Tu, Y., … Guo, C. (2015). FANCD2 and REV1 cooperate in the protection of nascent DNA strands in response to replication stress. *Nucleic Acids Research*, *43*(17), 8325–8339. https://doi.org/10.1093/nar/gkv737

Zellweger, R., Dalcher, D., Mutreja, K., Berti, M., Schmid, J. A., Herrador, R., … Lopes, M. (2015). Rad51-mediated replication fork reversal is a global response to genotoxic treatments in human cells. *The Journal of Cell Biology*, *208*(5), 563–579. https://doi.org/10.1083/jcb.201406099